2007

Structural and Signaling Elements Important for the Efficient Degradation of BHMT through Macroautophagy

Carol A. Mercer
Wright State University

STRUCTURAL AND SIGNALING ELEMENTS IMPORTANT FOR THE EFFICIENT DEGRADATION OF BHMT THROUGH MACROAUTOPHAGY

A dissertation submitted in partial fulfillment of the
requirements for the degree of
Doctor of Philosophy

By

CAROL A. MERCER
B.A., Wittenberg University, 1978

2007
Wright State University

WRIGHT STATE UNIVERSITY

SCHOOL OF GRADUATE STUDIES

March 30, 2007

I HEREBY RECOMMEND THAT THE DISSERTATION PREPARED UNDER MY SUPERVISION BY Carol Ann Mercer ENTITLED Structural and Signaling Elements Important for the Efficient Degradation of BHMT through Macroautophagy BE ACCEPTED IN PARTIAL FULFILLMENT OF THE REQUIREMENTS FOR THE DEGREE OF Doctor of Philosophy.

Patrick B. Dennis, Ph.D.
Dissertation Director

Gerald M. Alter, Ph.D.
Director, Biomedical Sciences
Ph.D. Program

Joseph F. Thomas, Jr., Ph.D.
Dean, School of Graduate Studies

Committee on
Final Examination

Patrick B. Dennis, Ph.D.

John Turchi, Ph.D.

Scott Baird, Ph.D.

Mark Mamrach, Ph.D.

John Paietta, Ph.D.

ABSTRACT

Mercer, Carol A., Ph.D. Biomedical Sciences Ph.D. Program, Wright State University, 2007. Structural and Signaling Elements Important for the Efficient Degradation of BHMT through Macroautophagy

Healthy cells maintain a dynamic and responsive intracellular environment that is marked by the synthesis and degradation of proteins, complex macromolecules and organelles. Autophagy, literally 'self-eating,' is a mechanism that delivers cellular cargo to the lytic compartment for digestion. Defects in the regulation of autophagy have been implicated in pathologies such as cancer and neurodegenerative disease, making the study of its regulation compelling. However, few studies have looked at the regulation of mammalian autophagy as a function of a specific cargo protein. Previous studies had indicated that the metabolic enzyme betaine homocysteine methyltransferase (BHMT) is degraded through an autophagic mechanism. One aim of this study has centered on the role of BHMT quaternary structure in determining the efficiency of autophagic sequestration and degradation. In these studies, an oligomerization deficient form of BHMT was used to show that modulation of the Class III PI3 kinase signaling pathway is likely involved in discerning monomeric from multimeric BHMT and that this has a role in the subsequent degradation of BHMT by autophagy.

The second aim has been to study to role of the nutrient-regulated mTOR pathway in the autophagic degradation of BHMT. It has been proposed that mTOR-mediated

inactivation of S6 kinase is required for induction of autophagy in mammals. However in *Drosophila melanogaster*, S6 kinase activity has been shown to be essential for induction of autophagy. The current study demonstrates that the inhibitory signal from mTOR to autophagy does not go through S6 kinase or subsequent phosphorylation of the ribosomal protein S6. The significance of these observations in terms of misfolded proteins, neurodegenerative diseases and therapeutics is discussed.

TABLE OF CONTENTS

ILLUSTRATIONS

TABLES

ACKNOWLEDGMENTS

I would like to sincerely thank my advisor, Dr. Patrick Dennis. I would not have done this without him. Every day was full of good conversation and good science. I would like to thank the all the members of my committee: Dr. Scott Baird, Dr. John Paietta, Dr. John Turchi, and Dr. Mark Mamrack. I am especially grateful to Dr. John Turchi, the first person I met at WSU and the one who convinced me that I would be accepted at WSU.

Thank you to the Biochemistry and Molecular Biology Department at Wright State University and to the Genome Science Department of the University of Cincinnati. Faculty members of both departments generously offered encouragement, ideas, and time. Thanks to the Biomedical Sciences Ph.D. program for funding and support.

Last, I would like to thank my family: Rob, Nick, Erin, Dad and Mom. I could not have done this without them. They offered support, encouragement and love at the times when I needed them most.

DEDICATION

To Rob, who encouraged, supported, and loved me.

To Dad, who inspired me.

I. INTRODUCTION

1.1. Introduction

Healthy cells maintain a dynamic and responsive intracellular environment that is marked by both the synthesis and degradation of proteins, complex macromolecules and organelles. Autophagy, literally 'self-eating,' is a mechanism that delivers cellular cargo to a lytic compartment for digestion. In basal conditions, this process removes cellular 'garbage' such as damaged or unwanted proteins, defective mitochondria, or excessive internal membranes[1]. Autophagy also responds to conditions of cellular stress. When nutrients are scarce, autophagy is induced to replenish the cell with essential building blocks such as amino acids, lipids and nucleic acids that are needed to maintain cellular processes necessary for survival. In metazoans, there are times in development when the need for new synthesis for cellular growth and proliferation is predominant, and the need for autophagy recedes[2]. Developmental periods of tissue remodeling tip the scales toward more autophagy and less synthesis in the autophagic death and removal of unwanted cells, as seen in *Drosophila*[3]. In the worm *Caenorhabditis elegans*, autophagy is important for normal dauer formation, allowing survival during long periods of limiting nutrients[4]. In mammals, the importance of autophagy to the whole organism is apparent in the neonate. Shortly after birth, before suckling is able to effectively provide nutrients, the newborn relies on autophagy, primarily of liver glycogen, to maintain circulating glucose levels and for survival[5]. There is an

increasing awareness of the significance of autophagy in human disease as defects in its regulation have been shown to contribute to cancer, aging, cardiomyopathy, myopathy, and neurodegenerative diseases[6, 7].

1.2. Types of autophagy

Autophagy is the lysosomal digestion of cytoplasmic cargo and occurs in all eukaryotic cells. There are three main types of autophagy: macroautophagy, chaperone-mediated autophagy (CMA) and microautophagy (Fig. 1). Macroautophagy is the most common type of autophagy and the terms autophagy and macroautophagy are often used synonymously. Distinct types of macroautophagy include the Cvt pathway (in yeast only), pexophagy (degradation of peroxisomes), mitophagy (degradation of mitochondria), and crinophagy (degradation of secretory vesicles)[6].

Macroautophagy and the yeast-specific Cvt pathway both require the formation of an enclosed double-membrane vesicle to sequester cargo destined for the lytic compartment. They share many of the same genes for the development of the sequestering vesicle, but differ in select genes that are pathway specific, in vesicle size, and in the nutrient conditions of activation. Macroautophagy is a non-specific degradation pathway in all eukaryotic cells that is active when nutrients are limiting. While non-lysosomal mechanisms exist for the degradation of protein, macroautophagy is the only cellular pathway to remove organelles and macromolecular complexes such as mitochondria and ribosomes respectively. The Cvt pathway is a biosynthetic pathway specific to yeast that delivers the hydrolytic enzymes aminopeptidase 1 (Ape1) and α-mannosidase to the vacuole. Ape1 is synthesized in the cytosol in an inactive form and assembles into a large, multimeric complex which is recognized by Atg19 (Fig. 2).

Figure 1. Schematic overview of macroautophagy, microautophagy, and chaperone-mediated autophagy. Macroautophagy involves the formation of a double-membrane autophagosome. Steps of macroautophagy include 1) induction at the pre-autophagosomal structure (PAS), 2) growth and elongation, 3) sequestration of cargo within the autophagosome, 4) fusion with the lysosome/vacuole to create the autolysosome, and 5) degradation of cargo. Microautophagy is the invagination of the lysosomal membrane for the direct import of cargo. Chaperone-mediated autophagy requires a KFERQ-like sequence on the substrate protein, recognition by hsc73, assembly of the chaperone complex and binding to lysosome associated membrane protein 2a (LAMP2a) at the lysosome. After the chaperone-mediated unfolding of the substrate protein, it is threaded through the lysosome membrane, binds the lysosomal hsc73 protein and is degraded.

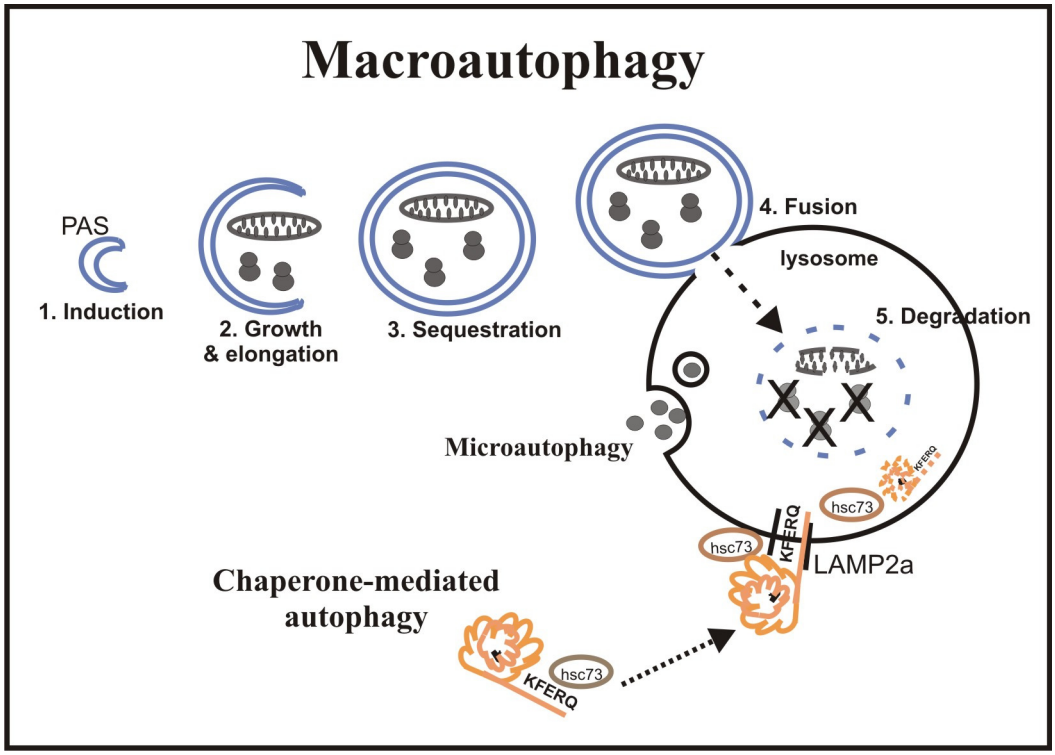
Macroautophagy
PAS
1. Induction
2. Growth & elongation
3. Sequestration
4. Fusion
lysosome
5. Degradation
Microautophagy
hsc73
KFERQ
LAMP2a
Chaperone-mediated autophagy

Figure 2. The Cvt pathway cargo recognition system. The Cvt pathway is a type of specific autophagy. Aminopeptidase 1, a substrate of the Cvt pathway, is a dodecamer which multimerizes into a larger Ape1 complex. The Ape1 complex is recognized by Atg19, which in concert with Atg11 and perhaps Atg1, delivers it to the pre-autophagosomal structure (PAS), where it directly interacts with Atg8. After Ape1 is delivered to the vacuole, it is proteolytically cleaved and becomes an active resident hydrolase.

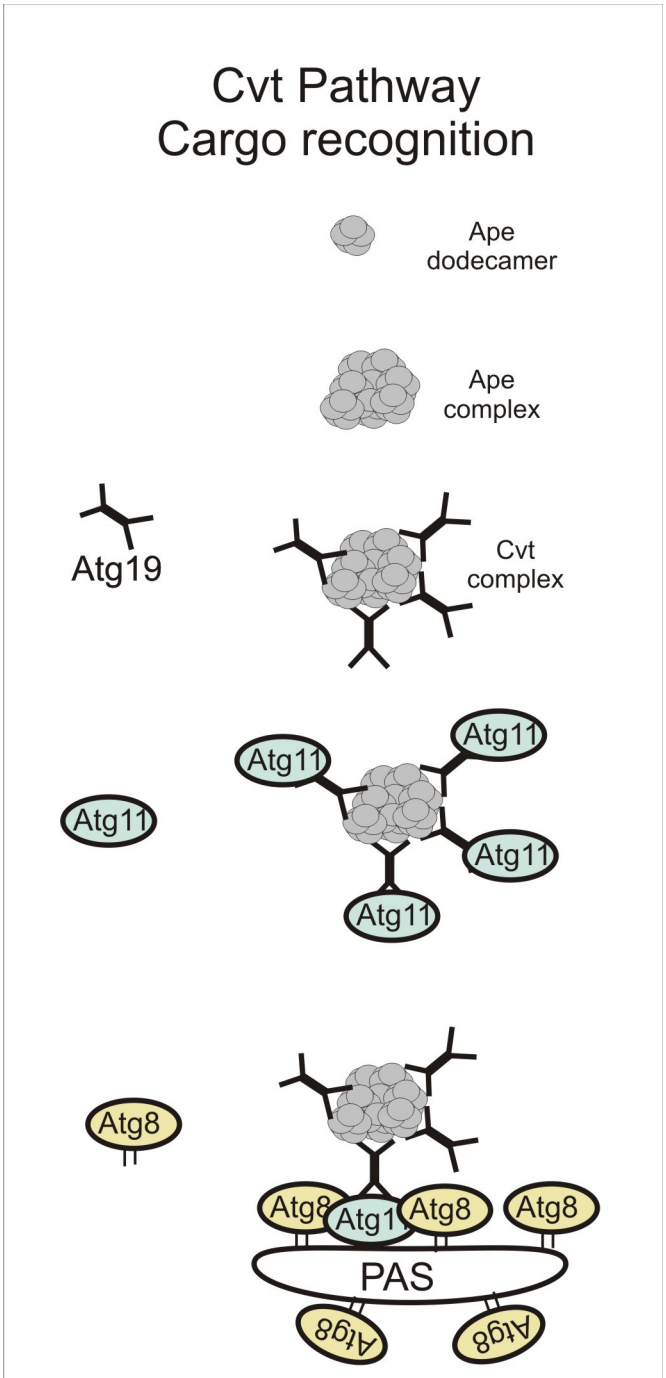

Adapted from Klionsky DJ, The molecular machinery of autophagy: unanswered questions. Journal of Cell Science, 2005. 118:7-18

Atg19 is an adapter protein that links the Ape1 dodecamer with Atg8 at the pre-autophagosomal membrane, in concert with Atg11 and other proteins that may include Atg1. Once in the vacuole, cleavage of in inhibitory peptide converts Ape1 into an active, resident enzyme. Phosphatidylinositol 3-phosphate (PI3P) is thought to be important for the Cvt pathway because some of the Cvt-specific proteins contain FYVE (first described in proteins Fab1, YOTB/ZK632.12, Vac1, and EEA1) or Phox homology (PX) PI3P binding domains[8].

Microautophagy involves invagination and fission of the lysosome membrane to create small intralysosomal vesicles. Little is know about this process in mammals, but in yeast, membrane-associated complexes form and mediate this process. The EGO complex, comprised of a Ras-related GTPase, Gtr2, Ego1 and Ego3, has been linked to the target of rapamycin (TOR) kinase. Nutrient depletion or inhibition of TOR with the drug rapamycin increases macroautophagy and the influx of membrane to the yeast vacuole. When rapamycin is removed, microautophagy is activated in a TOR-dependent manner to reduce the size of the vacuole[9]. It is not known if this type of TOR-mediated mechanism for microautophagy exists in higher organisms.

Chaperone-mediated autophagy (CMA) is an autophagy pathway in mammalian cells that responds to prolonged starvation. CMA is specific for proteins with a target recognition sequence similar to the KFERQ sequence identified in RNase A, the first known CMA substrate. Upon recognition of this motif by the heat shock cognate protein hsc73, the substrate protein is surrounded by a chaperone complex, and delivered to the lysosome. At the lysosome, the chaperone complex interacts specifically with lysosomal associated membrane protein 2a (LAMP2a) and facilitates the unfolding of the substrate

protein, allowing it to be threaded through the lysosome membrane to be degraded[10]. In CMA, proteins are imported and degraded one protein at a time. There are estimates that up to 30% of cytosolic proteins are degraded by CMA, but significantly, the LAMP2$^{-/-}$/LAMP1$^{-/-}$ double knockout mouse shows no defect in total protein degradation[11]. It may be that other autophagy pathways compensate for this defect as the selective knockout of the LAMP2a isoform results in a compensatory increase in macroautophagy[12].

1.3. The process of macroautophagy

Macroautophagy proceeds in a step-wise fashion that includes: 1) induction, 2) growth and elongation of a pre-autophagosomal structure (PAS), 3) sequestration of cargo within the double-membrane autophagosome, 4) fusion with the lytic compartment, and 5) degradation[13]. Genetic studies in *S. cerevisiae* have identified specific genes required for autophagy and for survival in nutrient-limiting conditions, leading to an increase in an understanding of some of the interactions and mechanisms involved in the autophagic process[14, 15]. A unified nomenclature system is now used that identifies these genes as autophagy-related genes (Atg) 1-27 (Table 1)[16]. Many of these genes, protein complexes and molecular mechanism are conserved in higher eukaryotes.

1.4. Molecular complexes in macroautopahgy

1.4.1. The ubiquitin-like conjugation systems

The formation of autophagosomes requires the function of two, novel, interrelated ubiquitin-like conjugation systems (Fig. 3)[17]. Atg8 and Atg12 are ubiquitin-like (UBL) modifiers which share the same E1-like activating enzyme Atg7. Atg8 and Atg12

ATG Proteins & Human Orthologs

Yeast	Human	Characteristics
ATG 1	hULK1/hULK2	Serine/Threonine protein kinase
ATG 2	hAtg2?	peripheral membrane protein
ATG 3	hAtg3	E2-like enzyme for Atg8/LC3
ATG 4	hAtg4B	Cysteine protease
ATG 5	hAtg5	Conjugated to Atg12
ATG 6	Beclin1	Part of Vps34 complex
ATG 7	hAtg7	E1-like enzyme
ATG 8	LC3B	Ubiquitinin-like protein
ATG 9	hAtg9	Integral membrane protein
ATG 10	hAtg10	E2-like enzyme for Atg12
ATG 11		Cargo recognition
ATG 12	hAtg12	Ubiquitinin-like protein
ATG 13		Modifies Atg1 activity
ATG 14		Part of Vps34 complex
ATG 15		Lipase
ATG 16	hAtg16	Part of Atg12-Atg5 complex
ATG 17		Modifies Atg1 activity
ATG 18	hAtg18	peripheral membrane protein
ATG 19		Cargo receptor for Cvt pathway
ATG 20		PX domain protein
ATG 21		Part of Cvt pathway
ATG 22		Integral membrane protein
ATG 23		Cvt vesicle completion
ATG 24		PX domain protein
ATG 25		Coiled-coil in macropexophagy
ATG 26		GRAM domain
ATG 27		PI3P binding protein

Table 1. List of known Atg proteins in yeast, with human orthologs. Right column lists brief discription of each.

Figure 3. The Ubiquitin-like conjugation systems of macroautophagy. Ubiquitin-like proteins Atg8 and Atg12 are activated by the E1-like enzyme Atg7 and ATP, transferred to their respective E2-like enzymes Atg3 and Atg10, and then conjugated to their targets. Atg8 is covalently attached to phosphatidylethanolamine and Atg12 is conjugated to Atg5. The Atg12-Atg5 heterodimer then forms a larger complex with Atg16.

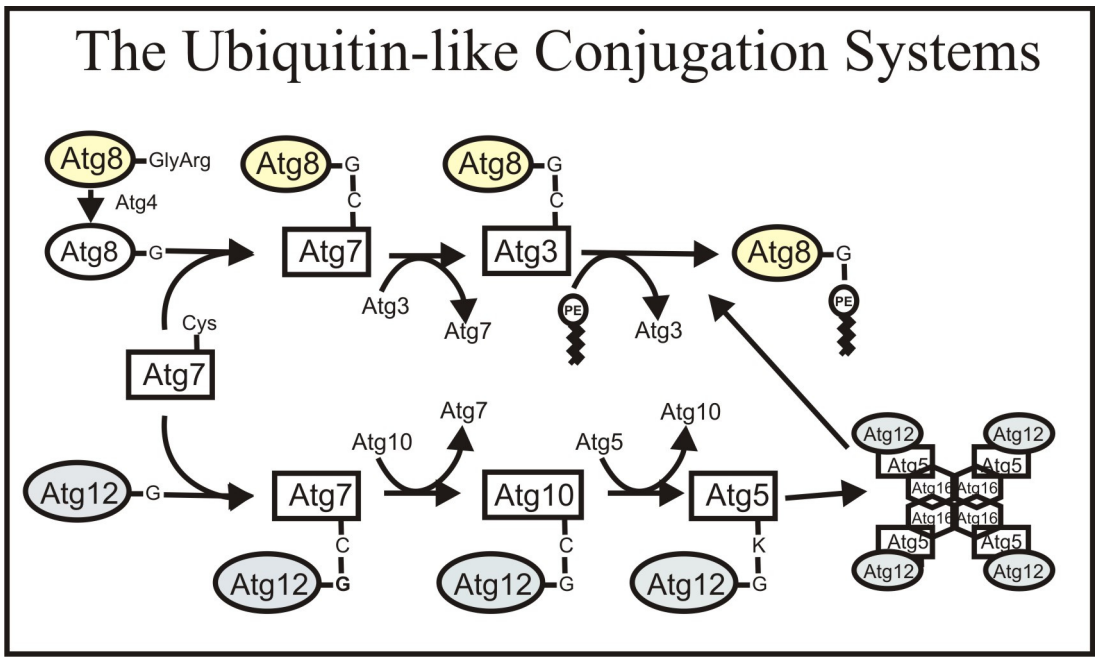
The Ubiquitin-like Conjugation Systems
Atg8
GlyArg
Atg4
Atg8
G
Cys
Atg7
Atg8
G
C
Atg7
Atg3
Atg7
Atg8
G
C
Atg3
PE
Atg3
Atg8
G
PE
Atg12
G
Atg7
C
Atg12
G
Atg10
Atg7
Atg7
C
Atg12
G
Atg10
C
Atg12
G
Atg5
Atg10
Atg5
K
Atg12
G
Atg12
Atg12
Atg5
Atg5
Atg16
Atg16
Atg16
Atg16
Atg5
Atg5
Atg12
Atg12

are then conjugated to their respective targets through the action of their specific E2-like enzymes, Atg3 and Atg10 respectively. Atg8 is translated in a pro-form that requires cleavage by the protease Atg4 to reveal a carboxy-terminal glycine necessary for conjugation. Atg8 is activated by Atg7 and ATP, transferred to Atg3, and then uniquely conjugated to phosphatidylethanolamine (PE). Atg8-PE remains associated with both inner and outer membranes of the expanding autophagosome, although Atg4-dependent cleavage of some Atg8-PE from the outer membrane is required for fusion with the vacuole (Fig. 3)[18]. In yeast, Δatg8 mutants form aberrantly small autophagosomes suggesting that Atg8 may be necessary for growth and elongation of the autophagosomes membrane[19].

The Atg8 conjugation system is well conserved in higher eukaryotes. In mammals, microtubule associating protein light chain (MAP-LC3) is the best known ortholog of Atg8 and is often used as a specific marker of autophagosomes[20]. Three isoforms of LC3 have been identified and are known as LC3A, LC3B and LC3C, with some overlapping and some specific distribution among cell types[21]. In addition to the LC3s, multiple other mammalian orthologs of Atg8 are known, although they are less well characterized in terms of autophagy. These include Golgi-associated ATPase enhancer of 16 kDa (GATE-16) and γ-aminobutyric acid receptor associated proteins (GABARAP-I and GABARAP-II) and Atg8L[22, 23].

Atg12 is also activated by Atg7 and ATP, transferred to its own E2-like enzyme Atg10, and conjugated to its only known target, Atg5[24]. The Atg5-Atg12 heterodimer then assembles into a higher molecular weight complex through interaction with Atg16[25]. The Atg5-Atg12 complex is found only on the outer, concave surface of the

growing autophagosome and may have a structural role in the curvature of the membrane. In addition, the Atg5-Atg12 complex may play a role in the recruitment and assembly of the other Atg proteins at the PAS. The Atg12-Atg5-Atg16 complex does not remain with the autophagosome but dissociates before fusion with the vacuole/lysosome.

The Atg12-Atg5 conjugation system is conserved in mammals[26]. Mice with total disruption of either Atg5 or Atg7 develop normally but die within 24 hours of birth[27, 28]. Early death is likely through a nutritional and energy collapse due to defective glycogen autophagy. Gene disruption of either Atg5 or Atg7 in the central nervous system results in a progressive, degenerative neurological phenotype causing death before 28 weeks. Neurons in these targeted knock-out mice are characterized by aggregates of poly-ubiquitinated protein and inclusion bodies[29, 30]. Protein aggregates, inclusion bodies, and autophagosomes are often observed upon biopsy or necroscopy of patients with neurodegenerative disease; however it had not been clear whether they were a cause or effect of the neurodegenerative process. The Atg5 and Atg7 targeted knock-out mice provide the first evidence that defects in autophagy can be a cause rather than a consequence of neurodegeneration.

1.4.2. The Class III PI 3-Kinase and Atg6 complex

In yeast, Atg6 associates with Vps34, a Class III PI3-kinase that phosphorylates the 3'-OH on the inositol ring of phosphatidylinositol to form phosphatidylinositol 3-phosphate (PI3P)[31]. Vps34 associates with the serine kinase Vps15, which has a role in the membrane localization and activation of Vps34 (Fig. 4). Vps34 activity or function may also be regulated by complexes of associating proteins: Vsp34, Vsp15, Atg6 and

Figure 4. The Vps34/Atg6 and Atg1 complexes in yeast. Class III PI 3-kinase Vps34 activity is controlled by its binding partners, Vps15, Atg6 and Atg14. Atg1 functions in complex with multiple Atg proteins. Some of the Atg proteins in complex with Atg1 are specific for the Cvt pathway, which has led to the proposal that the Atg1 complex acts as a switch between the Cvt pathway and macroautophagy. When TOR and Atg1 are active, the Cvt pathway is dominant, and when TOR is inactive, macroautophagy is preferred over the Cvt pathway.

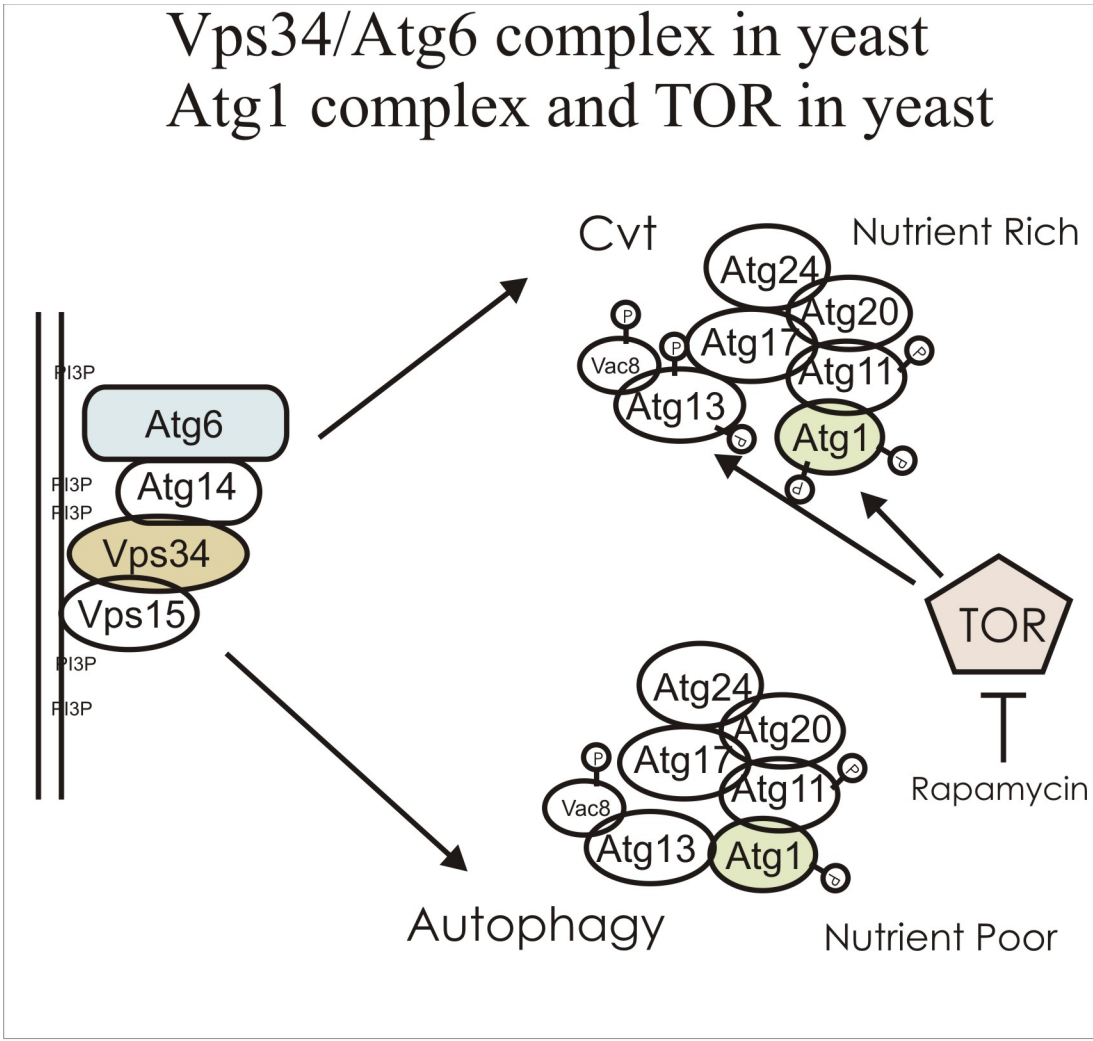

Adapted from Klionsky DJ, The molecular machinery of autophagy: unanswered questions. Journal of Cell Science, 2005. 118:7-18

Atg14 promote autophagy, and a modified complex with Vps38 in place of Atg14 favors the Cvt pathway[32]. Atg6 and Vps34 localize to the trans-Golgi. The production of PI3P may play a role in the recruitment of other Atg proteins to the pre-autophagosome structure. Vps34 activity is thought to promote autophagy, and the activity of Class I PI3 kinases suppresses autophagy. This is based on several pieces of evidence. First, an increase of PI3P increases degradation of long-lived protein, while the increase in PI(3,4)P2 or PI(3,4,5)P3, products of the Class I PI3 kinases, inhibits degradation[33]. Second, injection of Vps34 antisense oligonucleotides inhibits autophagosome formation in interphase cells[34]. And third, knockout mice for the myotubularin MTMR3, a member of a large family of lipid phosphatases that specifically remove the 3′ phosphate from PI3P, suffer from a large accumulation of autophagosomes in skeletal muscle, resulting in a severe, progressive myopathy[35]. Contrary to this data, two recent studies report that amino acids increase Vps34 activity which in turn activates the mTOR signaling pathway[36, 37]. It may be that hVps34 activity, like yeast Vps34, is also regulated by associating proteins. Wortmannin and 3-methyladenine (3MA) are traditionally used as autophagy inhibitors, and their effectiveness is thought to be through inhibition of Vps34 kinase activity[33].

Beclin1 is the mammalian ortholog of Atg6 and it has many of the same characteristics of yeast Atg6: it forms a complex with hVps34 at the trans-Golgi and it can complement autophagy in Δatg6 mutant yeast[38, 39]. Beclin1, originally described as a Bcl-2 binding protein[40], is the first autophagy protein whose disruption has been implicated in cancer[41, 42]. Beclin1 is mono-allelically deleted in 40-70% of human breast cancers, and its ectopic expression in MCF7 cells can induce autophagy and inhibit

tumorigenicity[38]. Total disruption of beclin1 in mice is embryonic lethal, but significantly, beclin1$^{+/-}$ mice have a high propensity to develop spontaneous tumors, providing genetic evidence that Beclin1 may play a role in tumor suppression[19, 42]. The association between Beclin1 and Bcl-2 suggests a potential molecular link between autophagy and apoptosis and a possible mechanism for the increased tumors in beclin1$^{+/-}$ mice. In one model, there is a balance between free Beclin1, free Bcl-2, and the Beclin1/Bcl-2 complex; increased free Beclin1 induces autophagy and inhibits tumors; increased Bcl-2 inhibits autophagy and increases oncogenesis[43]. Although further studies are needed to determine the accuracy of this model, it demonstrates the potential relevance of Beclin1 and autophagy in human disease.

1.4.3. The Atg1 Complex

Atg1 was the first Atg gene identified in the genetic screens in *S. cerevisiae* and is the only Atg gene that codes for a serine-threonine kinase[44]. In yeast, Atg1 is thought to be downstream of the target of rapamycin TOR signaling pathway[45]. There are two models of how TOR regulates Atg1 in yeast, and both place Atg1 within the context of a complex of associating proteins (Fig. 4). In the first model, Atg1 activity is regulated by its association with Atg13. When nutrients are plentiful and TOR signaling is active, Atg13 is hyperphosphorylated and forms a loose complex with Atg1 that prevents its activation. When nutrients are scarce and TOR signaling is off, the hypo-phosphorylated Atg13 forms a tight complex with Atg1 that results in increased Atg1 activity and autophagy[45]. In the second model, the Atg1 complex includes proteins that function in only one of the autophagy pathways, Cvt or macroautophagy. This led to the hypothesis that Atg1 activity is a switch that directs which pathway will be active. In the second

model, Atg1 activity is important for the Cvt pathway but is dispensable for autophagy[46]. The specific action or target of Atg1 activity is not known, however it may have a role in the trafficking of the only Atg integral trans-membrane protein, Atg9, between the PAS and autophagosome[47]. To date, no endogenous substrates of Atg1 catalytic activity are known.

Orthologs of Atg1 have been identified in many species from plants to humans and all have been implicated in the autophagy process. Defects in autophagy have been noted in Atg1 mutants in *Dictyostelium dicoideum*, *C. elegans*, and *Drosophila melanogaster*[4, 48, 49]. Mammals have at least two orthologs of Atg1, unc-51 like kinase 1 (hULK1) and hULK2[50, 51]. Consistent with the role of Atg1 in yeast, hULK1 is necessary for the localization of mAtg9 to LC3-marked membranes during autophagy induction[52]. Unlike yeast, in higher organisms, the Atg1 orthologs have not yet been shown to function downstream of TOR, nor has the connection between Atg1 and the TOR pathway been unambiguously established.

1.5. Macroautophagy and the TOR pathway in higher eukaryotes

In the field of autophagy, there is general agreement that autophagy must be tightly regulated because of the pathological consequences of deregulated autophagy. The protein kinase mTOR plays a central role in the ability of cells to sense growth signals, amino acid levels, and energy in order to make decisions that effect translation of new proteins, cell growth and proliferation (Fig. 5)[53]. It is generally accepted that mTOR also makes decisions that affect autophagy. If nutrients are readily available from the extracellular milieu, mTOR signals for the cell to grow. But when extracellular nutrients are scarce, mTOR signaling allows the cell to survive by increasing autophagy

Figure 5. The mTOR pathway and autophagy in mammals. mTOR senses mitogen signals through the PI3K/PKB pathway. Amino acids increase Vps34 activity and increase the mTOR signaling pathway. mTOR is a negative regulator of autophagy.

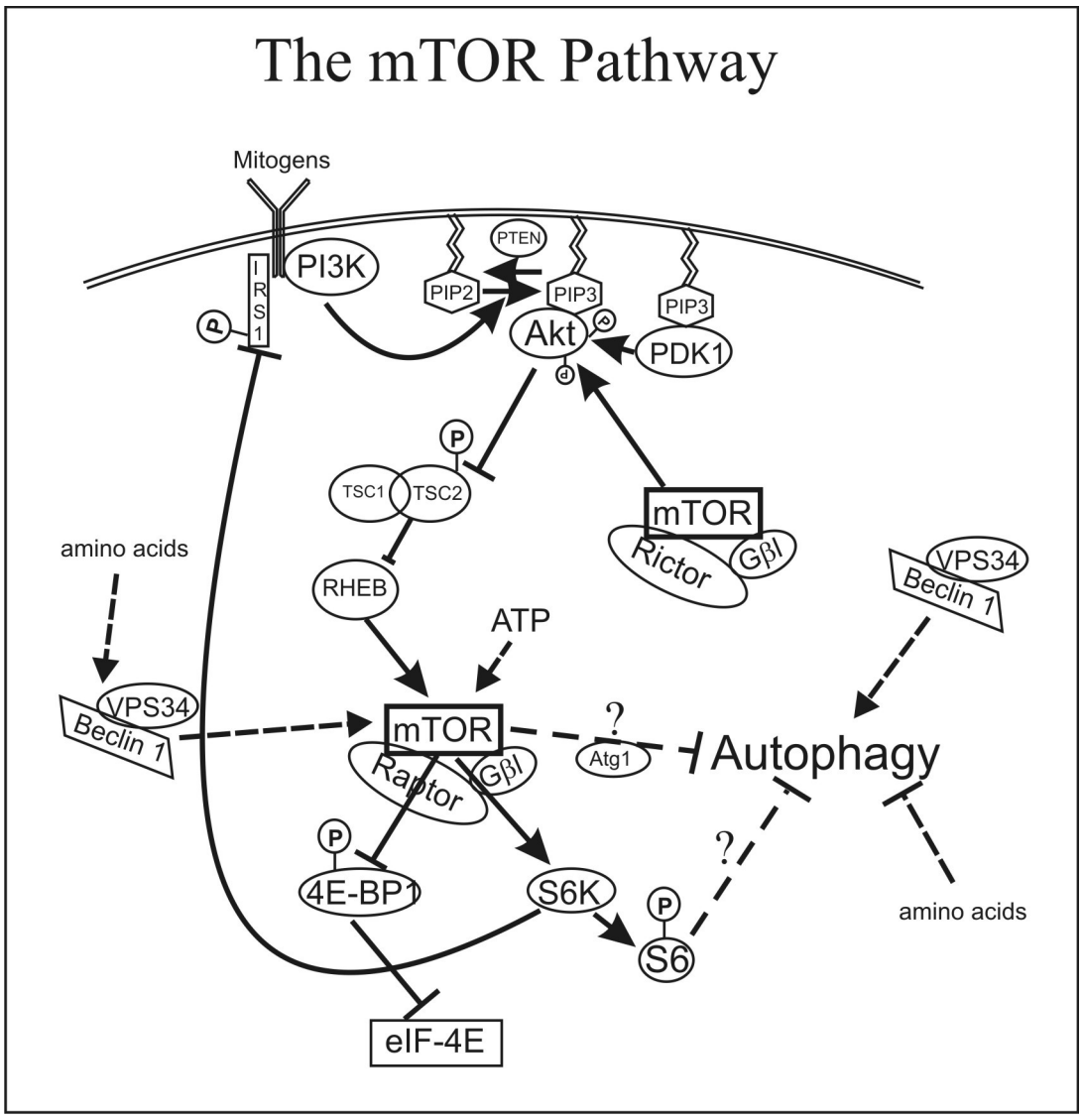
The mTOR Pathway
Mitogens
PI3K
IRS1
PTEN
PIP2
PIP3
PIP3
Akt
PDK1
TSC1
TSC2
RHEB
mTOR
Rictor
Gβl
amino acids
VPS34
Beclin 1
ATP
VPS34
Beclin 1
mTOR
Raptor
Gβl
?
Atg1
Autophagy
4E-BP1
S6K
S6
?
amino acids
eIF-4E

to degrade internal proteins for energy and raw materials necessary for survival.

In higher eukaryotes, the connection between mammalian mTOR and hULK1 is not obvious. In mammalian cells, it has been proposed that the regulation of autophagy involving mTOR may be through its downstream effector, p70S6 Kinase. mTOR phosphorylates p70S6K on T389, which leads to p70S6K activation and the phosphorylation of its downstream substrate, S6. Blommaart et al. (1995) demonstrated a strong negative correlation between phospho-S6 and autophagy in rat hepatocytes and proposed a model that the signal for autophagosome formation may be through dephosphorylation of S6[54]. For many years, this data supported a role for mTOR, p70S6K, and S6 in the regulation of autophagy. Although a recent paper suggests that hAtg1 (hULK1) is a negative regulator of mTORs downstream effector, p70S6K, the strongest data is based on ectopic expression of hAtg1[55]. Recently in *Drosophila*, it was demonstrated that some p70S6K activity was required for maximum autophagic activity[49]. The dilemma of an inactive mTOR and an active p70S6K is difficult to resolve, but it is proposed to be a self-limiting mechanism for autophagy.

mTOR responds to signals from growth receptors through the Class I PI 3-kinase/PKB pathway. Importantly, PTEN and TSC2 are two tumor suppressors on the PI3K/PKB/mTOR pathway that are involved in the regulation of mTOR[56]. In both mammals and *Drosophila*, positive signals through the PI3K/PKB pathway inhibit autophagy and negative signals induce autophagy[57, 58]. Amino acid stimulation of mTOR is independent of the PI3-kinase/PKB pathway[59]. It was recently shown by two laboratories that the amino acid input to the mTOR pathway is through the Class III PI 3-kinase Vps34[36, 37]. This interesting link between mTOR and Vps34 in the response to

amino acids is unexpected, as Vps34 activity is also thought to regulate the induction of autophagy[33]. However, as in yeast, it may be that the regulation of Vps34 occurs through its association with different binding partners. The link between Vps34/Beclin1 and mTOR puts another tumor suppressor, Beclin1, upstream of mTOR in a potential regulatory role. This brings one more layer of complexity and relevance to the pathways regulating autophagy.

1.6. Significance of autophagy

The significance of autophagy in maintaining the health of not just the cell, but the entire organism, is apparent in human disease. In cancer, the importance of maintaining the balance in the mTOR pathway between synthesis and autophagy is striking when one considers the tumor suppressors that keep this pathway in check. The down-regulation of autophagy may be one way that tumor cells use to gain an advantage in growth and proliferation. It suggests that negative regulators of the mTOR pathway may be effective therapeutics for certain types of cancer, and indeed, rapamycin has success in the treatment of renal cancer[60]. However, in certain cases, increased autophagy may actually promote tumor survival in harsh, non-vascular, nutrient-limiting conditions. It's even thought that some tumors are resistant to cell-damaging agents because of autophagy, underscoring the importance of understanding the regulation of this process[61].

While decreased autophagy may tip the scales in favor of cancer in proliferating cells, in differentiated cells, decreased autophagy may instead lead to degeneration and cell death. The selective loss of the autophagy-related genes Atg7 and Atg5 in the neurons of mice results in neurodegeneration with aging[29, 30]. Autophagy has long

been suspected of being involved in degenerative diseases of both the neural and muscular systems because of the appearance of autophagosomes in the post-mortem tissue or biopsies of patients with diseases such as Alzheimer's, Parkinson's, Huntington's, Inclusion-body myositis, and X-linked myopathy with excessive autophagy. These findings suggest that drugs which increase autophagy may be an effective treatment for patients with neurodegenerative disease, and in support of this, preliminary tests show that treatment with rapamycin can increase the autophagy-mediated removal of huntingtin aggregates[62].

Significantly, many of these diseases are associated with aging, and a decrease of autophagic or lysosomal function is thought to be part of the aging process[63]. If true, then more efficient autophagy should retard aging. This is supported by studies in *C.elegans* where loss of signaling to TOR increased longevity, presumably by increasing autophagy[4].

Autophagy can play a more acute role in human pathology by protecting cells from invading intracellular pathogens. Autophagy has recently been described as participating in the innate immune response to some bacteria and viruses. Autophagy can be either friend or foe to microorganisms. Some, such as *Coxiella burnetii* use autophagy to replicate while others such as *Streptococcus pyogenes* are removed from the cytoplasm by autophagy and destroyed[64]. Understanding the difference is likely to be important for therapeutics.

1.7. Thesis focus and significance

This research has focused on understanding the regulation and molecular mechanisms of mammalian macroautophagy. To aid in this study, new methods were

developed to unambiguously measure the induction and inhibition of autophagy. The macroautophagy-specific degradation of BHMT was used to study the importance of higher order structure on the efficiency of autophagic degradation. The data presented here support a hypothesis that modulation of the Class III PI3-kinase pathway may lead to the selective degradation of cargo based on quaternary structure. This is significant in terms of understanding the mechanism that cells use to remove potentially damaging protein aggregates by macroautophagy.

In addition, this study has sought to understand the relationship between mTOR, p70S6 Kinase and macroautophagy. Using the methods developed in the course of this study, the data show that the mTOR-dependent signal to autophagy does not go through p70S6 Kinase or S6. The signal to macroautophagy through other downstream effectors of mTOR is explored. Together, the data here confirm the importance of mTOR in the induction of autophagy and offer new insights into how the modulation of the Class III PI3-kinase and mTOR pathways may affect the clearance of cellular aggregates through macroautophagy.

II. MATERIALS AND METHODS

Cell lines and cell culture

HEK-293, T98G and A10 cells were purchased from ATCC. MCF7 cells were a kind gift of the Moscat-Diaz laboratory at UC/GRI, C2C12, A2780, NIH-3T3 cells from the Thomas-Kozma laboratory at UC/GRI, and H1299 cells from the Kadakia laboratory at WSU. Cells were maintained in a custom-prepared DMEM media, supplemented with 4-6mM final concentration L-glutamine and either 10% fetal calf serum or 10% Nu-Serum I (BD), at 37°C in 5% CO_2.

DMEM custom media (minus glucose, essential amino acids, L-glutamine, and serum) was prepared as follows. For five liters of basic media, combine 1g $CaCl_2$, 2g KCl, 488.5mg $MgSO_4$, 32g NaCl, 625mg NaH_2PO_4, 1ml of 0.5mg/ml $Fe(NO_3)_3$ stock, 5ml of 15mg/ml phenol red stock, 18.5gm $NaHCO_3$, 50ml Pen/Strep 5,000 I.U. Penicillin/5,000 µg/ml streptomycin (Cellgro/Mediatech: MT30-002-CI), 200ml MEM Vitamins 100x solution (Cellgro/Mediatech: MT25-020-CI), 200ml MEM non-essential amino acids (Cellgro/Mediatech: MT25-025-CI) in water, pH to 7.0, and sterile filter. 100mls of a 100x stock of either individual or 10 essential amino acids was prepared in water with the following: 660mg L-phenylalanine, 840mg L-arginine, 952mg L-threonine, 160mg L-tryptophan, 1462mg L-lysine, 300mg L-methionine, 420mg L-histidine, 1050mg L-isoleucine, 940mg L-valine, 1050mg leucine. 50mls of a 200x stock of tyrosine and cysteine was prepared in 1N HCl with 1040mg L-tyrosine and 630gm L-

cystine. A 10x, 250mM glucose solution was prepared in water. All solutions were sterile filtered.

Antibodies and reagents

The following antibodies were purchased from SantaCruz: GST (Z5), HA-probe (Y-11) GFP (FL), p-p70 S6 Kinase (Thr389), Beclin1 (D-18). Antibodies purchased from Cell Signaling include: Myc-Tag (9B11) LC3 (human) antibody (NB 100-2331) was purchased from Novus Biologicals. Leupeptin (Bachem), E64d, chloroquine and 3MA were purchased from Sigma. PMSF (Acros) was purchased from Fisher Scientific.

SDS-PAGE, immunoprecipitation, pull-downs, and western blot

Cells to be extracted were washed with ice-cold PBS and scraped into extraction buffer (EB)(50mM TRIS-HCl pH 8, 120mM NaCl, 5mM NaPPi, 10mM NaF, 30mM paranitrophenylphosphate, 1mM benzamidine, 0.1% NP-40, 0.2mM PMSF). In most cases, 1% Triton-X100 was added to the EB. Extracted cells were homogenized 10 strokes in a Dounce homogenizer and centrifuged to clear the supernatant of cellular debris. Total protein of cell extracts was determined by Bradford method. For whole cell extract (WCE) aliquots, SDS sample buffer was added and sample was boiled for 3 minutes before loading on SDS-PAGE gels. After SDS electrophoresis, protein was electrophoretically transferred to PVDF membrane, blocked with 1% BSA in TBS/Tween 20, incubated with primary antibody diluted in 1% BSA in TBS/Tween 20 overnight at 4°C. Blots were then incubated with either a species-appropriate HRP-conjubated secondary antibody, or with a species-appropriate biotin-conjugated second antibody followed by a HRP-strepavidin conjugate.

Cell fractionation and Sucrose Gradient

PBS-washed cells were scraped from a 10cm culture dish in 1ml of ice-cold PBS and centrifuged at 1000xg for 5 minutes. All steps were carried out at 4°C. The cell pellet was resuspended in 500ul homogenization buffer (HB) (10mM TRIS pH 7.5, 300mM sucrose, 0.2mM EDTA) and disrupted in a Dounce homogenizer with 10 strokes, followed by centrifugation at 540xg to pellet the nucleus and large membrane pieces. The supernatant was reserved in a separate 1.5ml eppendorf tube. The pellet was gently resuspended in an additional 500ul HB, centrifuged at 540xg for 5 minutes, and the supernatant combined with the reserved supernatant from the first spin. The combined supernatant was centrifuged for 12,000xg for 20 minutes to pellet the light membrane fraction (LMF). This pellet was then gently washed x3 with HB and centrifuged 5 minutes each at 12,000xg. The washed pellet was gently resuspended in 50 to 100ul HB for analysis. In some cases, the protein of the LMF was determined by Bradford analysis to normalize loading of sucrose gradients.

Percent sucrose solutions (60%, 45%, 35%, 27.5%, 20%, 15%) were prepared by dissolving sucrose in HB. All preparation steps of gradients were performed with ice-cold solutions and tubes. Discontinuous sucrose gradients were prepared within an hour of use by sequentially layering 1.8ml of 45% sucrose, 2.4ml of 35%, 1.6ml of 27.5%, 1.6ml of 20% and 2.4% of 15% in a 14 x 89mm polyallomer tube. Sample LMF in 1ml of HB was gently layered on top of prepared gradient. Gradients were centrifuged at 200,000xg for 2 hours at 2°C in a Sorvall SV41 rotor. 1ml fractions were collected by displacement, using 60% sucrose as the chase solution. Fractions were numbered with 1 being the top, least dense fraction and 10 the bottom, most dense fraction.

In-vitro Thrombin cleavage assay

Thrombin Protease (Amersham Biosciences 27-0846-01) was diluted in cold PBS to a concentration of 1 unit/ul. For on-bead cleavage, overexpressed GST-fusion protein was pulled out of cell extracts with glutathione agarose beads. Beads were washed with dilution buffer x1 and PBS x1, removing all excess PBS after final wash. 0.5ug of thrombin in 15-20ul of PBS was added to beads and incubated for 2 hours at room temperature. Reaction was stopped with SDS-sample buffer, boiled for 3 minutes and run on SDS-PAGE.

Trypsin Protection Assay

In 10 mM TRIS-HCl pH 7.5, dilute Trypsin-TPCK (Worthington) to 1mg/ml, Soybean Trypsin Inhibitor (STI) (Sigma T-9128) to 2mg/ml, and prepare a separate 1% Triton X-100 solution. To digest extra-vesicular protein, add dilute trypsin to sucrose fraction, incubate 5 minutes at 37°C, and stop with equal volume of STI and 0.1M PMSF. Amount of trypsin was determined experimentally. For digestion of intra-vesicular protein, add 1% Triton X-100 to a final concentration of 0.2%. Proceed as described above. After reaction has been stopped, total protein can be TCA precipitated, or individual tagged proteins can be isolated by affinity chromatography or immunoprecipitation.

Quick-change mutagenesis

Method for mutagenesis was patterned from Stratagene's QuikChange Site-Directed Mutagenesis Kit. Briefly, sense and antisense primers were designed to anneal to the same sequence with the mutated codon in the middle of the primer. Primers were between 25 and 45 bases in length, with a T_m greater than or equal to 78° (T_m=81.5+0.41(%GC)-(675/N)-%mismatch). PCR was performed with primer in excess

of plasmid template (125ng of each primer and 50ng of template) and with an annealing temperature of 55°C or less for 18-24 cycles. DNA polymerases used successfully include rTth DNA Polymerase XL (Applied Biosystems), Platinum Pfx DNA polymerase (Invitrogen) and Deep Vent DNA polymerase (New England Biolabs (NEB)). Dpn1 restriction enzyme (NEB) was added to finished PCR reaction to digest template and the mix was ethanol precipitated and reconstituted with sterile water. Successful production of product was checked on an agarose gel before being transformed into either XL1-Blue or DH5α competent cells.

TCA precipitation

Make a 100% solution of TCA (Fisher A322) in water. Add 100% TCA to dilute protein to a final concentration of 15-20%. Use higher percentage of TCA for smaller proteins. Mix and incubate on ice for a minimum of 2 hours. Centrifuge at 4°C at 12-13,000 xg for 20 minutes to pellet protein. Carefully remove and discard supernatant. Wash pellet x2 with ice-cold acetone. Allow pellet to air dry on ice and resuspend pellet in 1x SDS sample buffer.

Kinase assay

Immunoprecipitated hULK1 was incubated with 5μg MBP, 10mM $MgCl_2$, γ-^{32}P ATP, and reaction buffer (50mM Tris pH 7.5, 10mM NaCl, 1mM DTT, 10% glycerol) at 30º C for 30 min.

qPCR

Cells were detached by trypsin digestion and total RNA was extracted using the NucleoSpin RNAII extraction kit according to manufacturer's instructions. For RT-PCR analysis, 500ng of total RNA was reverse transcribed using ABgene Reverse-IT 1st

Strand Synthesis Kit using random hexamer primers according to manufacturer's recommendation. Conditions of RT-PCR: 70ºC for 5 min; put on ice; add Reverse-IT enzyme; 47ºC 60 min; 75ºC 10min. Final product was diluted 1:10 with nuclease-free water for qPCR. Primer sets for qPCR were purchased from Qiagen. Target genes were normalized to Actin or 18S.

III. RESULTS

3.1. Autophagy Assay Development

3.1.1. Autophagy Conjugation Systems

3.1.1.1. Atg12-Atg5 conjugation

Autophagosome formation requires the recruitment and assembly of autophagy-specific proteins to a pre-existing, or de-novo membrane structure that elongates and eventually fuses to form an enclosed, double-membrane autophagosome. hAtg12 and hAtg5 are covalently linked in an ubiquitin-like posttranslational modification, and then assembled with hAtg16 in a large multimeric complex that coats the convex side of developing autophagosomes. Like the ubiquitin conjugation system, the Atg12-Atg5 system requires the activity of E1- and E2-like enzymes, hAtg7 and hAtg10, which might be regulated by conditions known to induce autophagy[26].

One of the goals of this research project was to develop novel ways to study autophagy, and the hAtg12-hAtg5 conjugate was an attractive target because it was both specific and required for autophagosome formation. Conceptually, it was not unlike another specific marker of autophagosomes, LC3-II, whose levels were already being used to measure autophagy. At the time of this study, there were no reports in the literature on how an increase in autophagy might affect levels or regulation of the hAtg12-hAtg5 conjugate, but it seemed likely that a demand for new autophagosomes might require increased levels of conjugated hAtg12-hAtg5.

Because commercial antibodies were not available for either endogenous hAtg12 or hAtg5, both genes were cloned from a human B-cell cDNA library and subcloned into mammalian expression vectors downstream of the respective epitope tags HA and GST, for which antibodies were readily available. In a subcloning strategy that will be used for multiple reporters in this study, heamagglutinin (HA) epitope-tagged hAtg12 was placed in a bicistronic vector upstream of green fluorescent protein (GFP) under the translational control of an internal ribosome entry site (IRES). In this background, expression of GFP can be used for independent normalization of the upstream reporter gene (Fig. 6A).

HA-hAtg12$_{IRES}$GFP and GST-hAtg5 were co-transfected in HEK293 and maintained for 36 hours to allow for expression of the reporter genes. Cells were placed in either complete media, or media from which essential amino acids and serum had been removed for 4 hours, after which the cells were harvested. Aliquots of cell extract, normalized for protein, were immunoprecipitated with 12CA5 antibody to the HA epitope tag that was fused to HA-hAtg12$_{IRES}$GFP. Protein G purified antibody and attached protein were processed for western blotting with antibodies against GST or HA. Whole cell extracts (WCE) from these samples were processed for western blot and probed with an antibody against GFP. In a separate set of cell extracts, glutathione agarose beads were added to affinity purify GST-Atg5. These pulldowns were prepared for western blotting as above, and probed with antibody against GST.

A band of approximately 100 kDa was observed in the samples that were immunoprecipitated for HA-Atg12, and probed with antibody to GST-Atg5 (Fig. 6B, left, top panel). The 100 kDa band was slightly higher than the 85 kDa predicted molecular weight of the covalently linked fusion-proteins, but is not inconsistent with what is likely

Figure 6. Conjugation of GST-Atg5 and HA-Atg12. A. Schematic of epitope tagged HA-Atg12$_{IRES}$GFP and GST-Atg5. GFP under the translational control of an IRES has been placed downstream of HA-Atg12 to allow for normalization of transfection efficiency. B. Western blot of HEK293 cells co-expressing HA-Atg12 and GST-Atg5. Cells represented in left panel were immunoprecipitated with 12CA5 (anti-HA) and probed with antibody against GST (top) or HA (middle) showing conjugate and unconjugated Atg12. Expression of GFP is in bottom panel. Cells in the right panel were pulled down with glutathione agarose and probed with antibody against GST showing conjugate and unconjugated GST-Atg5.

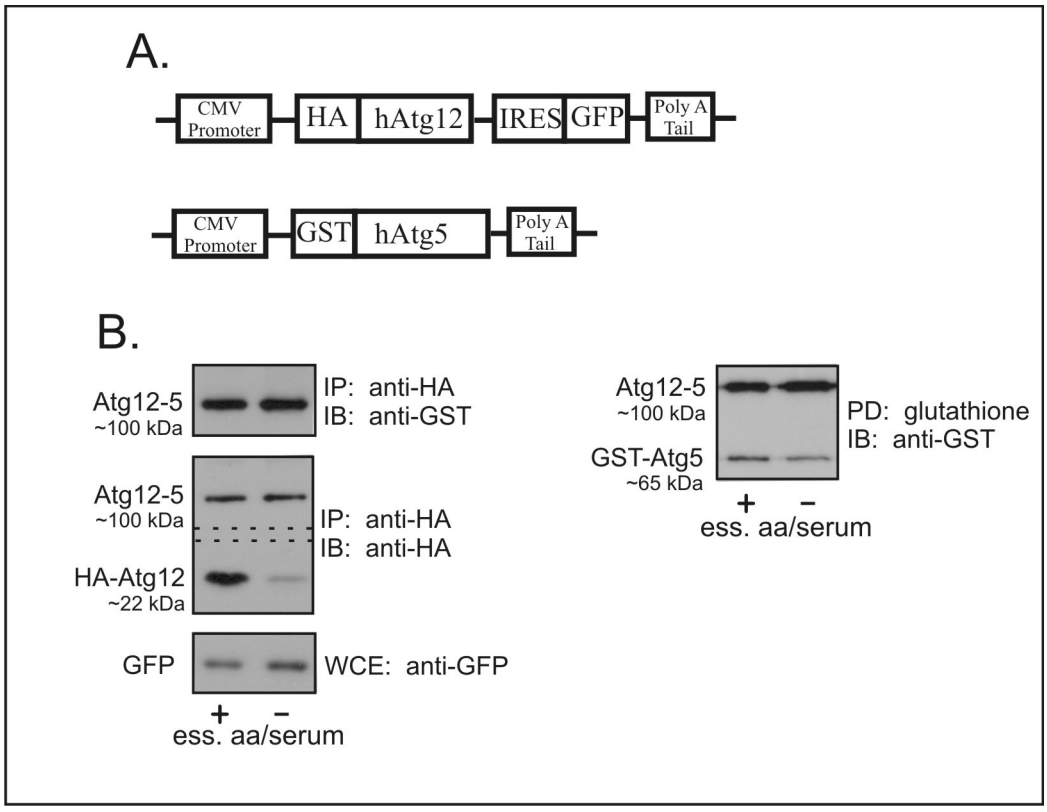
A.
CMV Promoter
HA
hAtg12
IRES
GFP
Poly A Tail
CMV Promoter
GST
hAtg5
Poly A Tail
B.
Atg12-5
~100 kDa
IP: anti-HA
IB: anti-GST
Atg12-5
~100 kDa
HA-Atg12
~22 kDa
IP: anti-HA
IB: anti-HA
GFP
WCE: anti-GFP
+
–
ess. aa/serum
Atg12-5
~100 kDa
GST-Atg5
~65 kDa
PD: glutathione
IB: anti-GST
+
–
ess. aa/serum

the slightly retarded migration of two covalently linked proteins. In support of this, a similar 100 kDa band was seen by western blot in the matched sets of 12CA5 IP samples probed with an antibody against HA for HA-Atg12. A second band at 22 kDa was observed on the blot probed with anti-HA that was likely unconjugated HA-Atg12 (Fig. 6B, left, middle panel). In the samples pulled down with glutathione and probed with antibody toward GST, two bands, one at 100 kDa and one at 65 kDa were found that were consistent with the GST-Atg5/HA-Atg12 conjugate (100 kDa) and with unconjugated GST-Ag5 (65 kDa) (Fig. 6B, right panel). These data show that the epitope-tagged proteins HA-Atg12 and GST-Atg5 were expressed as individual proteins and were competent for the conjugation reaction to form a covalent linkage.

Levels of the 100 kDa conjugated hAtg12-hAtg5 complex did not change when HEK293 cells were starved of essential amino acids and serum, compared to cells in compete media (Fig. 6B, left and right panels). Expression levels of free GST-Atg5 also showed little change in starvation conditions (Fig. 6B, right panel) However, levels of unconjugated HA-hAtg12 dropped significantly with amino acid starvation (Fig.6B, left middle panel). This was not due to differences in transfection efficiency, as expression levels of GFP, the second protein in the bicistronic message of HA-hAtg12$_{IRES}$GFP, were unchanged (Fig. 6B, bottom panel).

Under conditions of amino acid starvation, there is a general arrest of new protein synthesis. In the absence of newly translated protein, there are two possible explanations for the short half-life of unconjugated HA-Atg12. First, it could be conjugated into the covalent complex and consumed in the process of making new autophagosomes, or second, Atg12 may be degraded by another mechanism. Discriminating between the two

was important, because if unconjugated HA-Atg12 decreased due to consumption by the autophagosome-forming process, then HA-Atg12 levels could potentially be used to measure changes in autophagy. Cycloheximide was used to distinguish between the two possibilities because it serves two purposes; cycloheximide inhibits translation like amino acid starvation, and it inhibits autophagy. If decreased levels of Atg12 are due to autophagic consumption, then cycloheximide should protect levels of HA-Atg12 in starved cells. However, if Atg12 is degraded by another mechanism, cycloheximide should not protect levels of Atg12 levels.

HEK293 cells were co-transfected with HA-hAtg12$_{IRES}$GFP and GST-hAtg5. After allowing sufficient time for expression, control cells were incubated in either complete media or starvation media for 4 hours. Cycloheximide was added to a matched set of non-starved and starved cells for the duration of the 4 hour incubation. After harvesting, cell extracts were immunoprecipitated with anti-HA antibody 12CA5, run on SDS-PAGE and processed for western blotting as before. Consistent with previous observations, levels of unconjugated Atg12 were significantly decreased in the amino acid starved control cells (Fig. 7, lane 2). In the cycloheximide-treated cells, levels of HA-Atg12 were not protected in the starved cells and were also significantly decreased in cells maintained in complete media (Fig. 7, lanes 3 and 4). The cycloheximide results suggest that decreased levels of Atg12 in starved cells are not due to autophagic consumption and that degradation of Atg12 is not regulated by nutrients or mitogens.

The cycloheximide result supports the second explanation that Atg12 is likely degraded by another mechanism. Proteasome degradation is a major route for the removal and degradation of proteins. To test if Atg12 is degraded by the proteasome,

Figure 7. Levels of unconjugated HA-Atg12 in amino acid starved HEK293 cells. Western blot: HEK293 cells co-expressing HA-Atg12$_{IRES}$GFP and GST-Atg5 in complete media (lane 1), starvation media (land 2), and complete and starvation media with cycloheximide (lanes 3 & 4). Levels of unconjugated HA-Atg12 are not protected by cycloheximide. Conjugate levels do not change.

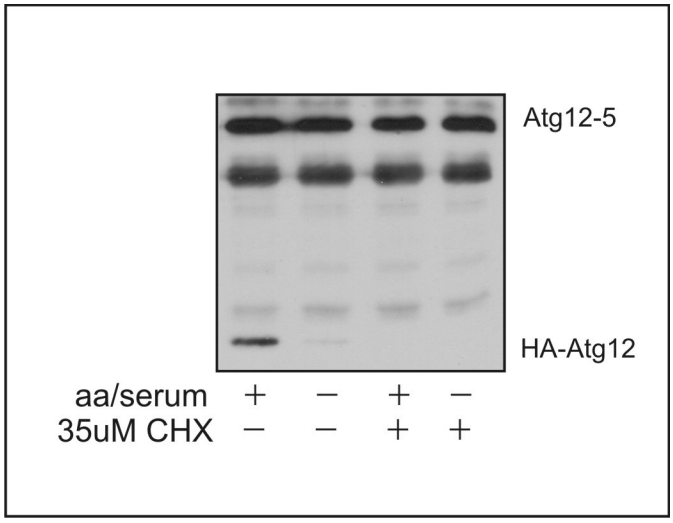
Atg12-5
HA-Atg12
aa/serum + − + −
35uM CHX − − + +

Figure 8. Unconjugated HA-Atg12 is degraded by the proteasome. Western blot: HEK293 cells co-expressing HA-Atg12$_{IRES}$GFP and GST-Atg5 were treated to conditions of complete media (lane 1), starvation media (lane 2), and starvation media with the proteosome inhibitor 20μm MG132 (lane 3). Levels of free Atg12 are protected in starved cells treated with MG132, suggesting degradation of Atg12 is proteasomal.

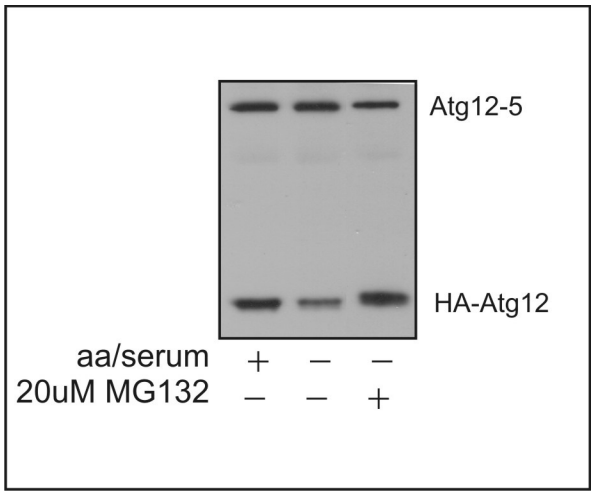
Atg12-5
HA-Atg12
aa/serum + – –
20uM MG132 – – +

HEK293 cells expressing both HA-Atg12$_{IRES}$GFP and GST-Atg5 were treated to conditions of complete media, amino acid and serum-depleted media, or starvation media with the proteasome inhibitor MG132. Levels of HA-Atg12 were completely protected by MG132 in starved cells (Fig. 8), confirming that levels of unconjugated HA-Atg12 are due to proteasome degradation and not consumption by the autophagic machinery. In all of these conditions, levels of the hAtg12-hAtg5 conjugate did not change (Figs. 7 & 8).

These results demonstrate that levels of the hAtg12-hAtg5 conjugate or of unconjugated HA-hAtg12 are not suitable readouts for the induction of autophagy. However, the stability of the hAtg12-hAtg5 complex in all conditions tested, the short half life of unconjugated hAtg12, and the potential role of the proteasome in regulating hAtg12 cytoplasmic levels are findings that may have physiological relevance.

3.1.1.2. LC3 conjugation

LC3-II has been extensively used as a marker of autophagosomes, both by western blotting and by fluorescent microscopy with a GFP-tagged LC3 reporter[20]. The specificity of the LC3 assay makes it a valuable tool to verify autophagosome formation and to validate that the lysosomal degradation pathway is macroautophagy.

At the beginning of this study, antibodies for endogenous LC3 were not yet available, and in a strategy similar to the one used for hAtg12, LC3 was cloned from a human B-cell cDNA library and subcloned into a mammalian expression vector with HA and myc epitope tags at the amino and carboxy termini respectively. The myc epitope tag at the carboxy-terminus of LC3 was added to slow the electrophoretic mobility of the proform of LC3 on SDS-PAGE to allow for better separation from LC3-I. A similar strategy had been successfully used with rat LC3, one of the first mammalian Atg8

orthologs identified[20]. It was expected that three forms of human LC3 would be seen on SDS-PAGE similar to rat LC3: the slowest migrating proform, the middle cleaved form, LC3-I, and the fastest migrating form with conjugated lipid, LC3-II. A year after LC3 was cloned, a study would report that humans have at least three different isoforms of LC3: LC3A, LC3B and LC3C. The LC3 in the tagged reporter was determined to be LC3B.

HA-LC3B-myc was transfected into HEK293 cells which were maintained for approximately 36 hours to allow for expression. Cells were washed into either fresh complete media or media deficient in essential amino acids and serum and incubated for four hours to induce autophagy. After harvesting, aliquots of cell extracts were normalized for equal protein, immunoprecipitated with an antibody to the HA epitope tag, and processed for western blotting with an antibody against HA. Three forms of LC3B, pro-LC3B, LC3B-I and the lipidated LC3B-II, were seen by western blot analysis (Fig. 9A). However, in contrast to the three bands seen with epitope tagged-LC3B and rat LC3, published immunoblots of human and mouse LC3 usually showed LC3-I and LC3-II, but not pro-LC3. Sequence analysis of the B-cell cloned LC3B reporter revealed two abnormalities. Specifically, an arginine was deleted from the central region of LC3B (ΔR) and an additional nine amino acids were inserted at the carboxy-terminus (+9aa) after the conserved TFG-glycine necessary for lipid conjugation (Fig. 9A).

The mutant HA-LC3B-myc reporter was tested for its response to known inhibitors of macroautophagy, 3MA and chloroquine (see Table 2). The autophagy and PI3K inhibitor 3MA is thought to block macroautophagy early in the formation of

Figure 9. Mutant HA-LC3B-myc reporter. A. The mutant HA-LC3B-myc reporter has an additional nine amino acids near the carboxy-terminus (in red), and a deletion of three nucleotides that code for an arginine (ΔR), also in red. Western blot is shown of mutant LC3B reporter in plus and minus amino acid conditions. B. The mutant LC3B reporter is shown in minus amino acid conditions (lane 1), and with autophagy inhibitors 10mM 3MA (lane 2) and 100μM chloroquine (lane 3). C. Restoration of the deleted arginine (R68/R69) of LCB3, with the '+9aa' insertion intact, yields a reporter that processes LC3B to LC3B-I and LC3B-II in a manner like endogenous or HA-tagged wild type LC3B (western blot)

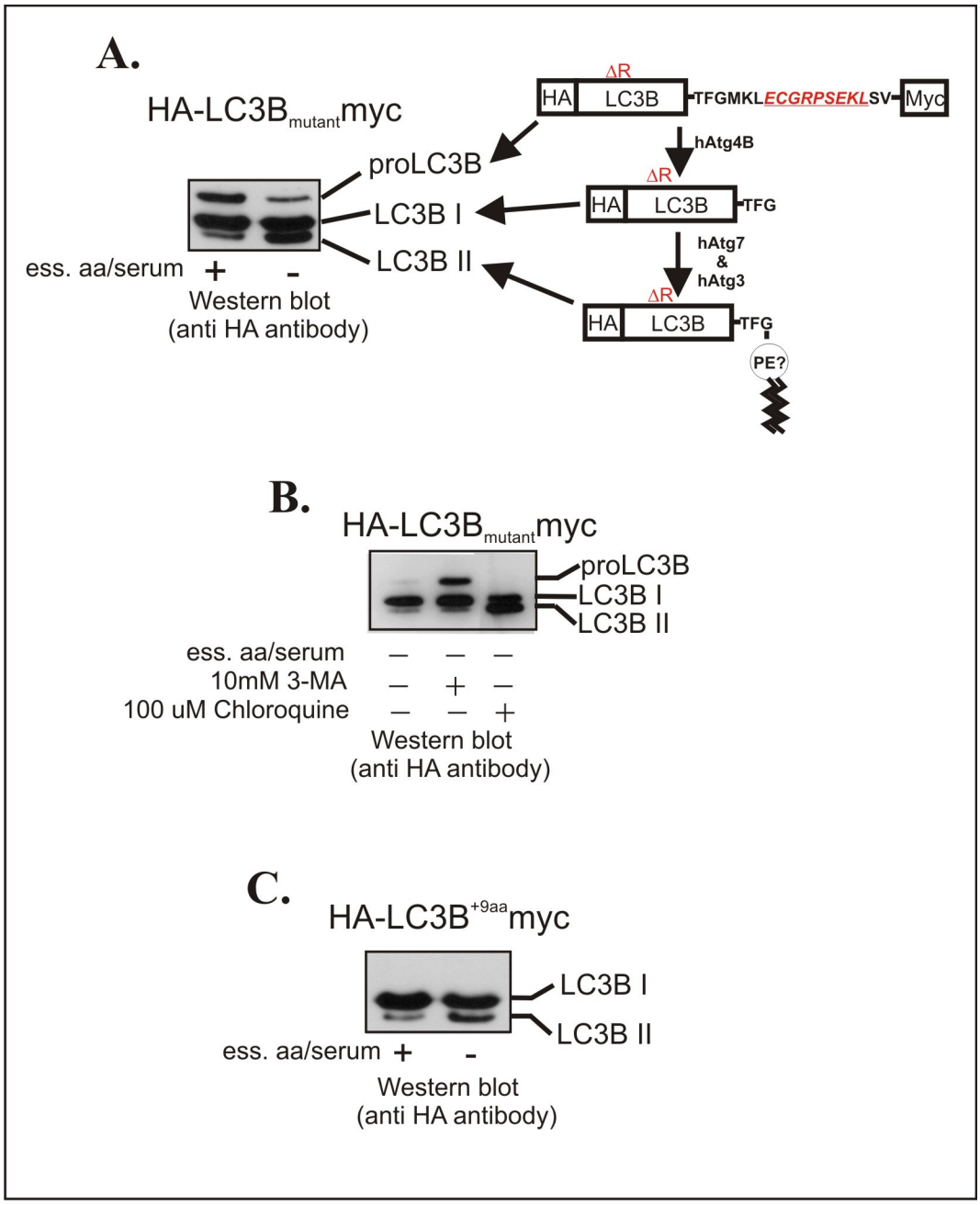
A.
HA-LC3B$_{mutant}$myc
ΔR
HA
LC3B
TFGMKLECGRPSEKLSV
Myc
hAtg4B
proLC3B
LC3B I
LC3B II
ess. aa/serum + -
Western blot
(anti HA antibody)
TFG
hAtg7
&
hAtg3
PE?
B.
HA-LC3B$_{mutant}$myc
proLC3B
LC3B I
LC3B II
ess. aa/serum — — —
10mM 3-MA — + —
100 uM Chloroquine — — +
Western blot
(anti HA antibody)
C.
HA-LC3B^{+9aa}myc
LC3B I
LC3B II
ess. aa/serum + -
Western blot
(anti HA antibody)

Table of pharmacological agents used in this study

	Type	Action and uses
3MA	PI3 Kinase inhibitor (Class III)	Thought to inhibit VPS34 at early step in autophagosome formation
bafilomycin A1	Vacuolar-type H+-ATPase inhibitor	Inhibits fusion of lysosomes & autophagosomes
chloroquine	lysomotrophic agent, increases lysosomal pH	Inhibits fusion of lysosomes & autophagosomes
cycloheximide	Inhibits translation elongation	Inhibits translation and autophagy
E64d	Inhibits cysteine proteases & calpains	Used to inhibit lysosomal cathepsins
leupeptin	Inhibits trypsin-like and cysteine proteases	Used to inhibit lysosomal cathepsins
MG132	Proteasome inhibitor	Reduces degradation of ubiquitin-conjugated proteins
pepstatin	Inhibits acid proteases	Used to inhibit lysosomal cathepsins
puromycin	Inhibits translation elongation	Inhibits translation and autophagy
rapamycin	Forms complex with FKBP12 to inhibit TOR	Inhibits mTOR, effects translation initiation, induces autophagy
vinblastine	Binds and disrupts microtubules	Inhibits membrane trafficking
W7	Calmodulin antagonist	Inhibits Ca+-calmodulin dependent signaling
wortmannin	PI3 Kinase inhibitor (Class I and Class III)	Thought to inhibit VPS34 at early step in autophagosome formation

Table 2. List of pharmacological agents. Drugs used in this study are listed in alphabetical order, with the pharmacological action and uses of each.

autophagosomes, although the exact mechanism is not known. Chloroquine blocks macroautophagy by preventing acidification of the lysosome and fusion, while allowing for the formation of autophagosomes. Large numbers of autophagosomes have been observed to accumulate with the use of chloroquine. After sufficient time to allow for expression, HEK293 cells transiently transfected with mutant HA-LC3B-myc were treated for four hours with complete media, starvation media, and starvation media with either 10mM 3MA or 100μM chloroquine. After harvesting, aliquots of cell extracts were immunoprecipitated with anti-HA antibody and processed for western blotting as before. The cells starved for amino acids and treated with 100μM chloroquine showed a strong accumulation of LC3B-II was seen as expected (Fig. 9B, lane 3). Interestingly, 3MA treatment resulted in a significant increase in the proform of LC3B (Fig. 9B, lane 2), suggesting that 3MA affected early LC3B processing.

The effect of 3MA on LC3B proform processing led to the investigation of which mutation, the ΔR deletion or the nine amino acid insertion, was responsible for the delayed cleavage. The abundance of the pro-form in the mutant LC3B suggests that its cleavage by Atg4B is impaired, although not completely inhibited. It was reasoned that the ΔR deletion (of R68 or R69) might affect cleavage by Atg4B because of its proximity to phenylalanine 80 (F77 in yeast), an amino acid essential for Atg4 binding and activity in yeast[65]. The R68 and R69 residues are highly conserved between Atg8 orthologs and species, making the importance of this region likely (Table 3). Alternatively, the proximity of the nine amino acid (+9aa) insertion to the glycine where Atg4B-mediated cleavage must occur might partially inhibit the activity of the protease. In order to determine which mutation was affecting LC3B processing, the mutant LC3B reporter was

				68	69				
hLC3B	K	I	I	**R**	**R**	R	L	Q	L
hLC3A	K	I	I	**R**	**R**	R	L	Q	L
hLC3C	S	I	I	**R**	**S**	R	M	V	L
hGABARAP-I	F	L	I	**R**	**K**	R	I	H	L
hGABARAP-II	F	L	I	**R**	**K**	R	I	H	L
hGATE-16	W	I	I	**R**	**K**	R	I	Q	L
Mouse LC3 alpha	K	I	I	**R**	**R**	R	L	Q	L
Rat LC3 alpha	K	I	I	**R**	**R**	R	L	Q	L
Drosophila Atg8a	F	L	I	**R**	**K**	R	I	H	L
Drosophila Atg8b	F	L	I	**R**	**K**	R	I	N	L
C.elegans lgg1	F	L	I	**R**	**K**	R	I	Q	L
C.elegans lgg2	S	I	V	**R**	**R**	R	L	Q	L
C.elegans lgg3	L	K	L	**R**	**K**	L	L	L	N
Dictyostelium Atg8	Y	E	I	**R**	**K**	H	M	T	K
S. cereviseae Atg8	Y	V	I	**R**	**K**	R	I	M	L
Arabidopsis	Y	I	L	**S**	**A**	R	L	H	L

Table 3. Sequence alignment of Atg8 orthologs. Basic residues that correspond to LC3B R68 and R69 are highly conserved.

repaired in a way that reinserted the arginine but left the '+9aa' insertion intact, so that the newly created HA-LC3B^{+9aa}myc mutant could be tested for expression by western blotting. HA-LC3B^{+9aa}myc was transiently transfected in HEK293 cells, and after sufficient time to allow for expression, washed into either complete or starvation media for four hours. Cell extracts normalized for equal protein were prepared for western blotting as described. Only the processed forms of the HA-LC3B^{+9aa}myc mutant, LC3B-I and LC3B-II, were observed by western blot, similar to other published reports of human LC3 (Fig. 9C). Although only a wild type or endogenous LC3 will be used in subsequent studies, the mutant LC3B construct is a unique reporter that may prove useful in future studies involving the early processing steps of LC3B.

To facilitate studies which utilize the HA-LC3B-myc reporter, an HA epitope-tagged wild-type LC3B-myc allele was made and stably integrated into HEK293 cells. Expression levels of the stable LC3B reporter are lower than the transiently over-expressed LC3B reporter, and were later found to be roughly equal to that of endogenous LC3 (data not shown). HA-LC3B^{wt}myc$_{4.1H}$ stably expressed in HEK293 cells has the benefit of an epitope tag without issues of variable transfection efficiency. HEK293 cells stably expressing HA-LC3B^{wt}myc$_{4.1H}$ were tested with either complete or starvation media for 4-5 hours. Cell extracts were collected and processed for western blot as before. The stably expressing HA-LC3B demonstrated increased LC3B-II levels with amino acid and serum starvation (Fig. 10A). However, unlike the transient reporter, levels of LC3B-I decreased in cells starved of amino acids. The decrease in LC3B-I is consistent with published reports of endogenous LC3-I and with early interpretations of the LC3 assay that rely on ratios of LC3-II/LC3-I to measure autophagy.

Figure 10. MG132 partially protects levels of LC3B-I in starvation conditions. A. HEK293 cells stably expressing HA-tagged wild-type LC3B-myc in complete media (lane 1) and starvation media (lane 2). B. HA-LC3B^{wt}myc$_{4.1H}$ stable cells in complete media (lane 1), starvation media (lane 2) and with the proteosome inhibitor MG132 (20μM) (lanes 3&4).

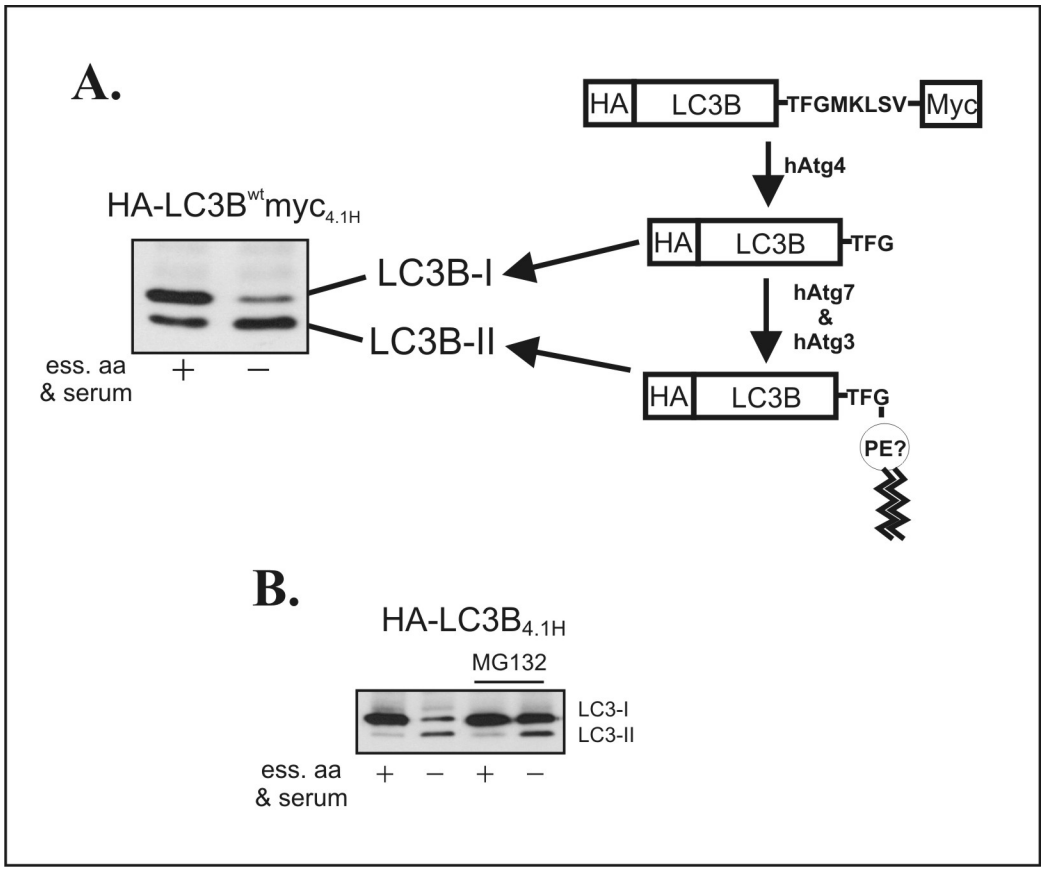
A.
HA
LC3B
TFGMKLSV
Myc
hAtg4
HA-LC3B^wtmyc4.1H
HA
LC3B
TFG
LC3B-I
hAtg7
&
hAtg3
LC3B-II
ess. aa
& serum
+
–
HA
LC3B
TFG
PE?
B.
HA-LC3B4.1H
MG132
LC3-I
LC3-II
ess. aa
& serum
+
–
+
–

Concerning the use of ratios, to interpret results from the LC3B assay, both a decrease in LC3B-I and an increase in LC3B-II are considered. This makes a starvation induced decrease in LC3B-I an important aspect of the LC3B assay. Although not generally accepted, some researchers have even interpreted decreased LC3-I levels alone as evidence of increased autophagy[66]. There are two possible interpretations to explain why LC3B-I levels decrease with starvation. The first, and most obvious, is that in the absence of new protein synthesis, LC3B-I levels drop as it is processed to LC3B-II when cells need more autophagosomes. The second is that LC3B-I, like unconjugated HA-Atg12, may be proteasomally degraded independent of conversion to LC3B-II. To test the latter, HEK293 cells stably expressing HA-LC3B^{wt}myc$_{4.1H}$ were incubated in complete or starvation media for four hours, either with or without the proteasome inhibitor MG132. Unexpectedly, levels of LC3B-I in starved cells were partially protected by MG132. In contrast, MG132 had no effect on LC3B-I in full media, and did not change levels of LC3B-II in either plus or minus amino acid media (Fig. 10B). This indicates that little LC3B-I was degraded proteasomally in conditions of complete media, and that LC3B-II was also not degraded proteasomally, as one might predict for a protein attached to a membrane degraded in the lysosome. However, the MG132 data showing protection of LC3B-I in minus amino acid media reveal that at a percentage of LC3B-I may be degraded proteasomally under autophagy-inducing conditions. Therefore, decreased levels of LC3B-I do not necessarily reflect conversion to LC3B-II and must be used cautiously in conjunction with LC3B-II to interpret levels of autophagy.

The stably expressing HA-LC3B-myc$_{4.1H}$ was tested under conditions known to inhibit autophagosome degradation. Chloroquine and bafilomycin A1 both inhibit

autophagy by increasing lysosomal pH to block fusion of lysosomes with autophagosomes. The block of fusion causes an accumulation of autophagosomes and an increase in LC3B-II levels. HEK293 cells stably expressing the HA-LC3B-myc reporter were starved of essential amino acids for 5 hours, with or without 100μM chloroquine or 100nM bafilomycin A1. After extraction, aliquots of cell extracts were normalized for protein concentration, immunoprecipitated with antibody to HA, and processed for western blotting. In the chloroquine and bafilomycin A1 treated cells, the accumulation of LC3B-II was much greater than that of control cells (Fig. 11), which was expected with strong lysosomal inhibition. However levels of accumulated LC3B-II in the inhibitor-treated cells were essentially the same in complete media as in media depleted of essential amino acids and serum (Fig. 11). The accumulation of LC3B-II in complete media was surprising because one would expect that more LC3B-II would accumulate in starved cells. In control cells, the increase of LC3B-II in starvation media was slight. The data show that LC3B-II levels reach a limit where no more is produced under plus amino acid and minus amino acid conditions. Without the lysosomal inhibitors, the accumulation of LC3B-II is largely determined by its rate of degradation. And surprisingly, LC3B-II is actively produced and degraded in the presence of amino acids and serum.

These finding raise questions about the induction of autophagosome formation. Does amino acid and serum starvation cause an actual increase in the rate of LC3B-II production? And is there a way to inhibit the lysosome to give optimal accumulation of LC3B-II when under starvation conditions? Since blocking lysosomal proteolysis and autophagosome fusion causes an accumulation of LC3B-II, it should be possible to see

Figure 11. LC3B-II with lysosome inhibitors. HEK293 cells stably expressing HA-LC3B^{wt}myc$_{4.1H}$ were incubated in complete and starvation media (lanes 1 & 2) with 100μM chloroquine (lanes 3 & 4) or 100nM bafilomycin A1 (5 & 6). LC3B-II levels in complete media approaches or reaches levels in starvation media, as seen by western blotting.

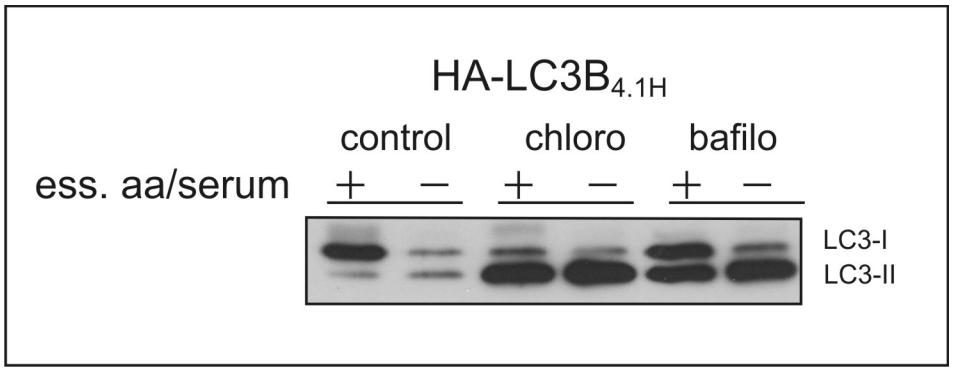
HA-LC3B4.1H
control
chloro
bafilo
ess. aa/serum
+ − + − + −
LC3-I
LC3-II

differences in rates of LC3B-II accumulation at early time points of lysosomal inhibition. To test this, HEK293 cells stably expressing the HA-LC3B-myc construct were pre-strong lysosomal block, and subsequently extracted at time points ranging from zero to starved for sixty minutes without inhibitors, then treated with 100μM chloroquine for a four hours. LC3B-II levels accumulated faster in starved cells compared to cells cultured in full media, consistent with amino acid and serum starvation inducing the synthesis of LC3B-II (Fig. 12A). The early time points of 20 and 40 minutes provided the most sensitive window to differentiate between LC3B-II levels in plus vs. minus amino acid conditions. Beyond that time, the difference between complete media and starvation media rapidly narrowed until LC3B-II levels reached a plateau with no detectable difference between the two treatments, consistent with the previous result (Fig. 11). The reason for this plateau effect is not known, but could be explained by a self-limiting mechanism that prevents excessive autophagosome formation. From this data, starvation induced increases in LC3B-II can be seen only at early time points under conditions of strong lysosomal inhibition.

Although a chloroquine time course was helpful in visualizing changes in autophagic induction, the window of differentiation was small in that the accumulated LC3B-II rapidly reached maximum levels with or without amino acids. In order to see changes in autophagy at long time points, it was tested whether partial inhibition of lysosomal degradation would allow for the accumulation of LC3B-II while still allowing its breakdown. In this way, a stronger LC3B-II signal could be observed while maintaining the ability to see regulation of LC3B-II at short and long time points. To test this, HEK293 cells stably expressing the HA-LC3B reporter were treated with decreasing

Figure 12. Lysosome inhibitors can validate LC3B-II induction and flux. A. Time course experiment of LC3B-II accumulation with 100μM chloroquine. At 120 minutes, levels of LC3B-II in plus and minus amino acid media are equal. B. Chloroquine dose response experiment. At lower doses, chloroquine controls autophagosome flux and increases the sensitivity of the LC3B-assay at longer time points. (western blot)

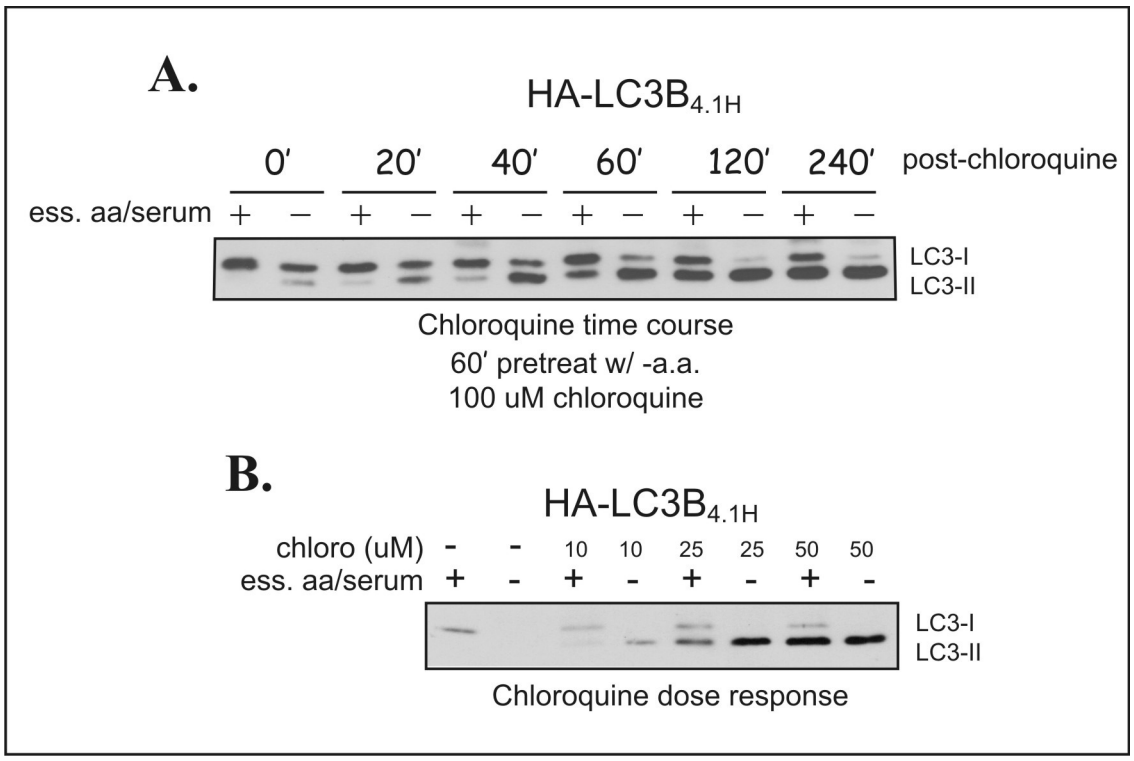
A.
HA-LC3B4.1H
0′
20′
40′
60′
120′
240′
post-chloroquine
ess. aa/serum + − + − + − + − + − + −
LC3-I
LC3-II
Chloroquine time course
60′ pretreat w/ -a.a.
100 uM chloroquine
B.
HA-LC3B4.1H
chloro (uM) - - 10 10 25 25 50 50
ess. aa/serum + - + - + - + -
LC3-I
LC3-II
Chloroquine dose response

conditions. At lower doses of 10μM and 25μM chloroquine, differences in LC3B-II levels between the two conditions were apparent (Fig. 12B). In principle, weak lysosomal inhibition enhances the sensitivity of the LC3B assay, without sacrificing the ability to see regulation by amino acid availability.

While chloroquine was useful, its potency occasionally made it difficult to correctly dose without reaching maximum LC3B-II accumulation. Chloroquine raises lysosomal pH, affecting many lysosomal hydrolases. Specific protease inhibitors may be less severe but still give the required result. E64d, combined with either leupeptin or pepstatin A, has been used in the literature as an effective inhibitor of lysosomal cathepsins. HEK293 cells stably expressing the HA-LC3B^{wt}myc$_{4.1H}$ reporter were treated with leupeptin and E64d, or pepstatin A and E64d, in either complete or starvation media for 5 hours. Control cells stably expressing HA-LC3B were incubated in either plus or minus amino acid media without inhibitors. HA-LC3B was immunoprecipitated from cell extracts and prepared for western blotting. Both leupeptin/E64d and pepstatin A/E64d were successful in increasing the window of sensitivity of the LC3B assay compared to control cells (Fig. 13) without the problem of maximal accumulation. This demonstrates that protease inhibitors can be successfully used for long time periods to control autophagosome flux and increase the sensitivity of the LC3B assay.

The experiments presented here emphasize some of the advantages and disadvantages of using a midpoint assay. In light of the current knowledge of LC3, LC3-II unquestionably has value for its specificity for autophagosomes. However, the transient nature of autophagosomes and the lack of specific knowledge of regulation of events at either formation or degradation, make correct interpretation difficult.

Figure 13. Protease inhibitors can control LC3B-II flux. HEK293 cells stably expressing HA-LC3B-myc were treated with leupeptin (10.0μM) + E64d (5.8μM) or pepstatin A (14.6 μM)+ E64d (29.2 μM) for five hours. This increases sensitivity of LC3B-II assay to flux. (western blot)

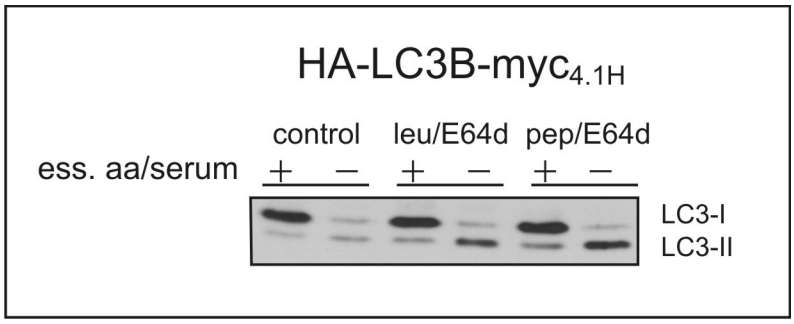
HA-LC3B-myc4.1H
control
leu/E64d
pep/E64d
ess. aa/serum
+ − + − + −
LC3-I
LC3-II

3.1.2. The BHMT assay

3.1.2.1. Assay development and pharmacological validation

Macroautophagy is a multi-step, biological process. The LC3 assay and electron microscopy (EM) are both valuable tools to semi-quantitatively assess levels of autophagosomes, but alone, they are inadequate to determine rate or level of autophagy. Optimally, one must consider delivery of cargo to the lysosome and its subsequent degradation. The importance of the lysosomal endpoint is widely acknowledged, and researchers in mammalian autophagy have developed biochemical methods to measure the degradation of long-lived proteins as a group[67]. However, these methods are neither sensitive nor specific for macroautophagy. One goal of this research was to develop and validate a functional, biochemical endpoint assay that would be reproducible, specific, and sensitive for macroautophagy. Ideally, this assay would measure the vesicular uptake, delivery and lysosomal degradation of cytoplasmic cargo. In a literature search to find proteins that might be useful in an autophagy endpoint assay, betaine homocysteine methyltransferase (BHMT) emerged as a promising candidate. BHMT, a metabolic, cytosolic enzyme in high abundance in liver and kidney, was identified by mass spectrometry as a protein that associated with purified autolysosomes in rat liver [68]. Although the authors were searching for autophagosome-specific membrane proteins, its presence in autolysosomes was likely due to engulfment as autophagosome cargo. In support of this, a specific carboxy-terminal degradation fragment of BHMT was found only within the lumen of leupeptin-treated rat autolysosomes. The authors concluded that a leupeptin-resistant cathepsin was able to

cleave BHMT to produce a discrete, 32kDa, lumenal fragment that could be visualized on SDS-PAGE.

Based on these observations, a BHMT plasmid-based autophagy reporter assay was developed for use in cell culture. In concept, the assay would measure levels of a BHMT lysosomal fragment similar to the one found in rat autolysosomes. In addition, if autophagic flux was high, levels of full-length BHMT might also be expected to decrease with increased autolysosomal consumption. The BHMT reporter was created using a subcloning strategy that fused a slightly truncated human BHMT cDNA downstream of a glutathione S-transferase (GST) epitope tag and upstream of a small epitope myc tag (Fig. 14A). This allowed for easy enrichment of full-length GST-BHMT and GST-fused fragments with glutathione agarose. Since commercial antibodies to the GST epitope tag were readily available, GST-BHMT and GST-fused fragments of BHMT could then be easily visualized on a western blot.

To determine if the chimeric GST-BHMT-myc would be a suitable reporter, it was necessary to 1) determine if GST-BHMT-myc, like rat BHMT, had a leupeptin-insensitive proteolytic cleavage site that could be seen by western blotting, and 2) test if degradation could be induced under conditions known to initiate macroautophagy. The GST-BHMT-myc reporter was transiently transfected into HEK293 cells and maintained in culture for 24-48 hours to allow for expression. HEK293 cells expressing GST-BHMT-myc were incubated for five hours under various media conditions previously shown to induce autophagy, such as amino acid deprivation and/or serum starvation. Aliquots of cell extracts, normalized for total protein, were incubated at 4ºC with glutathione agarose to purify and enrich GST-tagged BHMT and BHMT fragments

Figure 14. Leupeptin-dependent generation of GST-BHMT fragments. A. Schematic of the plasmid-based BHMT reporter, with a glutathione S-transferase (GST) epitope tag at the amino-terminus and a myc epitope tag at the carboxy-terminus. B. GST-BHMT fragmentation requires the protease inhibitors leupeptin (10ug/ml) and E64d (2ug/ml) (lanes 5-8 vs. 1-4). Levels of BHMT fragments increase in media depleted of 12 essential amino acids (lanes 7 and 8). Serum starvation does not increase levels of fragment 1 (lane 6 compared to lane 5, and lane 8 compared to lane 7). All data shown is obtained by glutathione pulldown and western blotting.

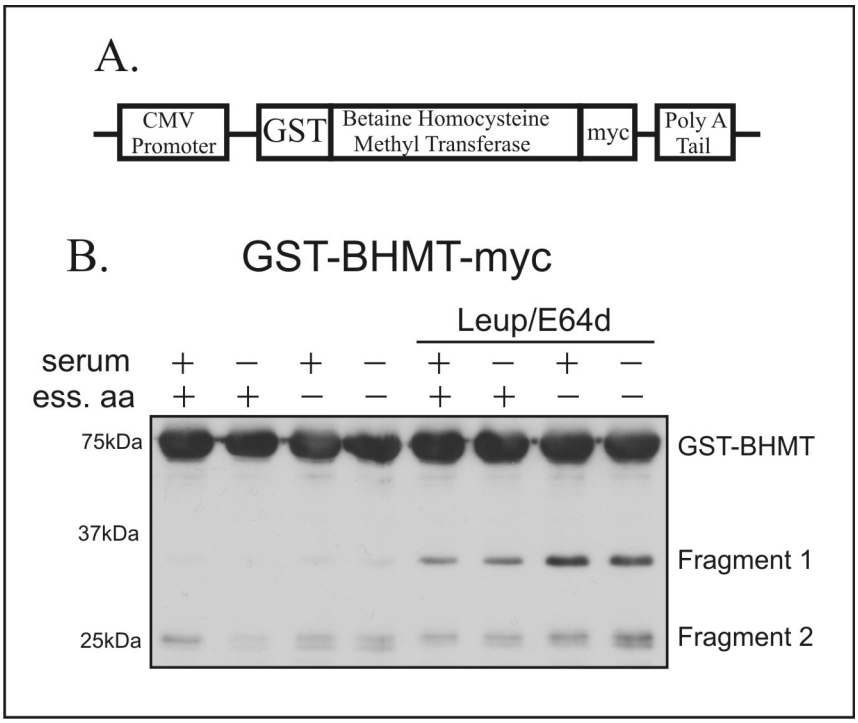
A.
CMV Promoter
GST
Betaine Homocysteine Methyl Transferase
myc
Poly A Tail
B.
GST-BHMT-myc
Leup/E64d
serum + − + − + − + −
ess. aa + + − − + + − −
75kDa
37kDa
25kDa
GST-BHMT
Fragment 1
Fragment 2

which were run on SDS-PAGE and probed with an antibody to GST. To test for GST-BHMT fragmentation, half of the cells received the protease inhibitors leupeptin and E64d. Leupeptin and E64d were chosen because they were both used to observe accumulation of BHMT fragmentation in the original study by Ueno et al[68]. In addition, the leupeptin/E64d cocktail has already been shown to have a modest, controlled effect on LC3B processing and thus on macroautophagy in the current study (see Fig. 13). It was expected that the proteases would slow the autophagic process to a rate that would allow the accumulation of partial degradation products within the autolysosome. If human GST-BHMT was proteolytically cut in a region similar to rat BHMT, generation of a fragment of approximately 35 kDa on SDS-PAGE was expected.

Consistent with these expectations, a fragment of approximately 35 kDa, labeled fragment 1, was observed on western blot in the leupeptin/E64d treated cells that was not seen in cells without protease inhibitors (Fig. 14B, lanes 5-8 compared to lanes 1-4). A second fragment, labeled fragment 2, was noted at 25 kDa which was the approximate size of either endogenous GST or of the epitope GST tag. Significantly, accumulation of the 35 kDa fragment increased in the absence of essential amino acids (Fig. 14B, lanes 7&8). Serum starvation alone, or in combination with essential amino acid starvation, did not alter the accumulation of fragment 1 (Fig. 14B, compare lanes 5 and 6, and lanes 7 and 8). These data show that BHMT fragmentation occurs in response to the specific removal of amino acids rather than serum. To see changes in the GST-BHMT fragments, it is necessary to partially inhibit macroautophagy with protease inhibitors. In all subsequent BHMT experiments, unless otherwise noted, leupeptin and E64d have been added to the media to visualize fragmentation. In addition, although serum deprivation

had no effect on induction of macroautophagy, the starvation media used to induce autophagy is generally deficient in both amino acids and serum for experimental convenience.

Expression of GST-BHMT requires the transient transfection of the expression plasmid. To compare levels of BHMT fragments between experimental conditions, it is necessary to normalize for differences of transfection efficiency. Normalization to the expression of the full length GST-BHMT-myc protein is not preferred because of its degradation during active autophagy. To address the issues of transfection efficiency and independent normalization of GST-BHMT, a bicistronic message under the control of a single CMV promoter was created by placing GFP downstream of GST-BHMT under the translation control of an IRES (Fig. 15A).

To validate that the generation of GST-BHMT fragments was due to macroautophagy, HEK293 cells were transiently transfected with the GST-$BHMT_{IRES}$GFP construct, and 48 hours later starved from serum and essential amino acids in the presence or absence of a panel of inhibitors known to inhibit macroautophagy; 3MA, wortmannin, bafilomycin A1, and puromycin. Wortmannin and 3-methyladenine (3MA) are PI3 Kinase inhibitors that are thought to inhibit autophagy through their inhibition of the Class III PI3 Kinase, Vps34. Bafilomycin A1, a potent inhibitor of the vacuolar H^+ ATPase (V-ATPase), prevents acidification of the lysosome and lysosome-fused vesicles. Puromycin, like cycloheximide, is an inhibitor of translation and autophagy. To exclude a role of the proteasome in the fragmentation of BHMT, the proteasome inhibitor MG132 was included in the panel of inhibitors. Each of the autophagy inhibitors prevented the accumulation of BHMT fragment 1 and fragment

Figure 15. The original BHMT assay with pharmacological inhibitors. A. Schematic of the GST-BHMT-$_{IRES}$GFP reporter plasmid. Placement of an IRES-GFP downstream of GST-BHMT in a bicistronic message allows for independent normalization of transfection efficiency. B. The BHMT assay. Fragmentation of GST-BHMT increases with amino acid and serum starvation and is inhibited with the macroautophagy inhibitors, 10mM 3MA, 100nM wortmannin, 100nM bafilomycin A1, and 50μM puromycin. The proteosome inhibitor MG132 does not effect fragmentation. All data shown is obtained by glutathione pulldown and western blotting.

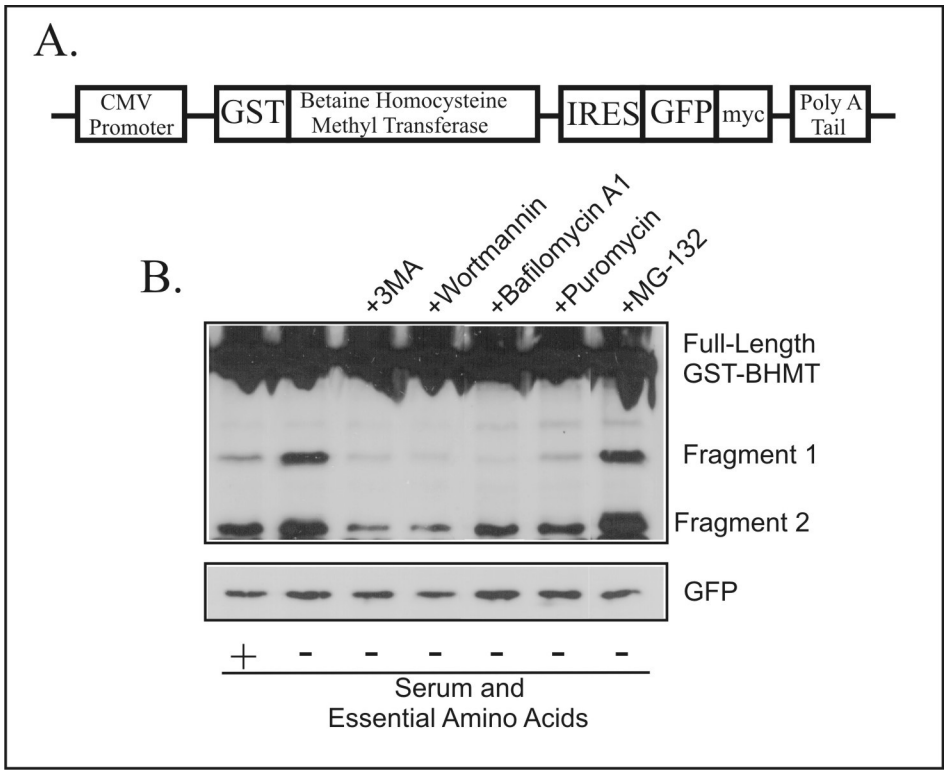
A.
CMV Promoter
GST
Betaine Homocysteine Methyl Transferase
IRES
GFP
myc
Poly A Tail
B.
+3MA
+Wortmannin
+Bafilomycin A1
+Puromycin
+MG-132
Full-Length GST-BHMT
Fragment 1
Fragment 2
GFP
+ - - - - - -
Serum and Essential Amino Acids

2. As expected, the proteasomal inhibitor MG132 had no effect (Fig. 15B, lanes 3 to 7). These data provide pharmacological validation that the GST-BHMT proteolytic fragments are generated through macroautophagic delivery of GST-BHMT to the lysosome.

Although levels of BHMT fragment 1 were consistently increased in conditions of autophagy induction and inhibited by autophagy inhibitors, fragment 2 was occasionally problematic; it was not always induced by amino acid starvation and did not always appear to be due to macroautophagy. If the cleavage sites responsible for the generation of fragment 1 and fragment 2 could be identified, then it might be possible to produce a more reliable readout for the induction and inhibition of autophagy. The initial rationale to test human BHMT as an autophagy reporter was based on the association of rat BHMT with autolysosomes[68]. Human BHMT and rat BHMT are 92% conserved at the amino acid level, making it likely that the cleavage site responsible for cleavage of human BHMT is at or near the cleavage site predicted by Ueno et al. in rat BHMT[68]. In support of this, the calculated molecular weight of the GST protein plus the first amino acids of BHMT up to the predicted cleavage site in BHMT is 35 kDa which corresponds well with the molecular weight estimated on SDS-PAGE for fragment 1.

In the crystal structure of rat BHMT, loop L2, which connects β2 and α2 of the $(\alpha/\beta)_8$ barrel, is not visible on electron density maps due to a high degree of mobility[69]. The cleavage site described by Ueno et al. is within this disordered, flexible loop region, L2, of BHMT (Fig. 16A). Proteolytic cleavage of human BHMT to generate fragment 1 might also occur somewhere in this flexible, exposed loop, potentially at the same E92 site described by Ueno et al[68].

Figure 16. BHMT fragment 1 cleavage site maps to loop 2 (L2). A. Crystal structure of overlapping subunits of rat BHMT, as published by Gonzalez et al[69]. The L2 loop is disordered and not visible on the electron density maps. Sequence of the L2 loop is conserved in human BHMT; ^ marks the only residue that is different between rat and human. Site of cleavage to generate peptide in Ueno paper is marked with an arrow. Sites considered as contenders for fragment 1 generation are similarly indicated. Engineered thrombin recognition site is noted, with mutations marked in red. B. Western blot of control and '$L2_{Thr}$' mutant. Starvation of the '$L2_{Thr}$' mutant generates two closely related fragments in lane 4. *In-vitro* thrombin cleavage assay has no effect on control but efficiently cleaves the '$L2_{Thr}$' mutant (lanes 7-8) to produce a band consistent with the upper band of the doublet.

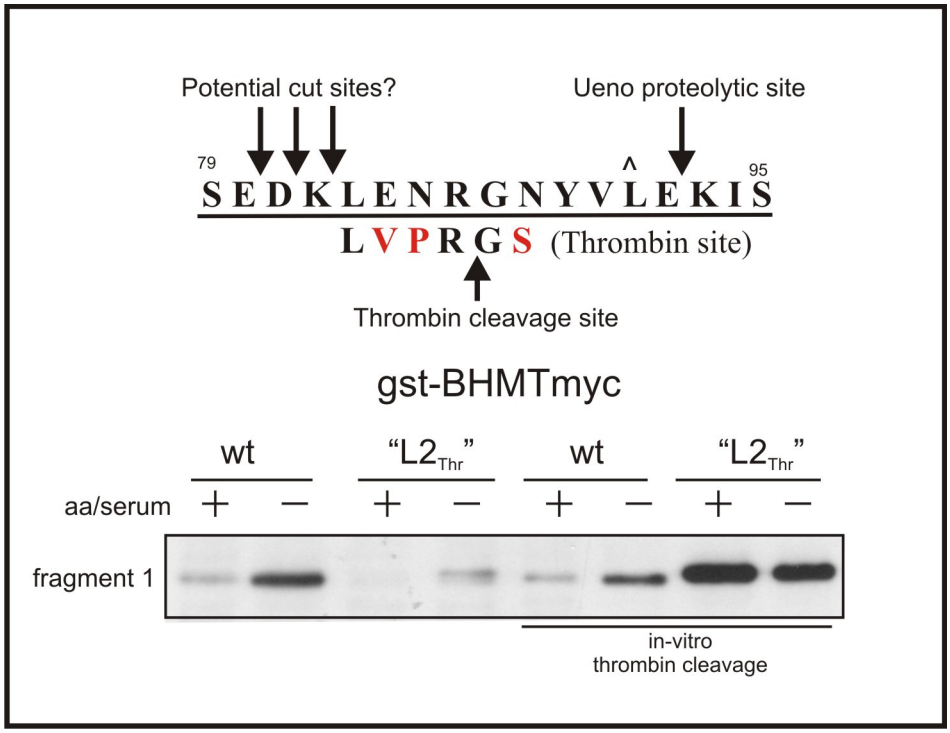
Potential cut sites?
Ueno proteolytic site
79
S E D K L E N R G N Y V L E K I S
95
L V P R G S (Thrombin site)
Thrombin cleavage site
gst-BHMTmyc
wt
"L2Thr"
wt
"L2Thr"
aa/serum
+ − + − + − + −
fragment 1
in-vitro
thrombin cleavage

While examining the L2 and surrounding regions of BHMT for potential protease recognition sites, it was noticed that L2 contained a sequence similar to a thrombin recognition site. The BHMT sequence LENRGN was different from a thrombin recognition site, LVPRGS, by just three amino acids, and was slightly upstream of the predicted E92 site (Fig. 16A). In an attempt to map the autophagy specific cleavage site in human BHMT, a strategy was designed to mutate the three amino acids necessary to introduce a thrombin cleavage site in the L2 loop of BHMT. If fragment 1 was produced by cleavage at E92 or somewhere downstream, and if the engineered thrombin site was not itself cleaved in vivo, then an *in-vitro* thrombin-generated fragment could be easily analyzed by mass spectrometry to obtain information on the precise cleavage site. However, it was possible that lysosomal thrombin-like proteases might cleave the introduced thrombin site either preferentially or in addition to the original cleavage site. In fact, the latter proved correct, as amino acid starvation of the GST-BHMT $L2_{thr}$ mutant resulted in the production of two, very closely associated fragments on SDS-PAGE (Fig. 16B, lane 4). The newly generated fragment seen in lane 4 migrated slightly slower on SDS-PAGE than control fragment 1, suggesting that the cleavage site for fragment 1 was not downstream as supposed, but rather was upstream of the engineered thrombin cleavage site.

To verify that the thrombin cleavage site was functional and that the upper band in lane four was generated by cleavage at the introduced thrombin recognition site, glutathione Sepharose pull-downs from control and GST-BHMT $L2_{thr}$ mutant cell extracts were treated with thrombin protease *in-vitro* and prepared for western blotting. Thrombin cleavage of the BHMT $L2_{Thr}$ mutant generated a band on SDS-PAGE identical

in size to the upper band of the doublet (Fig. 16B, lanes 7 and 8). *In-vitro* thrombin had no effect on GST-BHMT from control cells as expected (Fig. 16B, lanes 5 and 6). The results of the *in-vitro* thrombin cleavage assay confirm that the upper band was generated from the introduced site.

In an attempt to more closely map the fragment 1 cleavage site, mutations were made in the acidic and basic residues upstream of the thrombin cleavage site, E80A, D81A, K82Q, but they did not disrupt the production of fragment 1 (data not shown). To date, the exact proteolytic site responsible for fragment 1 is not known, although it is thought to be within a few amino acids upstream of the terminal amino acid, R86 produced by thrombin cleavage.

The inconsistencies that were observed in the generation of fragment 2 raised concerns that its cleavage was not entirely due to lysosomal proteases. Changes in levels of fragment 2 were not easily explained and distracted from the consistent, autophagy-related changes observed in levels of fragment 1. The goal of the BHMT assay was to create a clean and unambiguous reporter for macroautophagy, so it was necessary to make changes in the reporter that would preserve fragment 1, but eliminate fragmentation that generated fragment 2. If the site or region responsible for the generation of fragment 2 could be identified, then it might be possible to change it by mutation or deletion to make it a less favored substrate for its specific protease. Since the molecular weight of fragment 2 was very near the predicted molecular weight of GST alone (predicted to be 27 kDa), the linker region between GST and BHMT was examined for potential proteolytic sites. Sequence analysis of the GST-BHMT construct revealed a thrombin recognition site near the 3'end of the GST epitope tag (Fig. 17A in bold).

Figure 17. Mapping the major cleavage site responsible for fragment 2. A. Sequence analysis of the carboxy-terminal region of GST revealed a thrombin recognition sequence (bold and underlined). The twelve amino acids that were removed to make the $BHMT_{\Delta T}$ reporter are bracketed between the arrows. B. An *in-vitro* thrombin cleavage assay was performed with the original BHMT reporter to validate that the thrombin cleavage site was functional and capable of producing a fragment near the size of fragment 2. All data shown is by glutathione pull-down and western blotting.

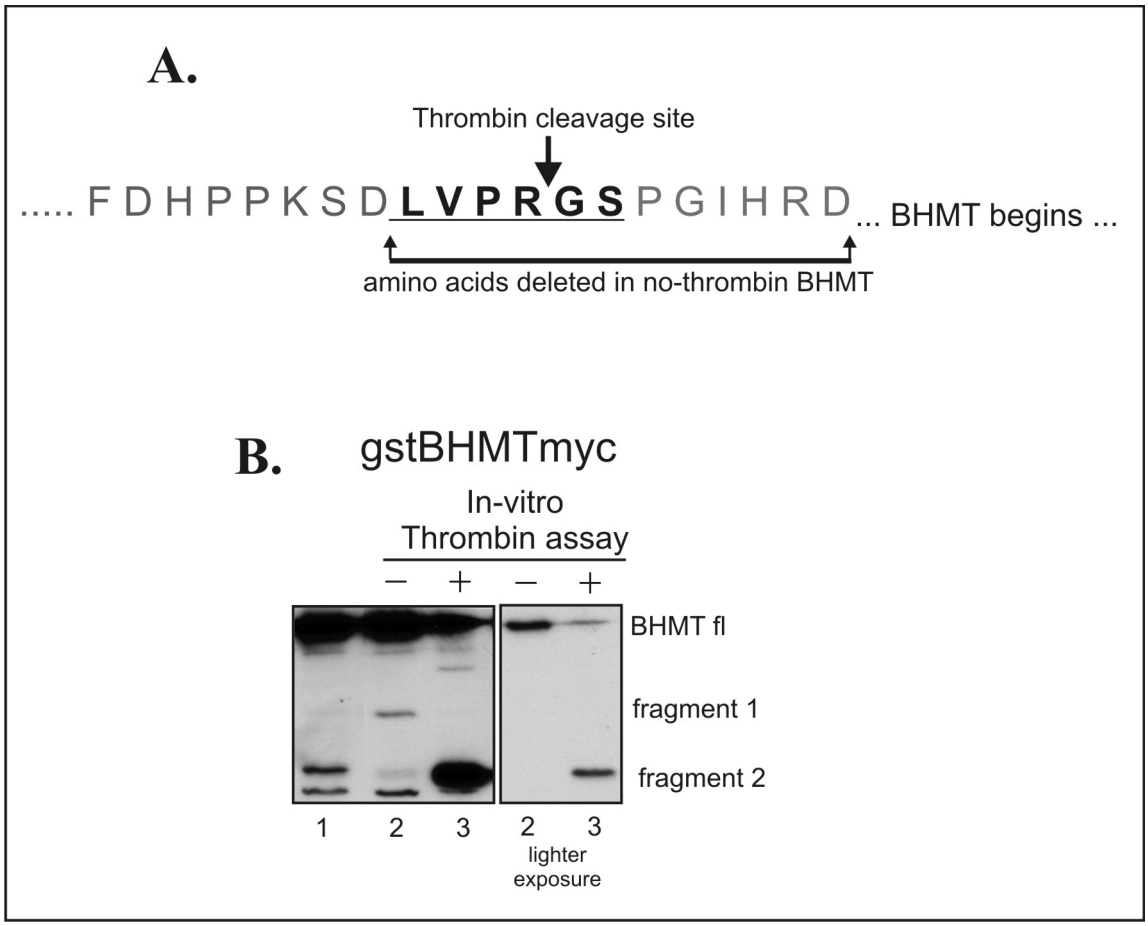
A.
Thrombin cleavage site
..... F D H P P K S D L V P R G S P G I H R D ... BHMT begins ...
amino acids deleted in no-thrombin BHMT
B.
gstBHMTmyc
In-vitro
Thrombin assay
– + – +
BHMT fl
fragment 1
fragment 2
1 2 3 2 3
lighter
exposure

The GST fused to BHMT was originally subcloned from the PGEX -2T cloning vector (accession number U13850). All PGEX vector GST sequences are identical from the amino-terminus through FDHPPKSD (Fig. 17A), but vary in the protease recognition sites and sequences that follow. The thrombin recognition site in the original vector was designed to allow cleavage and release of protein fused to GST for purification purposes. Thrombin cleavage of the GST-BHMT reporter could be useful in narrowing the region of the proteolytic site responsible for the generation of fragment 2, by generating a defined fragment that could be compared to the size of fragment 2. It was also possible that the thrombin cleavage site itself might be responsible for generation of fragment 2 as was observed with the $L2_{Thr}$ form of BHMT. Since thrombin-like proteases exist in both the cytoplasm and the lysosome, cleavage at this site would explain why fragment 2 appeared to be of lysosomal origin in some experiments, but not others.

An *in-vitro* thrombin cleavage assay was performed to determine the size of a thrombin-released GST-BHMT fragment on SDS-PAGE compared to fragment 2. HEK293 cells were transiently transfected with the GST-BHMT-myc reporter construct and extracted after 48 hours. GST-BHMT-myc was affinity-purified on glutathione Sepharose beads from 300µg of cell extracts. PBS-washed glutathione beads with bound GST-BHMT were incubated at room temperature for 2 hours in 20µl of PBS with 0.5µg thrombin. A negative control was processed in the same manner without thrombin. Samples were prepared for western blotting with an antibody against GST. Independent glutathione pull-down was included as a control for the size of fragment 2 (Fig. 17B, lane 1). Negative thrombin assay control is shown in Fig. 17B, lane 2. The fragment released by *in-vitro* thrombin cleavage ran on SDS-PAGE at a molecular weight equal to that of

fragment 2 (Fig. 17B, lane 3 compared to lane 1). It seemed likely that the thrombin recognition site was responsible for the generation of fragment 2 *in-vivo*.

The amino acids in the carboxy-terminal region of the GST tags vary between the different PGEX vectors, and are likely not essential for glutathione interaction or antibody recognition. Therefore, a PCR strategy was used to remove the thrombin recognition site plus six additional amino acids from the linker region between the GST tag and BHMT to create a new reporter called $GST_{\Delta T}$BHMT myc (Fig. 17A).

The new $GST_{\Delta T}$BHMTmyc reporter was tested to determine if it retained the ability to generate fragment 1 in conditions known to induce and inhibit macroautophagy, and to see if deletion of the thrombin cleavage site had removed the cleavage site responsible for the generation of fragment 2. HEK293 cells were transiently transfected with GST-BHMT-myc as a control and the $GST_{\Delta T}$BHMTmyc construct. After allowing sufficient time to allow for expression, the cells were starved from serum and essential amino acids in the presence or absence of a panel of macroautophagy inhibitors: 3MA, wortmannin, chloroquine, and bafilomycin A1. The proteasome inhibitor MG132 was included as before. Glutathione pull-downs were performed from cell extracts and prepared for western blotting. The $GST_{\Delta T}$BHMT reporter was as fully responsive to induction of autophagy by amino acid starvation and to the effects of macroautophagy pharmacological inhibitors in the generation of fragment 1 as the original reporter (Fig. 18B). $GST_{\Delta T}$BHMT fragment 1 migrated slightly faster on SDS-PAGE as expected due to the deletions in the GST linker regions. Although the ΔT modification seemed to reduce the level of fragment 2, it did not completely eliminate generation of a second fragment (Fig. 18B, lane 2 compared to lane 1). On closer examination, the original

Figure 18. The GST-BHMT$_{\Delta T}$ assay. A. Schematic of the GST-BHMT$_{\Delta T}$ reporter construct. B. GST-BHMT$_{\Delta T}$ produces two consistently lysosomal fragments with amino acid and serum starvation. BHMT fragmentation is inhibited by the autophagy inhibitors, 10mM 3MA, 100nM wortmannin, 100μM chloroquine, or 100nM bafilomycin A1. GST-BHMT$_{\Delta T}$ fragmentation was not inhibited by the proteasome inhibitor MG132. All data shown is obtained by glutathione pull-down and western blotting.

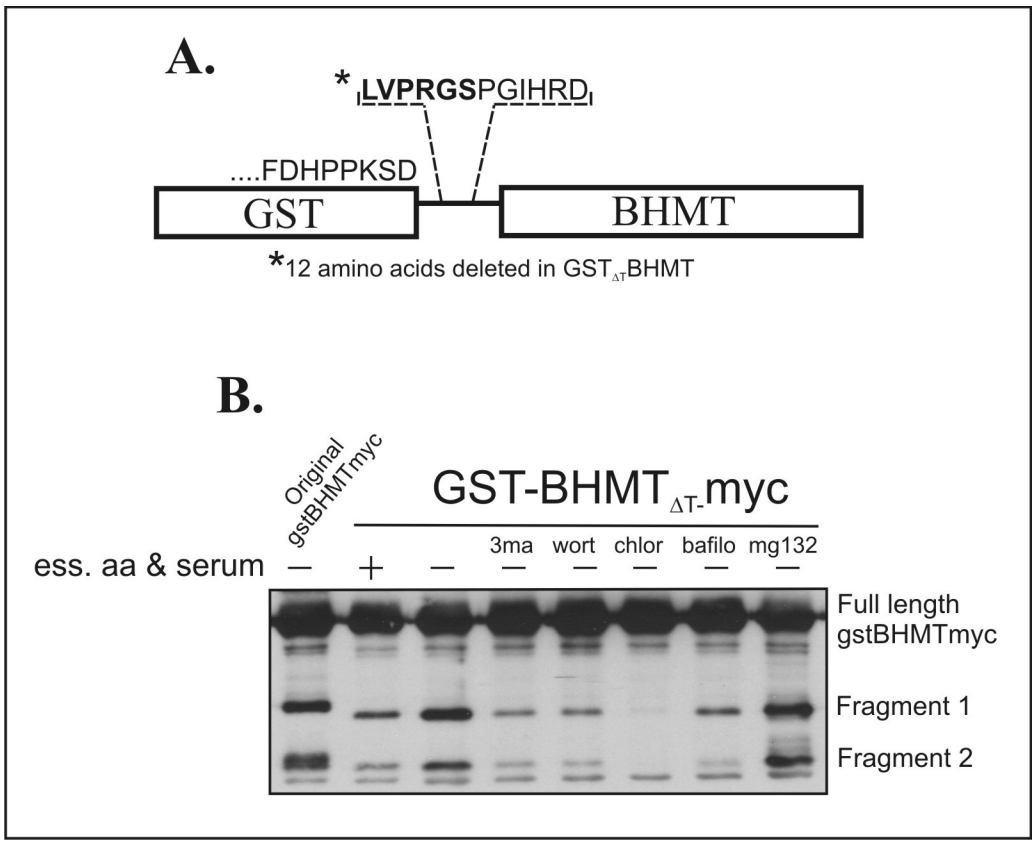
A.
*LVPRGSPGIHRD
....FDHPPKSD
GST
BHMT
*12 amino acids deleted in GST$_{\Delta T}$BHMT
B.
Original gstBHMTmyc
GST-BHMT$_{\Delta T}$-myc
3ma
wort
chlor
bafilo
mg132
ess. aa & serum
— + — — — — — —
Full length gstBHMTmyc
Fragment 1
Fragment 2

GST-BHMT-myc reporter fragment 2 is actually a doublet. The larger, slower migrating fragment was eliminated in the $BHMT_{\Delta T}$ background, but the smaller fragment remained. Unlike the original fragment 2, generation of the smaller fragment, called fragment 2′ in the ΔT background, correlated well with fragment 1 under conditions of autophagic induction and inhibition.

Although both fragments 1 and 2′ were now consistent in their response to autophagic induction and inhibition, it was possible that the overall signal observed in the generation of fragment 1 might be diluted by subsequent cleavage to fragment 2′. If this were true, the elimination of the fragment 2′ cleavage site might increase the generation of fragment 1 and the overall signal strength. To do this, two things were considered. First, it was assumed that either the same or a similar lysosomal cathepsin was responsible for the generation of both fragment 1 and the remaining 2′, since both fragments were generated in the presence of the protease inhibitors leupeptin and E64d. Second, the size of fragment 2′ again suggested that the cleavage site must be near the end of GST. Ueno et al. indicated the intralysosomal carboxy-terminal fragment of rat BHMT was cleaved between glutamate E92and lysine K93 to produce the carboxy-terminal peptide identified by mass spectrometry[68]. With this information, point mutations were made in the carboxy-terminal region of GST that changed two aspartates to glycines (D214G, D220G), and a lysine to a glutamine (K218Q) (Fig. 19A).

While making these modifications, an additional mutation was made in GST to address a potential KFERQ-like chaperone-mediated autophagy (CMA) site. Although it seemed unlikely that GST-BHMT was imported via CMA, Majeski and Dice reported that glutathione GST was a known CMA substrate[10]. The identified site, NKKFE was

found in the GST fused to BHMT, so a N43A mutation was introduced that was known to destroy substrate recognition by the CMA complex (Fig. 19A).

The new $GST_{mod}BHMT$ construct was subcloned as before to create a bicistronic message with a downstream IRES-GFP (Fig. 19A). HEK293 cells were transiently transfected with $GST_{mod}BHMT_{IRES}GFP$ and maintained in culture for 36 hours to allow for expression of the reporter and GFP. GFP expression on western blot is shown for normalization (Fig. 19B, bottom panel). Cells were treated for five hours with or without leupeptin (10ug/ml) and E64d (2ug/ml), which was essential to observe fragment 1 at a molecular weight of approximately 35 kDa by western blotting (Fig. 19B, lanes 5-8 compared to lanes 1-4). Serum starvation of cells with the full cocktail of essential amino acids was not sufficient to induce an increase in fragment 1 (Fig. 19B, lanes 5 vs. lane 6). Depletion of essential amino acids was sufficient to increase levels of fragment 1, with the presence of dialyzed serum having no effect (Fig. 19B, lanes 7 and 8). The deletions and mutations in the $GST_{mod}BHMT$ reporter did not prevent the starvation-induced generation of fragment 1. Protease inhibitors were still necessary to see fragment 1, which was now the only fragment observed.

The deletions and mutations in the $GST_{mod}BHMT$ reporter had successfully eliminated the generation of fragment 2 and it seemed prudent to verify that the extensive modifications had not affected the generation of fragment 1 with autophagy inhibitors. The $GST_{mod}BHMT$ reporter was transiently transfected into HEK293 cells and treated for 5 hours with complete media and starvation media with the panel of macroautophagy inhibitors as before, including wortmannin, 3MA, bafilomycin A1, chloroquine, and puromycin. Aliquots of cell extracts were pulled down with glutathione Sepharose and

Figure 19. Leupeptin-dependent generation of GST_{mod}BHMT fragment 1. A. Schematic of the $GST_{mod}BHMT_{IRES}$GFPmyc reporter; the thrombin recognition site has been removed and N43A, D214G, K218Q, and D220G mutations have been made in GST. B. GST_{mod}BHMT fragmentation requires the protease inhibitors leupeptin (10ug/ml) and E64d (2ug/ml). Levels of BHMT fragment 1, but not fragment 2, increase in media depleted of 12 essential amino acids (lanes 7 and 8). All data shown is obtained by glutathione pulldown and western blotting.

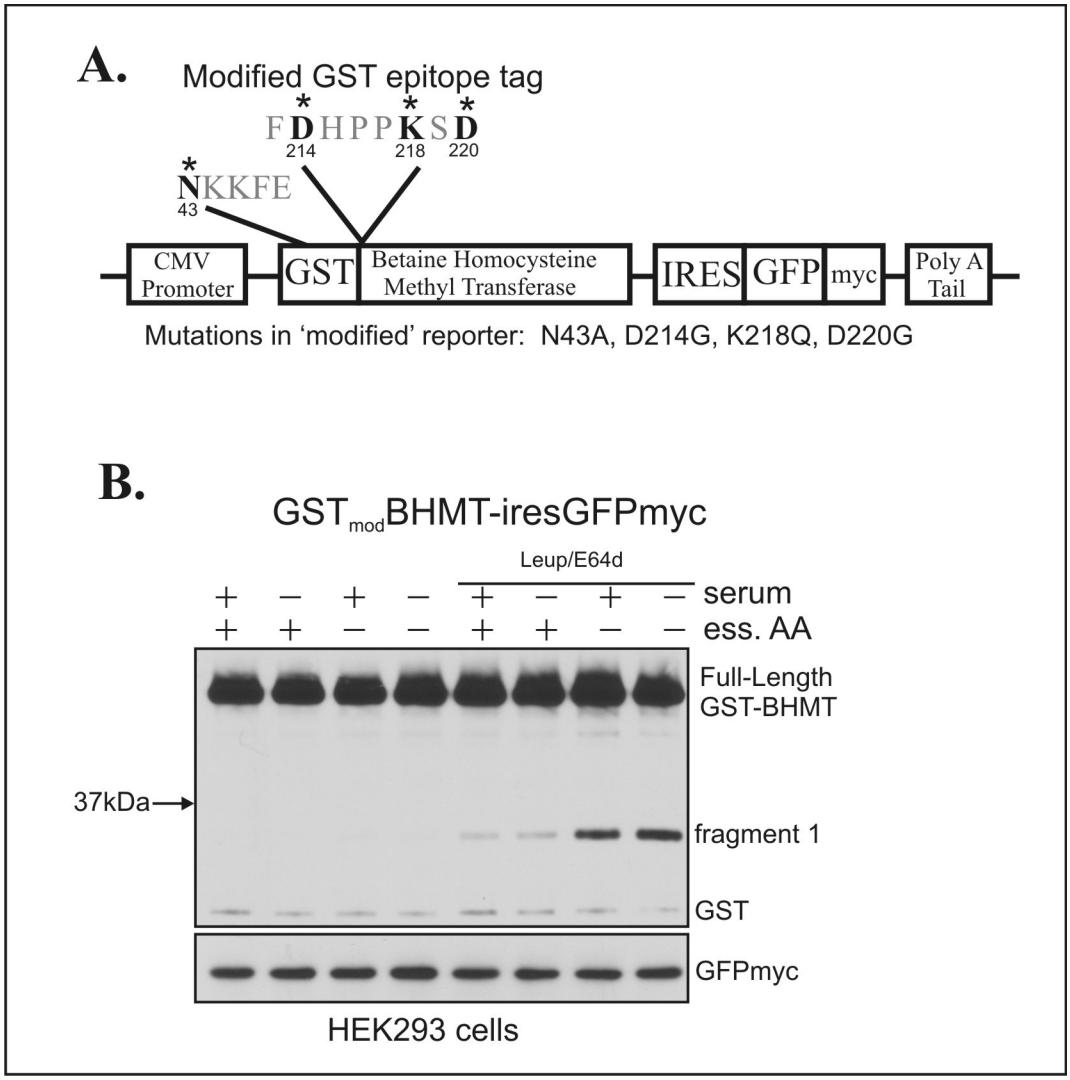
A.
Modified GST epitope tag
F D H P P K S D
214 218 220
N K K F E
43
CMV Promoter
GST
Betaine Homocysteine Methyl Transferase
IRES
GFP
myc
Poly A Tail
Mutations in 'modified' reporter: N43A, D214G, K218Q, D220G
B.
GST mod BHMT-iresGFPmyc
Leup/E64d
+ − + − + − + − serum
+ + − − + + − − ess. AA
Full-Length GST-BHMT
37kDa
fragment 1
GST
GFPmyc
HEK293 cells

prepared for western blotting. GST_{mod}BHMT demonstrated increased fragment 1 accumulation with amino acid starvation that was effectively blocked with the panel of autophagy inhibitors (Fig. 20). Increased fragmentation of this reporter was also observed in cells treated with 40nM rapamycin, an agent reported to induce macroautophagy in the presence of full amino acids[54], providing further evidence that GST_{mod}BHMT was a reporter for macroautophagy (Fig. 20 lane 3). A band near the molecular weight of fragment 2 was observed, but is likely endogenous GST, as it was also observed in extracts from untransfected cells (data not shown).

Recently, it was reported that intact microtubules were necessary for macroautophagy in hepatocytes and that their disruption with the drug vinblastine allowed and potentiated autophagosome formation, but inhibited the vesicular trafficking necessary for fusion with lysosomes[70]. Vinblastine was also recently tested for its effects on chaperone-mediated autophagy (CMA) by Finn et al., who showed that vinblastine did not inhibit CMA in IMR90 cells[71]. For further validation that BHMT fragmentation was the result of macroautophagy and not CMA, the BHMT assay was tested with the pharmacological agent vinblastine. HEK293 cells stably expressing GST_{mod}BHMTmyc were starved of essential amino acids and serum for 5 hours. Cells were treated with decreasing doses of vinblastine from 50μM to 5μM, with 100μM chloroquine as a positive control for maximum lysosomal inhibition. Amino acid starved cells served as a control for generation of fragment 1. After the cells were harvested, glutathione pull-downs from cell extracts were processed for western blotting. The starvation-induced generation of fragment 1, seen in lane 1, was inhibited by chloroquine, seen in lane 2, as expected (Fig. 21). Generation of BHMT fragment 1 was inhibited by

Figure 20. The BHMT assay with $GST_{mod}BHMT_{IRES}GFPmyc$. Western blot of modified BHMT reporter in plus and minus amino acid media and with a panel of pharmacological agents: 40nM rapamycin, 100nM wortmannin, 10mM 3MA, 100n bafilomycin A1, 100μM chloroquine, 50μM puromycin. The band marked with an * is not specific for cells expressing the GST-BHMT constructs and is most likely endogenous GST.

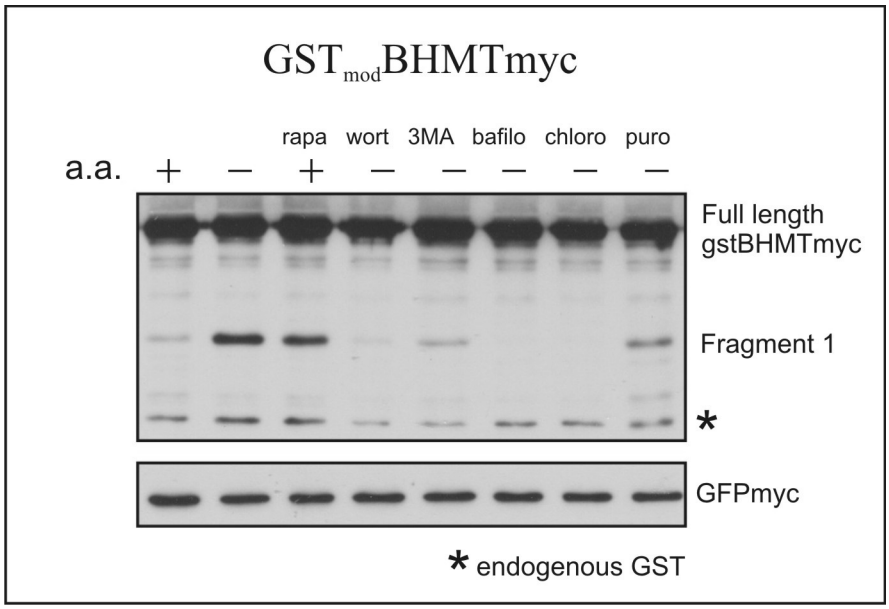
GST mod BHMTmyc
rapa
wort
3MA
bafilo
chloro
puro
a.a.
+
−
+
−
−
−
−
−
Full length
gstBHMTmyc
Fragment 1
*
GFPmyc
* endogenous GST

Figure 21. Validation of the BHMT assay with vinblastine. Western blot of HEK293 cells stably expressing GST_{mod}BHMT-myc. Amino acid starved cells represented in lanes 3-6 were treated with 50μM, 25μM, 10μM and 5μM vinblastine repectively. Lane 1 represents cells in starvation media, and lane 2, starvation media with 100 μM chloroquine as a control for a block of lysosomal degradation. Western blot of endogenous LC3 is shown in the bottom panel. BHMT fragmentation and LC3-II are inversely related in amino acid starved cells with chloroquine or higher doses of vinblastine.

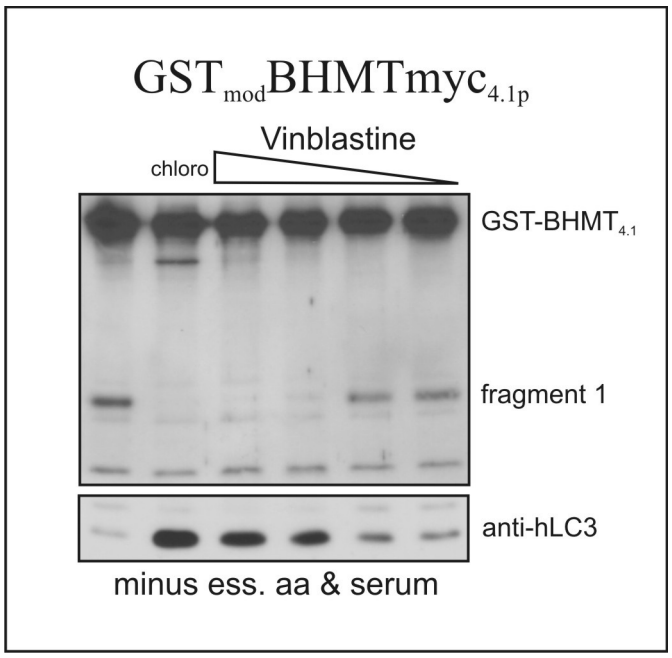
GST$_{mod}$BHMTmyc$_{4.1p}$
Vinblastine
chloro
GST-BHMT$_{4.1}$
fragment 1
anti-hLC3
minus ess. aa & serum

vinblastine in a dose dependent manner, and at 50 μM was as effective as chloroquine at inhibiting BHMT fragmentation (Fig. 21, lanes 3-6). Western blot of endogenous hLC3 shows an inverse correlation between levels of LC3-II and BHMT fragment 1, confirming that vinblastine blocks macroautophagy at a late stage, causing an accumulation of autophagosomes. The vinblastine data provide additional pharmacological validation that the BHMT assay does not measure chaperone-mediated autophagy, but is specific for macroautophagy.

The pharmacological inhibitors of BHMT fragmentation strongly argue that the BHMT assay specifically measures macroautophagy. The lysosome inhibitors convincingly demonstrate that BHMT fragmentation is lysosomal and the macroautophagy inhibitors wortmannin and 3MA, and vinblastine suggest it is not due chaperone-mediated autophagy (CMA). However, the effects of any of these inhibitors on microautophagy are not known, and therefore the pharmacological data cannot rule out microautophagy as a mechanism of BHMT lysosomal import.

3.1.2.2. Validation of the BHMT assay by modulating levels of known autophagy genes.

Silencing of a macroautophagy-specific gene by short-interfering RNA (siRNA) would unambiguously validate that BHMT is delivered to the lysosome by macroautophagy. Beclin1, the human ortholog of yeast Atg6, was chosen as one target for siRNA. The expression of Beclin1 is thought to promote autophagy through its interaction with the Class III PI3 Kinase, Vps34[72]. Over-expression of Beclin1 increases macroautophagy in MCF7 cells and monoallelic deletion of Beclin1 promotes tumorigenesis in part due to suppressed macroautophagic activity[38]. pSilencer DNA plasmid vectors (Ambion), designed with a short hairpin (sh) insert, were used to express

target-specific sequences to be processed into siRNA that would silence certain Atg genes. In a manner similar to the HA-LC3B-myc reporter, the GST_{mod}BHMTmyc reporter was stably integrated into HEK293 cells. This eliminated issues related to the co-transfection of shRNA plasmids with a BHMT reporter plasmid, especially when multiple transfections were required for efficient gene silencing. HEK293 cells that stably expressed GST_{mod}BHMT were transfected twice with pSilencer plasmids to achieve a transfection efficiency of approximately 90%. Three different shRNA sequences targeting Beclin1 successfully lowered Beclin1 expression by approximately 60% (Fig. 22). Significantly, in the cells with shRNA targeting Beclin1, generation of BHMT fragment 1 in amino acid and serum starved cells was decreased by approximately 60% (Fig. 22). This provides the first direct evidence that an autophagy specific gene is necessary for the BHMT assay to generate fragment 1 and that the BHMT assay is measuring the process of macroautophagy.

A second gene of interest in macroautophagy is human unc 51-like kinase 1 (hULK1). hULK1 is an ortholog of yeast Atg1, the only protein kinase identified in the initial genetic screens in *S. cerevisiae*[44]. In yeast, one model suggests that Atg1 activity increases with autophagy induction in response to the decreased phosphorylation of Atg13, an associating protein in complex with Atg1[45]. The phosphorylation of Atg13 is downstream of the target of rapamycin (TOR). Inhibition of yeast TOR by nitrogen starvation or by its inhibitor rapamycin decreases phosphorylation of Atg13 and increases the activity of Atg1. However, this model is not universally accepted, as Abeliovich et al. reports that Atg1 activity is not required for macroautophagy, although it is required for the Cvt pathway[46]. Although hULK1 was first described in 1998 as

Figure 22. Validation of the BHMT assay by silencing Beclin1 with shRNA. Plasmid vectors with three different short hairpin inserts designed to target Beclin1 mRNA with siRNA were transfected twice in HEK293 cells stably expressing GST_{mod}BHMT-myc. Cells were treated to conditions of plus and minus amino acid media. Levels of BHMT fragment 1 are decreased in cells with decreased levels of Beclin1. Western blot for Beclin1 verifies that levels of endogenous Beclin1 decreased with each shRNA targeting Beclin1.

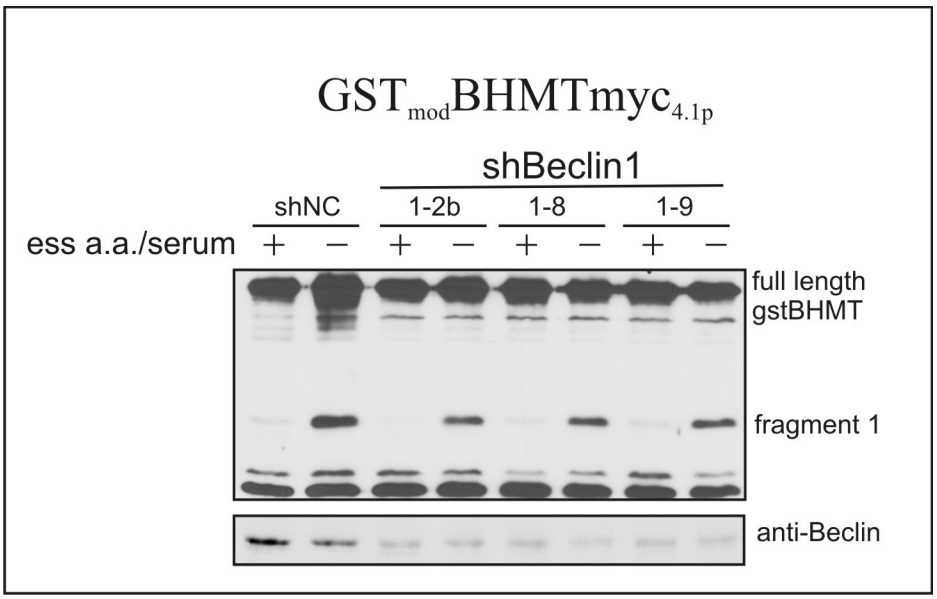
GST mod BHMTmyc 4.1p
shBeclin1
shNC
1-2b
1-8
1-9
ess a.a./serum
+ − + − + − + −
full length
gstBHMT
fragment 1
anti-Beclin

an Atg1 ortholog, data that suggests a role in autophagy has only recently been published. It was shown that shuttling of the mammalian autophagy-related protein mAtg9 between the trans-Golgi and autophagosomes is inhibited in cells in which hULK1 transcript levels are decreased by shRNA, providing the first evidence that human hULK1 plays a role in mammalian macroautophagy[52].

Because hULK1 is a kinase, it seemed likely that conditions known to induce or inhibit autophagy might change its specific activity. This is supported by data in *S. cerevisiae* that Atg1 activity increases in conditions known to induce autophagy[45]. To test this, it was necessary to create and express an epitope-tagged hULK1 because hULK1 antibodies that were commercially available were not sensitive enough for immunoprecipitation or western blotting of the endogenous protein. hULK1 was cloned from a human cDNA library and subcloned into a mammalian expression vector with an HA epitope tag at the amino-terminus and a myc tag at the carboxy-terminus. To make a catalytically inactive allele of hULK1, the invariant lysine in subdomain two of the catalytic domain, known to disrupt ATP binding in other kinases, was mutated to a glutamine (K39Q) by site directed mutagenesis. The HA-tagged hULK1^{KD} mutant migrated faster on SDS-PAGE than HA-ULK1-myc, in a band shift consistent with loss of phosphorylation (Fig. 23A). To test the activity of HA-hULK1-myc and HA-hULK1^{KD}, the two kinases were tested in an *in-vitro* kinase assay with myelin basic protein (MBP) as a generic substrate. In the conditions tested, HA-ULK1-myc was catalytically active toward MBP and was able to autophosphorylate as expected. The KD mutant was not active toward MBP and did not autophosphorylate (Fig. 23B).

To test the specific activity of hULK1, HEK293 cells expressing HA-ULK1-myc

Figure 23. Expression and activity of HA-hULK1-myc and HA-hULK1^{KD}myc. A. Western blot of HA-tagged hULK1 and the slower-migrating HA-tagged kinase dead hULK1^{KD}. B. *In-vitro* kinase assay: The epitope-tagged wild type hULK1 can autophosphorylate and phorphorylate MBP in vitro. HA-hULK1^{KD}myc shows no evidence of catalytic activity.

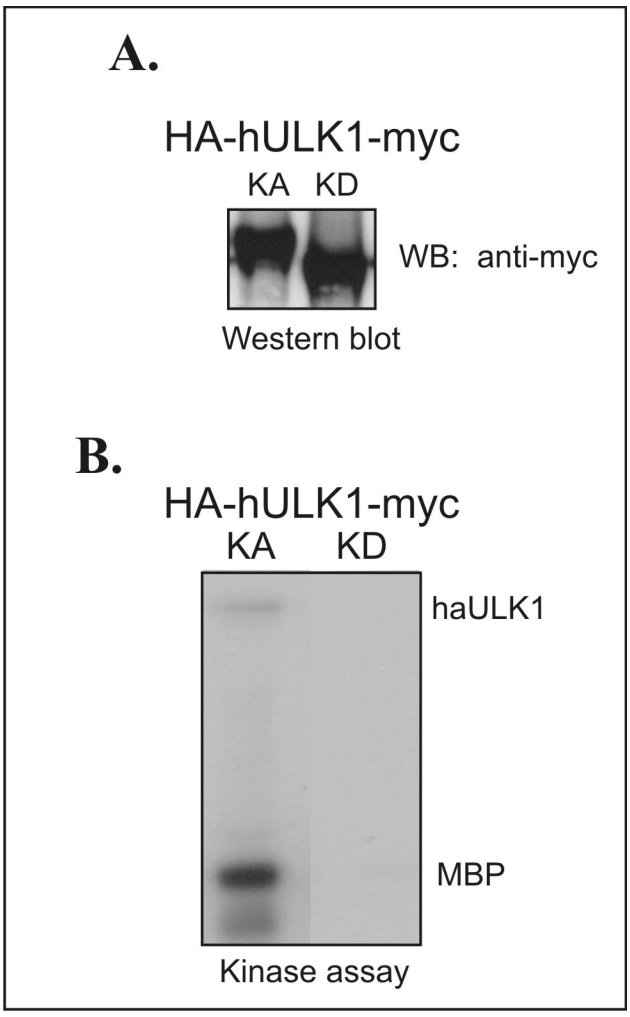
A.
HA-hULK1-myc
KA KD
WB: anti-myc
Western blot
B.
HA-hULK1-myc
KA KD
haULK1
MBP
Kinase assay

Figure 24. Specific activity of HA-hULK1-myc in conditions known to induce or inhibit macroautophagy. HEK293 cells expressing HA-hULK1-myc were treated to conditions known to induce autophagy, such as minus essential amino acids and rapamycin treatment, or to conditions known to inhibit autophagy, such as 10mM 3MA, 100nM wortmannin, and 100μM chloroquine. Top panel shows expression of HA-hULK1-myc by western blotting. Middle and bottom panels are autorads showing autophosphorylation of HA-hULK1-myc and phosphorylation of the generic substrate, myelin basic protein (MBP).

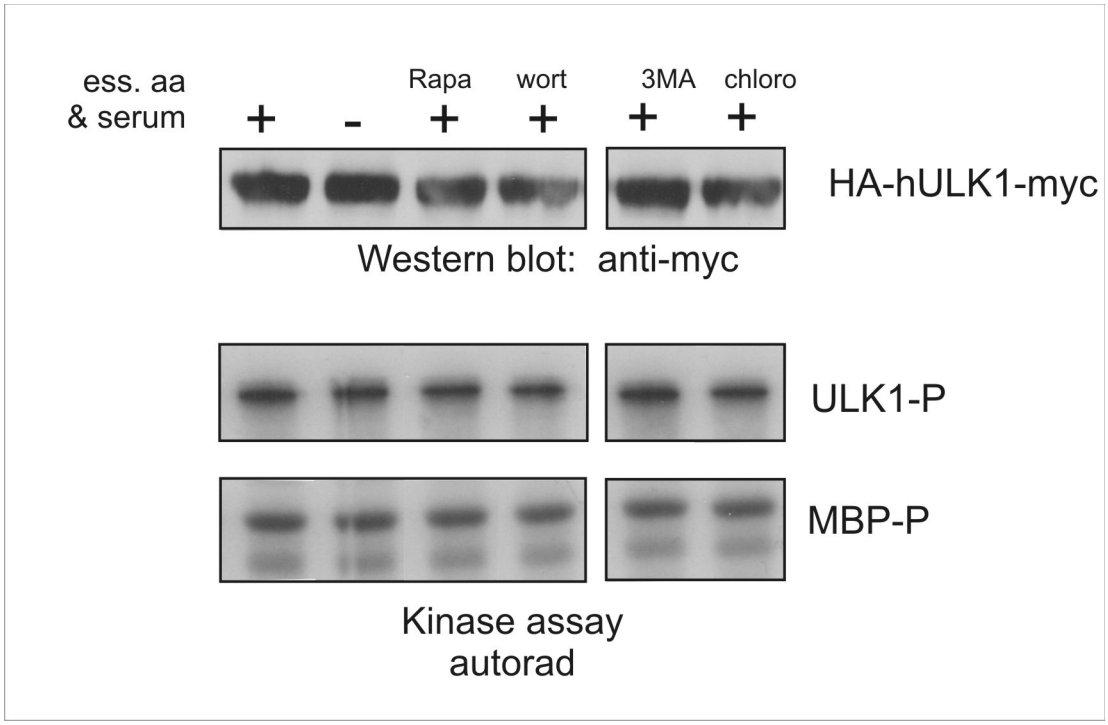
ess. aa
& serum
Rapa
wort
3MA
chloro
+
-
+
+
+
+
HA-hULK1-myc
Western blot: anti-myc
ULK1-P
MBP-P
Kinase assay
autorad

were tested under conditions known to induce autophagy such as amino acid starvation or treatment with 40nM rapamycin, as well as conditions that inhibit autophagy such as treatment with 100nM wortmannin, 10mM 3MA or 100μm chloroquine. After four hour treatment and extraction, HA-ULK1-myc was immunoprecipitated from cells extracts and tested for activity toward MBP in an *in-vitro* kinase assay. As a control of expression, a western blot of HA-hULK1-myc in crude extracts is shown in the top panel (Fig. 24). Autophosphorylation of hULK1 and phosphorylated MBP are shown in the bottom two panels of Figure 24. Unlike in yeast, the specific activity of HA-hULK1-myc did not change in starvation conditions, with rapamycin treatment, or in any of the other conditions tested.

Protein kinase function can be regulated by mechanisms other than changes in specific activity. Expression levels regulate the function of some kinases and could be a mechanism of regulation for hULK1. Although endogenous hULK1 cannot be seen by western blotting with the available antibodies, qPCR is a testable method to determine if amino acid starvation affects levels of hULK1 mRNA. Total RNA was extracted from HEK293 cells that were maintained in either complete or starvation media for approximately 7 hours. Each condition was repeated in triplicate. After reverse transcription to cDNA with random primers, qPCR was performed on each sample, in duplicate, with primers specific to hULK1 and its isoform hULK2. Quantitation is expressed as fold change, normalized to two housekeeping genes, actin and 18S (Fig. 25). Amino acid starvation did not significantly change levels of either hULK1 or hULK2 mRNA, compared to cells in complete media. Regulation of hULK1 does not seem to occur at the transcriptional level.

Figure 25. hULK1 and hULK2 transcript levels are unchanged in amino acid starved cells. T98G cells were maintained in complete media or media depleted of essential amino acids and serum for 6 hours. After extraction of total RNA and RT-PCR, qPCR was performed with primers to either hULK1 or hULK2. Relative levels of hULK1 and hULK2 mRNA in amino acid starved cells are compared to cells in complete media. Fold change is normalized to two housekeeping genes: actin and ribosomal 18S.

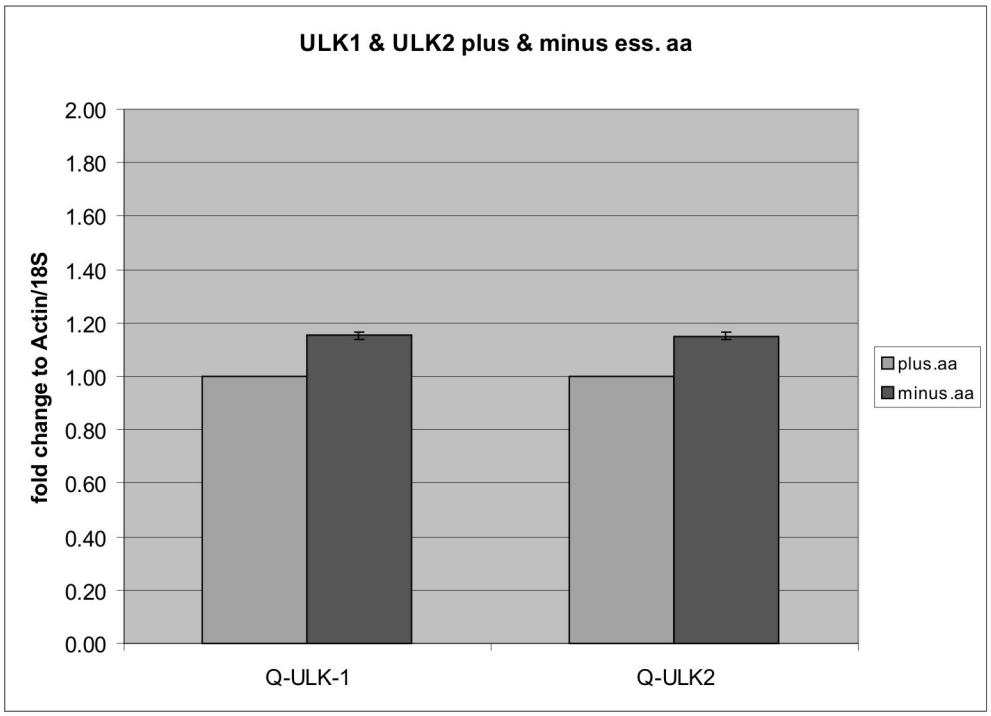
ULK1 & ULK2 plus & minus ess. aa
fold change to Actin/18S
2.00
1.80
1.60
1.40
1.20
1.00
0.80
0.60
0.40
0.20
0.00
Q-ULK-1
Q-ULK2
plus.aa
minus.aa

Figure 26. HA-hULK1^{KD}myc inhibits starvation-induced BHMT fragmentation. HEK293 cells were cotransfected with $GST_{mod}BHMT_{IRES}GFP$ and either HA-hULK1^{KD}myc or empty plasmid. Generation of fragment 1 is inhibited in cells expression HA-hULK1^{KD}myc. Expression levels of GFP and hULK1 by western blotting are shown in the bottom two panels.

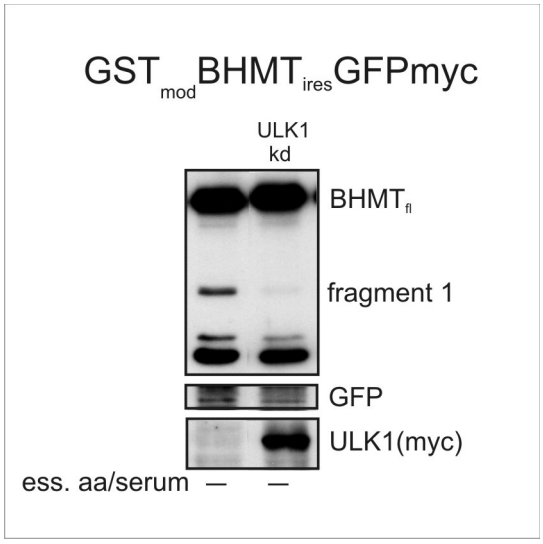
GST mod BHMT ires GFPmyc
ULK1
kd
BHMT fl
fragment 1
GFP
ULK1(myc)
ess. aa/serum — —

Although the specific activity of hULK1 did not change observably under conditions that modulate autophagy, it was tested how disruption of hULK1 signaling might affect autophagy as judged by BHMT fragmentation. One easy way to test this is to use the kinase dead allele of hULK1 as a dominant interfering mutant. The catalytically inactive HA-hULK1^{KD} allele was co-expressed in HEK293 cells with the BHMT reporter. After sufficient time to allow for expression, the cells were starved of essential amino acids and serum for approximately 5 hours and extracted. Expression of the catalytically inactive hULK1^{KD} mutant consistently inhibited the generation of BHMT fragment 1 in starved cells (Fig. 26). The dominant interfering effect of the hULK1^{KD} mutant on the assay suggests that ULK1 activity may be important for autophagy.

There is a caveat to the use of a dominant-interfering allele. The effects of its over-expression can occur through sequestration of either downstream effectors or upstream regulatory proteins. Therefore, the dominant-interfering effect of hULK1^{KD} on the BHMT assay might not be specific for ULK1 alone. To address this caveat, a strategy was implemented to decrease the expression of endogenous hULK1 by shRNA. hULK1 mRNA levels were measured by qPCR to assess the effectiveness of silencing. Two shRNAs were designed to target the three prime untranslated region (3′ UTR) of hULK1. hULK1 sh3′12 and sh3′13 were the most effective in decreasing hULK1 message by approximately 90% and 80% respectively, as measured by qPCR (Fig. 27A). Significantly, when transfected into HEK293 cells stable expressing GST$_{mod}$BHMT, each of these hULK1 shRNAs inhibited the ability of BHMT to generate fragment 1 in amino acid starvation conditions (Fig. 27B). Therefore, the effectiveness of hULK1 silencing

Figure 27. shRNA-targeted depletion of hULK1 inhibits BHMT fragmentation. A. Plasmid vectors with two different short hairpin inserts designed to target hULK1 mRNA with siRNA were transfected twice in HEK293 cells stably expressing GST_{mod}BHMT-myc. Cells were treated to conditions of plus and minus amino acid media. qPCR derived from cells expressing sh3′12 and sh3′13 shows significant knockdown of hULK1 mRNA to 90% and 80% of normal levels. Fold change is normalized to the housekeeping gene, ribosomal subunit L32. This is typical of three independent experiments. B. The BHMT assay is shown in HEK293 cells stabling expressing GST_{mod}BHMT, with a non-specific shNC or the two shRNA hairpins targeting hULK1. Generation of fragment 1 is inhibited in cells expressing the shULK1 3′12 and 3′13.

A.

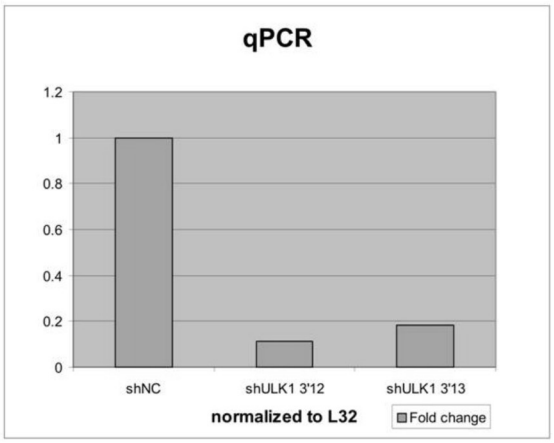
qPCR
1.2
1
0.8
0.6
0.4
0.2
0
shNC
shULK1 3'12
shULK1 3'13
normalized to L32
Fold change

B.

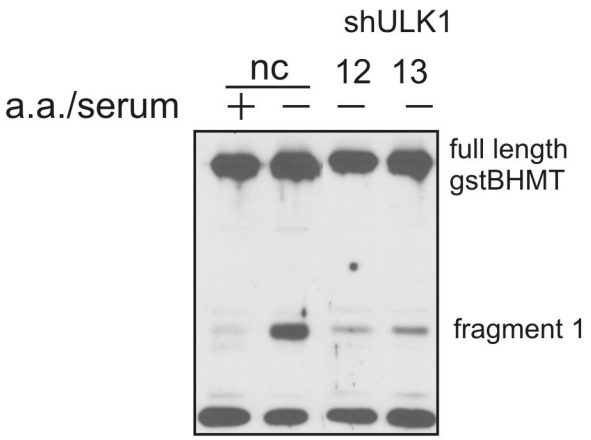
GST mod BHMTmyc 4.1H
shULK1
nc
12
13
a.a./serum
+
—
—
—
full length
gstBHMT
fragment 1

on BHMT fragmentation provides further validation of the BHMT assay by targeting a second autophagy specific gene, and also demonstrates with an endpoint assay that loss of ULK1 alone is sufficient to inhibit autophagy.

3.1.2.3. Sensitivity of the BHMT assay to amino acids

In the development and validation of the BHMT assay, essential amino acid starvation was the predominant condition used to induce macroautophagy in cell culture. For starvation experiments, cells were maintained in culture media that lacked the twelve essential amino acids but contained levels of glutamine and non-essential amino acids normal for Dulbeccos's modified essential media (DMEM). Except for the harsh nutrient deprivation seen in ischemia, cells in a physiological setting are rarely forced to respond to total starvation. However, circulating levels of amino acids are known to fluctuate: being lower during fasting, in the perinatal period, and in times of poor nutrition; and higher after the ingestion of a protein-rich meal. To test the response of the BHMT assay to changes in levels of available essential amino acids, HEK293 cells expressing the $GST_{mod}BHMT_{IRES}GFP$ reporter were incubated in culture with steadily decreasing concentrations of the essential amino acids for six hours. Aliquots of cell extract normalized for total protein were pulled down with glutathione agarose and prepared for western blotting. Expression of GFP in WCE is shown on western blot as a normalization control for the BHMT reporter (Fig. 28). It was expected that cells might respond to changes in amino acid levels in a linear fashion and that this would be reflected in increasing levels of BHMT fragment 1. However, only minor increases in fragment 1 were seen in the range of amino acid concentrations between 100% and 20% (Fig. 28A). The major increase in levels of BHMT fragment 1 was found only after the

Figure 28. The BHMT assay is sensitive to physiologic levels of essential amino acids. A. HEK293 cells expressing $GST_{mod}BHMT_{IRES}GFP$ were maintained in media containing decreasing concentrations of 12 essential amino acids for 6 hours. Essential amino acids in this experiment are listed in Table 4. Significant increase of BHMT fragmentation is seen at levels less than 20%. B. The experiment describe in A was repeated with the same conditions, except with titration points in the lower concentration range. Concentration of essential amino acids must be less than 10% of normal DMEM media to generate significant levels of BHMT fragmentation. All data shown is by western blotting.

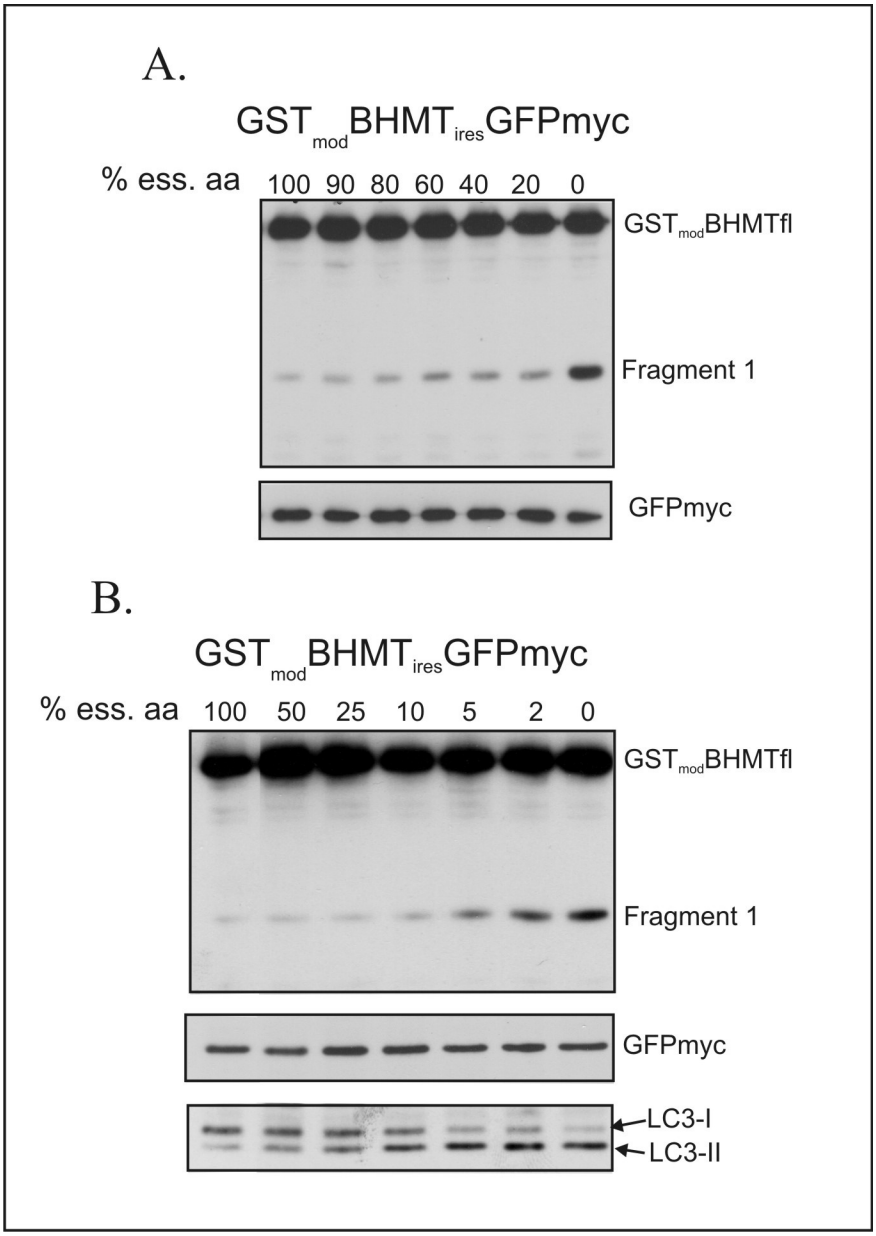
A.
GST mod BHMT ires GFPmyc
% ess. aa
100 90 80 60 40 20 0
GST mod BHMTfl
Fragment 1
GFPmyc
B.
GST mod BHMT ires GFPmyc
% ess. aa
100 50 25 10 5 2 0
GST mod BHMTfl
Fragment 1
GFPmyc
LC3-I
LC3-II

Amino acid	Adult Reference Range (uM)	DMEM (uM)
Leucine	72-201	450
Isoleucine	30-108	415
Valine	119-336	451
Arginine	15-128	848
Histidine	72-124	203
Lysine	116-296	625
Methionine	10-42	116
Phenylalanine	35-85	215
Threonine	60-225	449
Tryptophan	10-140	44
Cysteine	5-82	145
Tyrosine	34-112	308

*Reference values from Hospitals In-Common Laboratory, Inc. Version 15-Jan-2004

Table 4. Comparison of amino acid levels in DMEM with adult plasma reference ranges. Levels of essential amino acids in DMEM compared to levels in human adult plasma reference ranges. Normal reference ranges are from Hospitals in Common Laboratory, Inc. Version 15-Jan-2000.

concentration of essential amino acids had decreased by more than 80% of normal culture conditions.

To further define the percentage of essential amino acids required for BHMT fragmentation, HEK293 cells expressing the $GST_{mod}BHMT_{IRES}GFP$ reporter were tested in conditions as before, but with a titration of essential amino acids more specific for the ranges between 25% and 0%. Significant accumulation of BHMT fragment 1 was noted only when essential amino acids fell below 10% (Fig. 28B). Expression of endogenous LC3 at each of the titration points correlate well with the BHMT assay (Fig. 28B bottom panel). On careful examination of the amino acid composition in DMEM, it was noted that for cultured cells, amino acid levels in DMEM are up to 6 times greater than the mean reference values for circulating amino acids in human plasma (Table 4). Therefore, the window of response noted with the BHMT assay is likely within the physiological range.

Some of the essential amino acids play a regulatory role in macroautophagy, based on inhibition of intracellular proteolysis. In rat hepatocytes cultured from fetal, suckling or weaned animals, Bloomaart et al. showed that intracellular levels of leucine, isoleucine, lysine, phenylalanine and tyrosine increased in linear fashion in response to extracellular levels of the same[73]. Amino acids within this group effectively decreased proteolysis independent of hormonal levels. These experiments are difficult to perform and are not necessarily specific for macroautophagy. The BHMT assay provides an excellent means to test the effects of these and the other essential amino acids on the induction of macroautophagy. To test the response of the BHMT assay to small changes in the amino acid content of the media, cultured cells expressing $GST_{mod}BHMT_{IRES}GFP$

were deprived of select essential amino acids, while all other amino acids were maintained at DMEM levels. Removal of either leucine or arginine alone was able to moderately induce autophagy, while loss of isoleucine, valine, lysine, methionine, phenylalanine or tryptophan caused only a mild increase in fragmentation (Fig. 29). The removal of the three branched-chain amino acids as a group induced autophagy to levels approaching the loss of all essential amino acids. No change was noted with the removal of histidine or threonine (Fig. 29). Levels of LC3-I and LC3-II in the selectively-starved extracts are shown by western blotting with antibody against endogenous LC3, showing some response to the loss of individual amino acids, although with less sensitivity (Fig. 29). A caveat that must be considered in the interpretation of these results is that although amino acid depletion was presumed, intracellular levels of amino acids were not measured in this experiment. However, it has been shown that intracellular levels of free branched chain amino acids decrease 90% with a 30 minute starvation period in HEK293 cells[74]. The data from this experiment suggest that full induction of macroautophagy needs the additive effects of a small number of essential amino acids, particularly the branched chain amino acids. The BHMT assay provides a degree of sensitivity to look at small changes in macroautophagy not possible with the LC3 assay. Future experiments using the BHMT assay will be able to determine what combination of essential amino acids is sufficient to induce a full macroautophagy response.

3.1.2.4. The BHMT assay is functional in multiple cell lines

The BHMT assay depends on the activity of a lysosomal cathepsin to cleave BHMT in a specific region of the protein to generate fragment 1. Multiple isoforms of cathepsins are expressed to varying degrees in different cell types[75]. To determine if

Figure 29. Sensitivity of the BHMT assay to single essential amino acids. HEK293 cells expressing $GST_{mod}BHMT_{IRES}GFP$ were incubated in specially prepared DMEM media missing one or more essential amino acids for 6 hours. A. The BHMT assay was tested for sensitivity to the loss of leucine, isoleucine, and valine individually and in combination. B. The BHMT assay was tested for sensitivity to the loss of each of the following essential amino acids: arginine, histidine, lysine, methionine, phenylalanine, threonine, and tryptophan. A.and B. Western blot of GFP is shown as a control of reporter expression in middle panel. Bottom panel is a western blot with antibody against endogenous LC3 from same samples that were starved for individual amino acids.

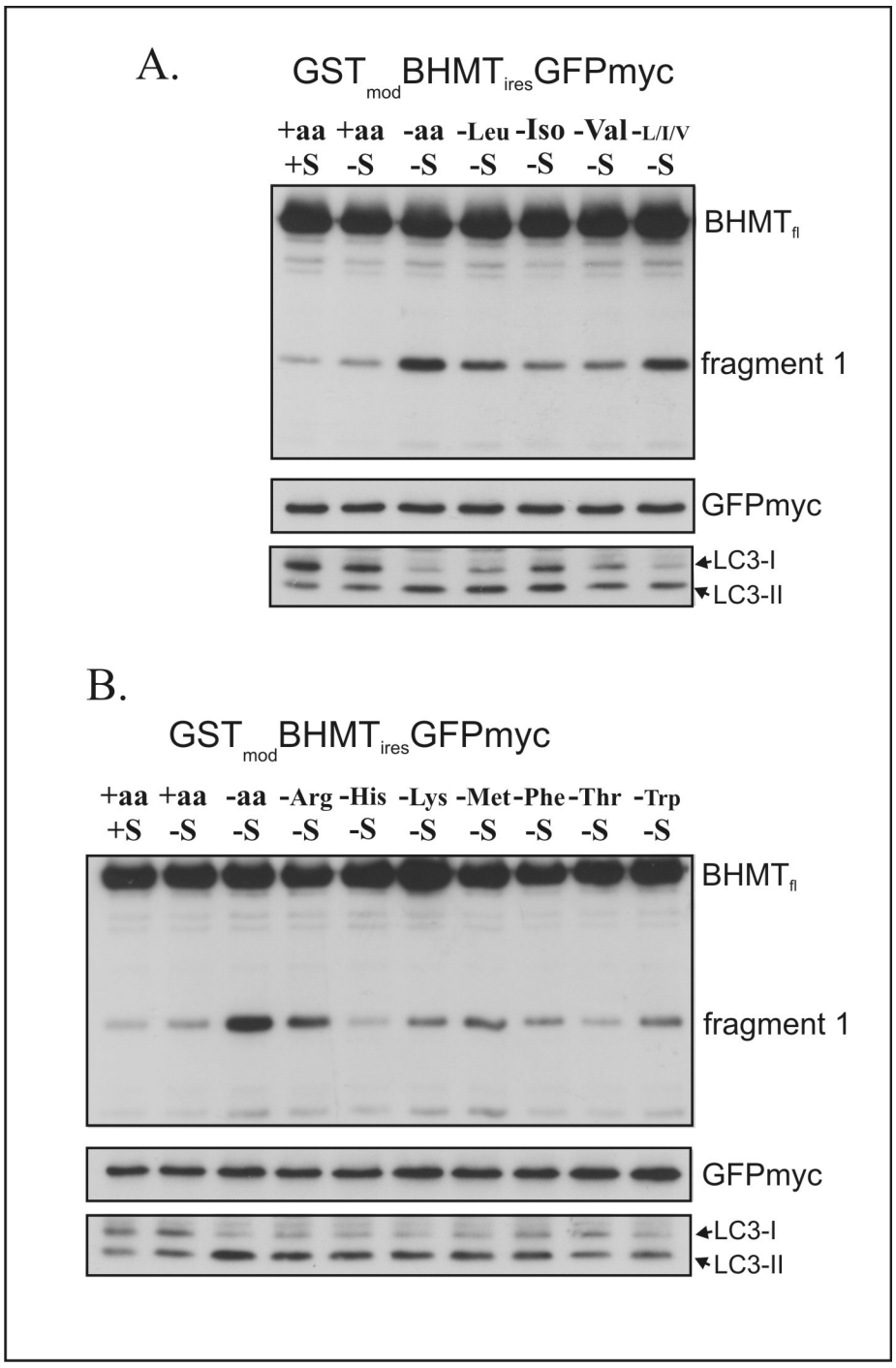
A.
GST mod BHMT ires GFPmyc
+aa +S
+aa -S
-aa -S
-Leu -S
-Iso -S
-Val -S
-L/I/V -S
BHMT fl
fragment 1
GFPmyc
LC3-I
LC3-II
B.
GST mod BHMT ires GFPmyc
+aa +S
+aa -S
-aa -S
-Arg -S
-His -S
-Lys -S
-Met -S
-Phe -S
-Thr -S
-Trp -S
BHMT fl
fragment 1
GFPmyc
LC3-I
LC3-II

the BHMT assay was cell type specific or capable of functioning in a broad range of cells, the $GST_{mod}BHMT_{IRES}GFP$ reporter was transiently transfected into an array of cells from human, mouse, and rat (Fig. 30 and data not shown). Cells were starved of essential amino acids and serum for 6 hours to induce autophagy, and the autophagy inhibitors 3MA and chloroquine were added to starved cells to validate that fragmentation was due to macroautophagy. After treatment, cells were harvested and WCE and glutathione pull-downs were prepared for western blotting as before. The expression of GFP by western blotting is shown as a control for transfection of the BHMT reporter (Fig. 30, second row of panels from the top). Western blot with antibody against endogenous LC3 is included for comparison and for validation of chloroquine dosage (Fig. 30, third row of panels from top). Cancer cells were chosen with known mutations or deficiencies that have been reported to effect macroautophagy. Immortal, but not transformed cells of mouse origin, NIH3T3 and C2C12, were included to test the efficacy of the BHMT assay in a non-tumor cell setting. Starvation induced BHMT fragmentation was observed in all of the cell lines selected (Fig. 30 top panels). However, the degree of increase over basal varied between cell lines. In each case, BHMT fragmentation was sensitive to 3MA and chloroquine, indicating that accumulation of fragment it was due to an induction of autophagy.

In summary, the BHMT assay is effective in transformed and non-transformed cells of varying species. In the present form, its usefulness is limited to cells in culture that can be transfected to a level of efficiency that allows sufficient expression of the reporter. Fragmentation of BHMT accurately reflects the state of macroautophagy when LC3-II levels alone are ambiguous.

Figure 30. The BHMT assay is functional in multiple cell lines.

$GST_{mod}BHMT_{IRES}GFP$ was transiently transfected into T98G cells, MCF7 cells, H1299 cells, NIH3T3 cells, and C2C12 cells, which were tested under conditions known to induce and inhibit macroautophagy for 6 hours. Levels of BHMT fragment 1 increased in all cells with amino acid starvation and were inhibited by the autophagy inhibitors 10mM 3MA and 100μM chloroquine. Western blot of GFP is shown as a control for transfection efficiency between conditions. Western blot for endogenous LC3 is shown in the bottom panel for comparison.

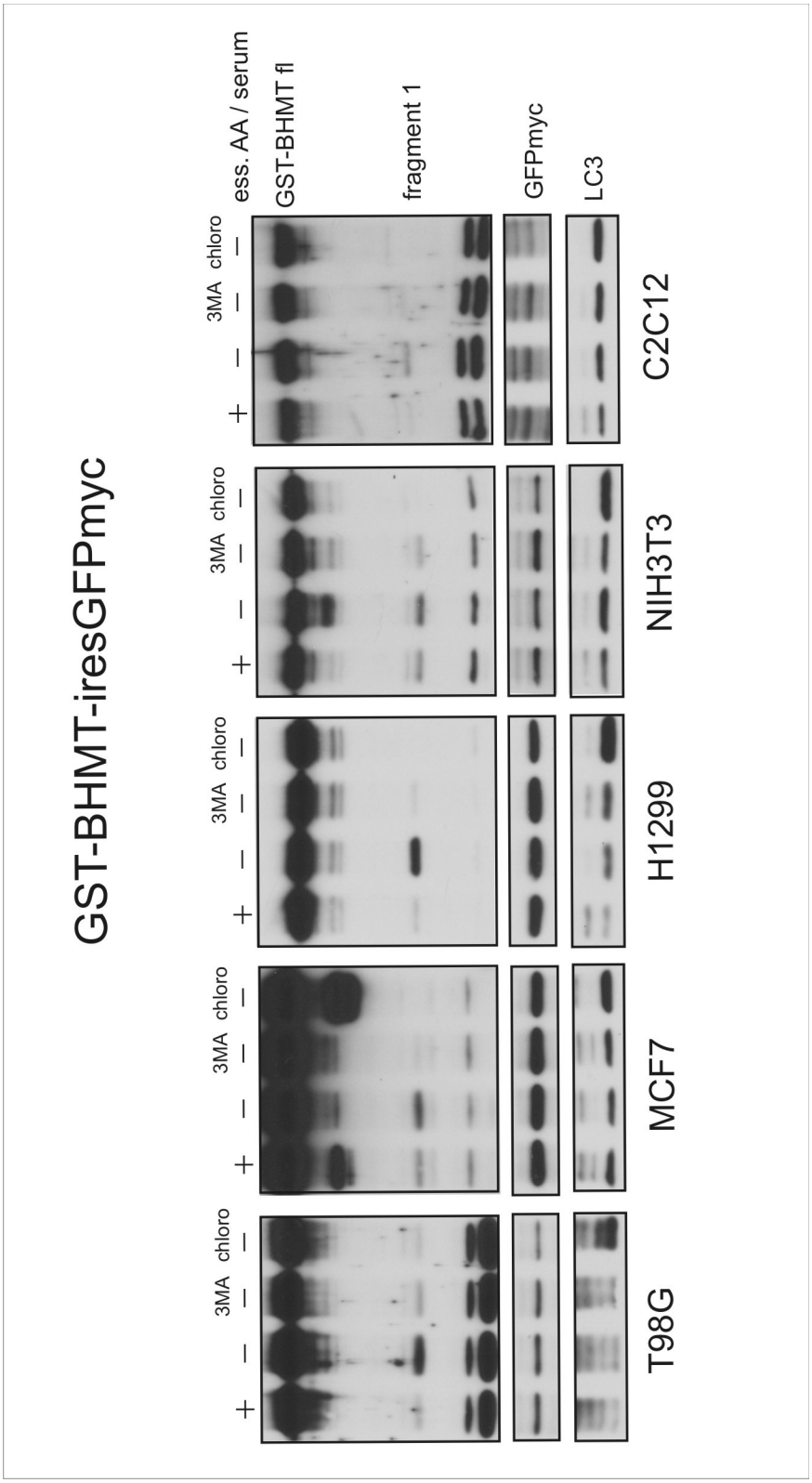
GST-BHMT-iresGFPmyc
ess. AA / serum
3MA
chloro
GST-BHMT fl
fragment 1
GFPmyc
LC3
T98G
MCF7
H1299
NIH3T3
C2C12

3.1.2.5. Example of the BHMT and LC3 assays with W7

Ultimately, the value of the BHMT assay lies in its ability to provide an endpoint assessment of autophagy. Its use is not mutually exclusive with the LC3 assay which is valued for its specificity in autophagosome formation, but complements the LC3 assay by providing a read-out for the autolysosomal completion of autophagy. By using these two assays together, one can gain insight into how a signaling pathway or experimental condition affects the autophagic pathway. To demonstrate the value of using both an endpoint assay and a midpoint assay to assess regulation of autophagy, examples in the literature were sought for which the BHMT assay would bring clarification.

The role of Ca^{2+}/calmodulin-dependent protein kinases in the regulation of autophagy is ambiguous, at least in part due to the difficulties of measuring autophagy. Early in the study of autophagy, one method loaded cells with [^{3}H]raffinose and measured the sedimentable [^{3}H]raffinose to assess autophagic sequestration. With this method, a study in 1992 reported that Ca^{2+}/CamK-II activity inhibited autophagy, and that autophagy was restored by the use of the calmodulin inhibitor W-7[76]. Later, the same group published that W-7 had little or no effect on autophagy[77]. Various other studies have suggested a role for the Ca^{2+}/calmodulin dependent kinase, Death-Associated Protein kinase (DAPk) and the Ca^{2+}/calmodulin-dependent protein kinase, elongation factor 2-kinase (EF2-Kinase) in the induction of autophagy[78, 79]. Methods used to monitor autophagy in these studies included electron microscopy, monodansylcadaverin (a marker of acidic vesicles), and LC3. The conflicts in the conclusions of these studies and the ambiguities of the methods used to measure protein

autophagy raise questions about the role of calcium and the Ca^{2+}/calmodulin-dependent kinases in autophagy.

Based on what has been reported, the calmodulin inhibitor W-7 could inhibit, increase, or have no effect on autophagy. The BHMT assay in conjunction with the LC3 assay may be able to resolve whether Ca^{2+}/calmodulin-dependent protein kinases are necessary for the induction of autophagy. W-7 was chosen for this experiment because its effect on EF2 can be easily assessed by western blotting. During amino acid starvation, EF2 Kinase activity increases in a Ca^{2+}/calmodulin dependent manner, and increases the phosphorylation of EF2. The activity of EF2 Kinase and the effectiveness of W-7 can be determined by the use of a phospho-specific antibody that recognizes EF2 (Fig. 31, bottom panel). To test the effects of W-7 on autophagy, W-7 was added to HEK293 cells stably expressing either GST-BHMT or HA-LC3B reporter and maintained in either complete media or starvation media for six hours. Normalized aliquots of cell extracts were pulled down with either glutathione agarose of antibody to HA and prepared for western blotting. In the extracts from HA-LC3B cells, LC3B-II levels were the same between the control and W-7 treated cells (Fig. 31, second panel from the top). Based on the LC3B assay alone, W-7 appears to have no effect on autophagy. In contrast, W-7 strongly blocked the generation of BHMT fragment 1 in starvation conditions (Fig. 31). The BHMT assay unambiguously demonstrates that W-7 inhibits autophagy. Together, the results show that the inhibitory effects of W-7 on autophagy do not interfere with the early steps of LC3 processing and autophagosome formation, but appear to be at a later step,

Figure 31. Example of BHMT and LC3B assays with the calmodulin inhibitor W7. HEK293 cells stably expressing either $GST_{mod}BHMTmyc_{4.1}$ or HA-LC3B-myc were treated for 6 hours in complete or starvation media, with the calmodulin inhibitor W7 (1μM). Cell extracts were pulled down with glutathione agarose or antibody to HA and prepared for western blotting. A. Western blot in top panel shows BHMT fragmentation upon amino acid starvation (lane 2) which is inhibited by W7 (lane 4). Western blot showing LC3B is in bottom panel. LC3B-II levels increase with starvation in control and W7-treated cells in a similar manner. B. Western blot of cell extracts from $GST_{mod}BHMTmyc_{4.1}$ and HA-LC3B-myc cell extracts with a phospho-specific antibody that recognizes phosphorylated eEF2. Phosphorylation of EF2 is decreased in cells treated with W7.

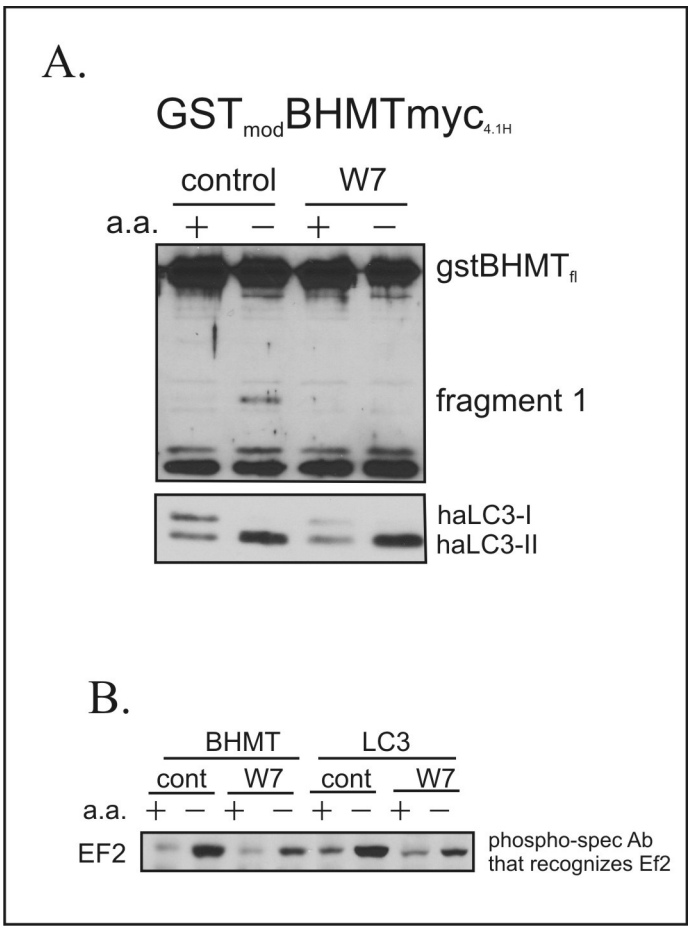
A.
GST mod BHMTmyc 4.1H
control
W7
a.a. + − + −
gstBHMT fl
fragment 1
haLC3-I
haLC3-II
B.
BHMT
LC3
cont
W7
cont
W7
a.a. + − + − + − + −
EF2
phospho-spec Ab
that recognizes Ef2

In conclusion, the BHMT assay is a novel endpoint assay for macroautophagy, whose specificity has been validated pharmacologically and by shRNA targeting known autophagy genes. Its effectiveness has been demonstrated in multiple cell lines. The BHMT assay alone, or in combination with the LC3 assay, provides a unique method to study macroautophagy in cell culture.

3.2. The BHMT assay and higher order structure

3.2.1. The carboxy terminus of BHMT is important for generation of fragment 1

In the process of developing the BHMT assay, it was evident that the generation of fragment 1 was lost with severe modification or truncation of the carboxy-terminus. It was originally expected that a carboxy-terminal fragment might be generated from a BHMT reporter, similar to the peptide of rat BHMT originally identified by mass spectrometry. To help capture what was expected to be the carboxy-terminal fragment, constructs were made that fused a GST epitope tag to the carboxy-terminus of BHMT, with a variety of amino-terminus epitope tags. Two examples are shown (Fig. 32A). No fragmentation of the HA-BHMT-GST reporter was observed in any of three experimental conditions: incubation in complete media, starvation media, or complete media with rapamycin (Fig. 32B, lanes 4-6). When the amino-terminal GST-tagged BHMT reporter was fused to a second carboxy-terminal GST tag to create a GST-BHMT-GST reporter, the presence of a carboxy-terminal GST was detrimental to generation of the observed fragment 1, even though the fusion protein expressed at approximately the same level as GST-BHMT-myc (Fig. 32, lanes7-9). The data led to a hypothesis that a functional carboxy-terminus was important for generation of GST-BHMT fragment 1.

Figure 32. Carboxy-terminus of BHMT is important for generation of fragment 1. A. Schematic of three early BHMT reporters: GST-BHMT-myc, HA-BHMT-GST and GST-BHMT-GST. B. Each reporter was expressed in HEK293 cells and incubated in complete media, media starved of essential amino acids and serum, or media with 40nM rapamycin for 5 hours. Western blot of glutathione agarose pull-downs shows that fragment 1 only accumulated in cells transfected with the GST-BHMT-myc reporter (lanes 1-3). Cells transfected with a GST epitope tag at the carboxy-terminus did not generate observable fragmentation with either amino acid and serum starvation or with rapamycin (lanes 4-9).

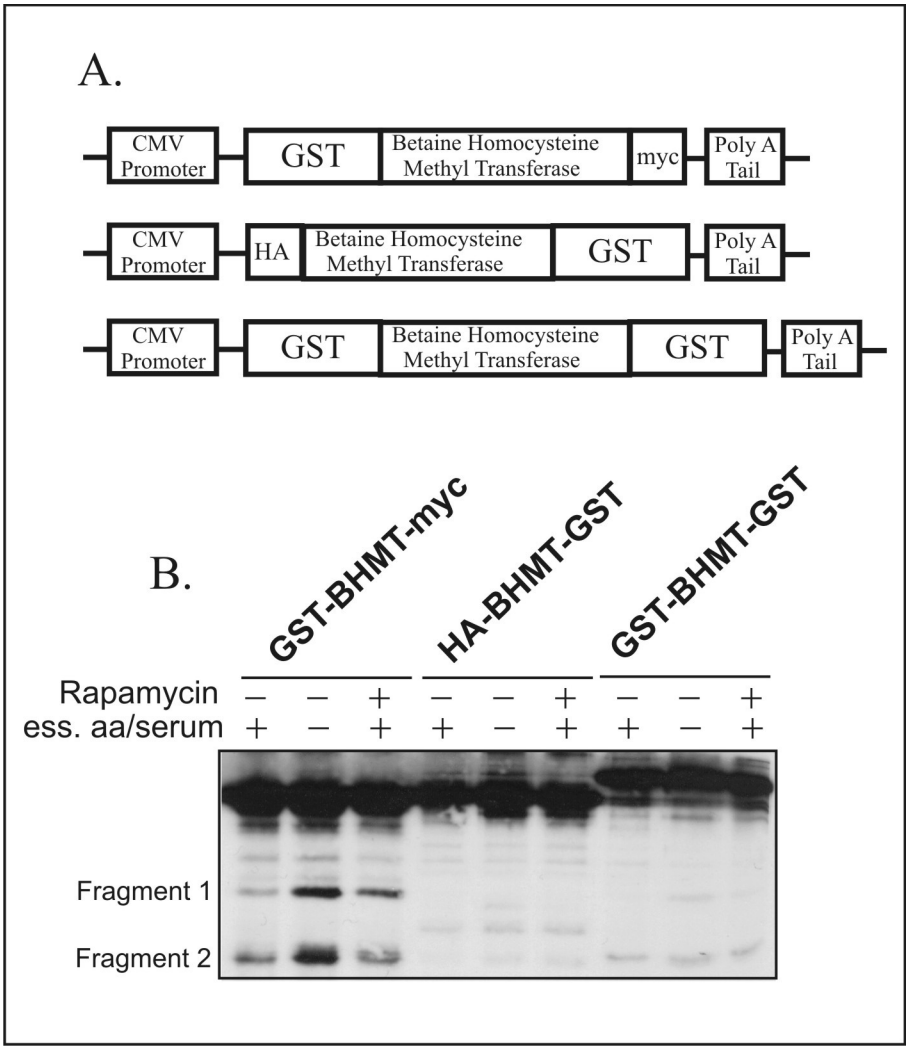
A.
CMV Promoter
GST
Betaine Homocysteine Methyl Transferase
myc
Poly A Tail
CMV Promoter
HA
Betaine Homocysteine Methyl Transferase
GST
Poly A Tail
CMV Promoter
GST
Betaine Homocysteine Methyl Transferase
GST
Poly A Tail
B.
GST-BHMT-myc
HA-BHMT-GST
GST-BHMT-GST
Rapamycin
ess. aa/serum
Fragment 1
Fragment 2

The original GST-BHMT$_{wt}$ is in fact a 9 amino acid truncation mutant that could correctly be designated ΔC9. It seemed likely that if the carboxy-terminus was important, restoring the carboxy terminus to full length might make BHMT a better reporter. Conversely, it was predicted that a more severe carboxy-terminal truncation of BHMT might make a poorer reporter. To test this, truncated GST-BHMT$^{\Delta C142}$ was made that deleted 142 amino acids from the carboxy-terminus. This construct did not produce fragments with amino acid starvation and expressed poorly, most likely due to instability (data not shown). Separately, a GST-BHMT full length reporter was made that restored the nine carboxy-terminal amino acids that had been truncated in the original reporter. The full length reporter produced fragments 1 and 2 in a manner identical to the original reporter, suggesting that the moderate ΔC9 truncation of the original reporter was tolerated without adversely affecting the readout (Fig. 33). For the remainder of this document, the term full length, original, or GST-BHMT$_{wt}$ will refer to the original ΔC9 construct.

The above data raised questions about the nature of the carboxy-terminal and its role in the generation of GST-BHMT fragment 1. How much of the carboxy-terminus could be truncated without losing the ability to generate fragment 1? To answer this question, a number of progressive carboxy-terminus truncation mutants of BHMT were produced. Each mutant was compared to the original GST-BHMT$_{wt}$ construct in the ability to generate fragment 1 when expressed in cells starved of essential amino acids. The autophagy inhibitors 3MA and bafilomycin A1 were tested with each mutant to validate that any fragment generated from the truncation mutants was due to macroautophagy. GST-BHMT$^{\Delta C24}$ generated fragment 1 in a manner identical to the

Figure 33. BHMT assay with full length GST-BHMT. HEK293 cells were transfected with either the original BHMT reporter (ΔC9) or with a carboxy-terminal restored full length GST-BHMT. After starvation of essential amino acids and serum, cell extracts were pulled down with glutathione and prepared for western blotting. Both BHMT reporters generated fragment 1 upon amino acid starvation in a similar manner. Minor truncation of original reporter is not detrimental to fragment formation.

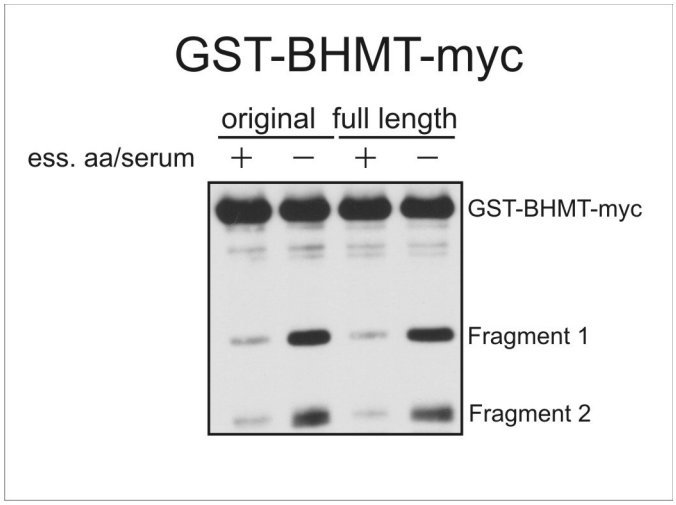
GST-BHMT-myc
original
full length
ess. aa/serum
+
−
+
−
GST-BHMT-myc
Fragment 1
Fragment 2

Figure 34. The BHMT assay with truncation mutants: ΔC24 and ΔC51. Truncation mutants of BHMT were created with a PCR and sub-cloning strategy to remove either 24 or 51 amino acids from the carboxy-terminus. BHMT and the truncation mutants were transfected into HEK293 cells and treated with starvation media to induce autophagy or starvation media with the autophagy inhibitors 10mM 3MA or 100nM bafilomycin A1. Compared to control BHMT, truncation of 24 amino acids from the carboxy-terminus of BHMT does not prevent generation of fragment 1 with starvation (lanes 3-6), but fragment 1 does not accumulate in starved cells expressing ΔC51 (lanes 7-9).

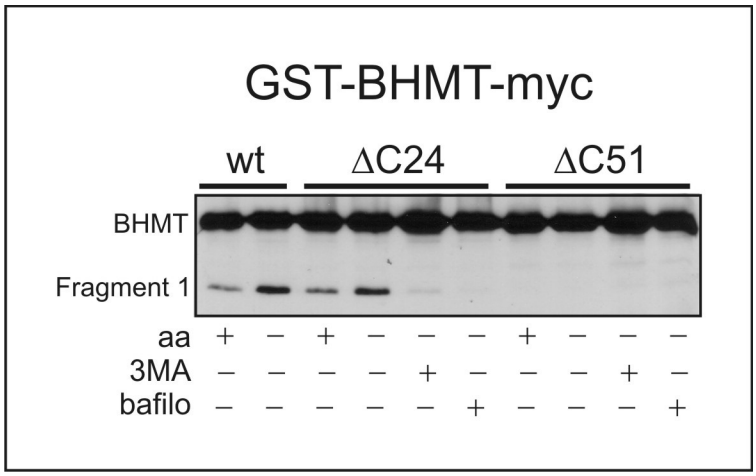
GST-BHMT-myc
wt
ΔC24
ΔC51
BHMT
Fragment 1
aa + − + − − − + − − −
3MA − − − − + − − − + −
bafilo − − − − − + − − − +

control (Fig. 34, lanes 3-6). However, deletion of an additional 27 amino acids in GST-BHMT$^{\Delta C51}$ created a truncation mutant that failed to generate fragment 1 under amino acid starvation conditions, in spite of the fact that its expression and stability was equal to either control or ΔC24 (Fig. 34, lanes 7-9). Further truncations (ΔC92 and ΔC115) produced proteins that expressed poorly and were likely unstable and degraded (data not shown). The data confirm that the carboxy terminus of BHMT is important in the generation of fragment 1.

Rat BHMT exists as a homo-tetramer. Each subunit is an $(\alpha/\beta)_8$ barrel with an extended dimerization arm, a hook region, and a linker region leading to a long alpha-helix at the carboxy-terminus (Fig. 35). The carboxy-terminus of BHMT is important for the interaction between subunits, and oligomerization is essential for enzymatic activity of the endogenous enzyme[80]. The two subunits that form a dimer interact with each other through both the dimerization arm, which extends from one subunit and imbeds in the structure of its dimer partner, and the hook, a region of intertwining complementary strands between the two subunits. The long carboxy-terminal alpha-helix of each subunit interacts with a subunit of the second dimer pair, linking the two dimers to form the complete tetramer. It is likely that truncation of the BHMT carboxy-terminus, or fusion of bulky epitope tags to the carboxy end, might disrupt the ability of the subunits to interact.

This raised a question about whether it was catalytic activity or oligomerization of BHMT that might be important to be recognized as a substrate for the autophagy. If activity was important, then a catalytically inactive BHMT mutant should not generate fragment 1 in starvation conditions. BHMT is a metabolic enzyme that transfers one

Figure 35. BHMT structure. BHMT structure is shown with interaction of 3 of the 4 subunits. BHMT is a dimer of dimers. Two subunits interact with each other through the dimerization arm (as labeled) and hook regions (shown in enlarged box). The carboxy-terminal alpha-helix of each subunit then interacts with a subunit of the other dimer to form a tetramer. Oligomerization of subunits is required for an active enzyme. The truncations that affect the original BHMT reporter (ΔC9) and the ΔC24 mutant are in the carboxy-terminal alpha helix as labeled on the dark blue subunit. The ΔC51 truncation and the W352A mutation are in the hook region of the dimerization arm as labeled. The region of the disordered L2 loop that is likely cleaved to generate fragment 1 is labeled in red.

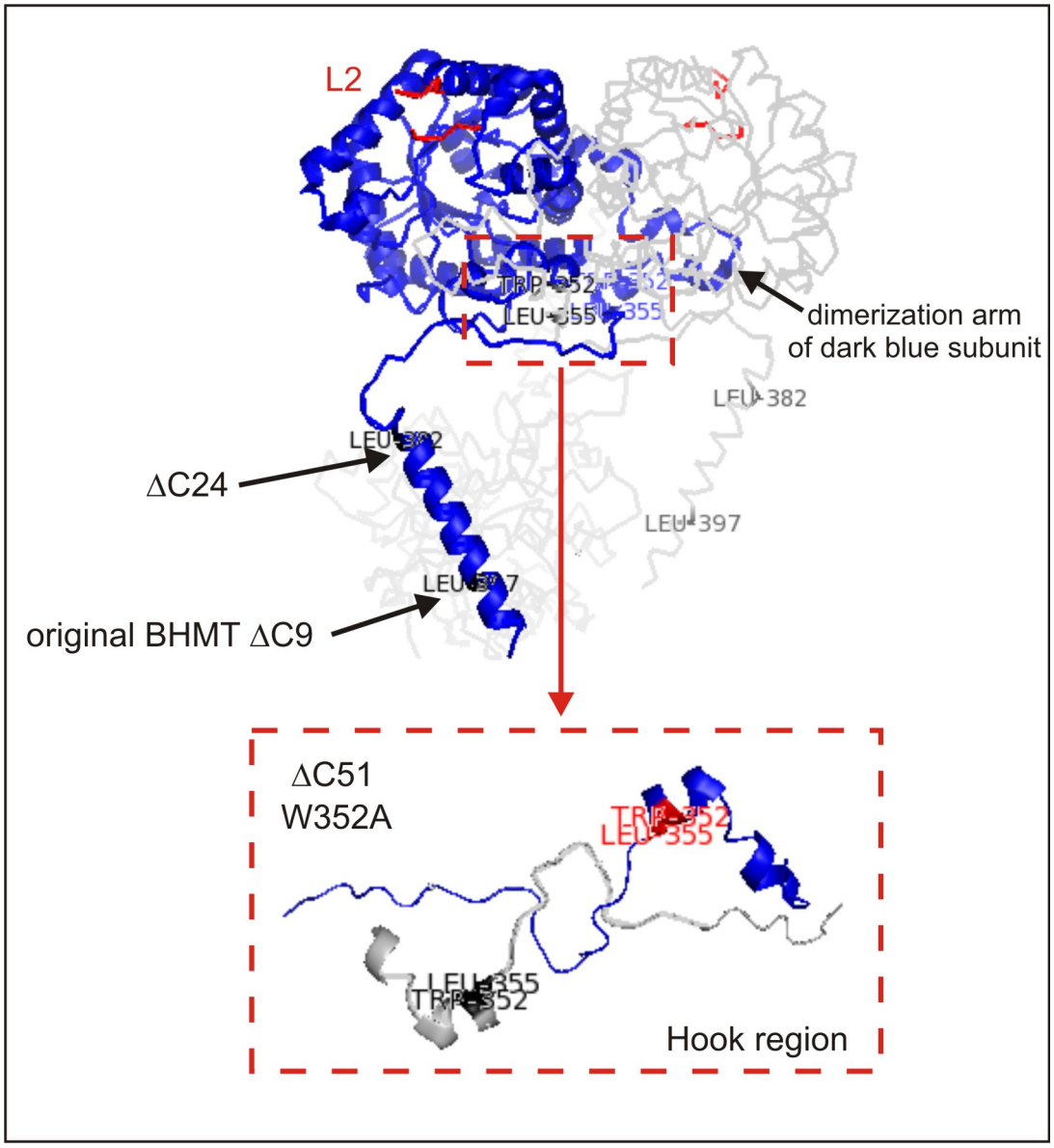
L2
dimerization arm
of dark blue subunit
ΔC24
original BHMT ΔC9
ΔC51
W352A
Hook region

methyl group from betaine to homocysteine to generate methionine. It contains a Zn^{2+} ion, coordinated by three cysteine residues (C217, C299 and C300) which are necessary for its activity[81]. To test whether catalytic activity of BHMT effected its ability to be processed by macroautophagy, a mutation reported to kill catalytic activity, C217A[81], was introduced by site directed mutagenesis. HEK293 cells transiently transfected with GST-BHMT-myc and the mutant GST-BHMT^{C217A}myc were incubated for 4 hours in complete media, starvation media, or starvation media with the autophagy inhibitor 3MA. After the cells were harvested, glutathione pull downs of cell extracts were processed for western blotting. Both control and GST-BHMT^{C217A} reporters generated similar levels of starvation induced fragment 1 that was inhibited by the autophagy inhibitor 3MA (Fig. 36). These data suggest that catalytic activity of BHMT does not play a role in its ability to generate fragment 1 in starved cells.

It appeared there was correlation between the ability to generate fraction 1 and the ability to form multimers. The results obtained with the ΔC51 truncation of BHMT initiated a search for a single mutation that would affect oligomerization without truncating large regions of the protein. A study by Szegedi and Garrow found that mutation of a tryptophan in the dimerization arm of BHMT, W352A, impaired the stability of subunit dimerization[80]. The W352A point mutation was made in the original GST-BHMT reporter so that oligomerization would be disrupted. The W352A mutant was expressed at levels identical to control GST-BHMT, and cells were cultured under the same conditions described in Figure 34. Like the ΔC51 truncation mutant, the W352A point mutant did not generate fragment 1 under starvation conditions (Fig. 37). These data show that the predicted ability of BHMT to oligomerize correlates with the

Figure 36. Catalytic activity of BHMT is not required for fragmentation. The C217A mutation in BHMT is known to kill enzymatic activity, and was introduced in BHMT by site directed mutagenesis. HEK293 cells were transfected with either control BHMT or $BHMT^{C217A}$ and treated with starvation media to induce autophagy or starvation media with 10mM 3MA to inhibit autophagy for 6 hours. Cells were extracted and prepared for western blotting as previously described. The control and C217A mutant BHMTs both generated fragment 1 in starvation conditions that was inhibited by 3MA.

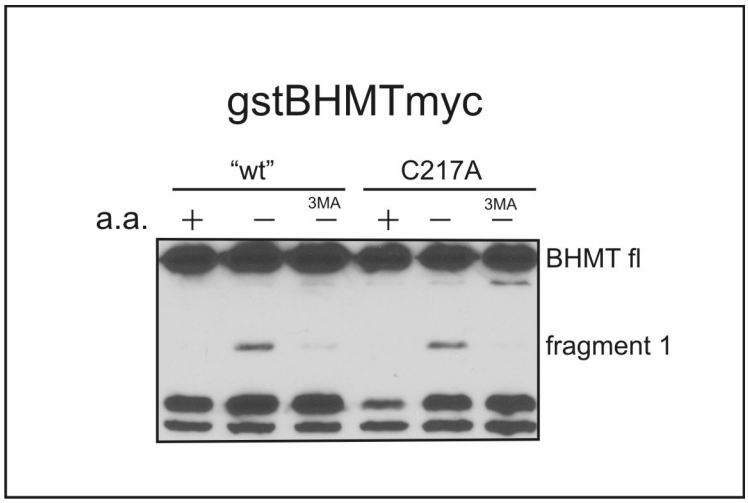
gstBHMTmyc
"wt"
C217A
a.a.
+
−
3MA
−
+
−
3MA
−
BHMT fl
fragment 1

Figure 37. The BHMT^{W352A} point mutant in the BHMT assay. A mutation, W352A, was introduced into BHMT by site directed mutagenesis that was reported to prevent oligomerization and activity. HEK293 cells were transfected with either control or GST-BHMT^{W352A} mutant and treated to conditions identical to the previous experiment with the truncation mutants (Fig. 34). Cells were extracted and prepared for western blotting as previously described. Fragment 1 did not accumulate in the BHMT^{W352A} mutant extracted from amino acid starved cells.

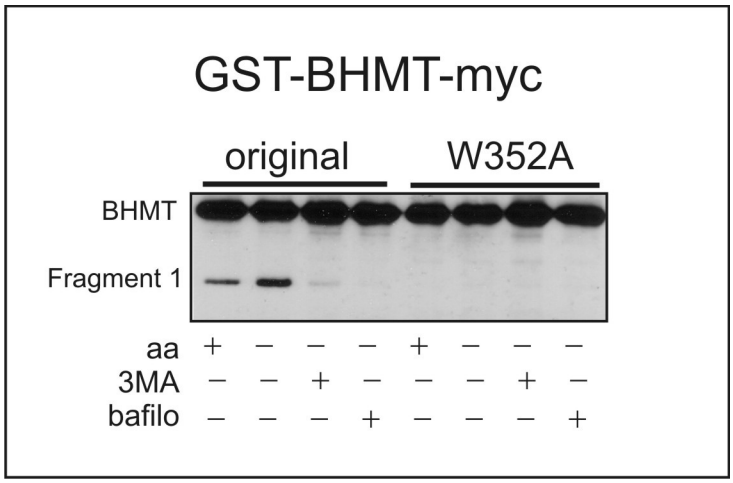
GST-BHMT-myc
original
W352A
BHMT
Fragment 1
aa + − − − + − − −
3MA − − + − − − + −
bafilo − − − + − − − +

ability to generate intralysosomal fragment 1.

It was necessary to determine if the GST-tagged BHMT mutants could or could not oligomerize as predicted. To do so, the original BHMT cDNA was sub-cloned downstream of a HA epitope tag and co-expressed in HEK293 cells with each of the GST-tagged BHMT constructs. To demonstrate interaction, glutathione beads were added to cell extracts to pull out the GST-BHMT mutants, and the beads were gently washed so as not to disrupt interacting proteins. The purified GST-BHMT complex was then run on SDS-PAGE, transferred to PVDF membrane, and probed with an antibody to the HA epitope tag. Expression levels of the GST and HA tagged proteins show that all expressed at equivalent levels (Fig. 38, bottom two panels). As expected, the two mutants that were able to generate fragment 1, GST-BHMTwt and GST-BHMT$^{\Delta C24}$, were able to pull down HA-BHMT$_{wt}$, indicating multimerization (Fig. 38, lanes 1 and 2). In contrast, the two mutants that disrupted the hook region of the dimerization arm by either truncation (GST-BHMT$^{\Delta C51}$) or mutation (GST-BHMT^{W352A}) were either unable to pull down HA-BHMT$_{wt}$ in the case of the former, or pulled down very small amounts of HA-BHMT$_{wt}$ in the case of GST-BHMT^{W352A} (Fig. 38, lanes 3 and 4). The ability of GST-BHMT^{W352A} to pull down a small amount of HA-BHMT$_{wt}$ is consistent with the published report that the W352A mutant is able to form dimers, but in complexes that are less stable than wild-type BHMT.

The data above demonstrate that the ability of the BHMT mutants to assemble inversely correlates with the ability to generate fragment 1 with starvation. How does oligomerization affect the ability of BHMT to generate fraction 1 with starvation? Two possibilities are likely: 1) Quaternary structure of BHMT is required for the lysosomal

Figure 38. The carboxy-terminal of BHMT is important for oligomerization. HEK293 cells were co-transfected with HA-BHMT and each of the GST-tagged BHMT mutants: wt, ΔC24, ΔC51, and W352A. After allowing time for expression, cells were harvested and cell extracts were processed for glutathione pull-down and western blot. Membrane was probed with antibody against HA to demonstrate interaction between subunits. Interacting subunits were demonstrated between HA-BHMT and GST-BHMT (lane 1) and HA-BHMT and GST-ΔC24 (lane 2). No interaction was found between HA-BHMT and GST-ΔC51 (lane 3). A small amount of GST-W352A associated with HA-BHMT, consistent with the ability of this mutant to form unstable dimers (lane 4). Each mutant expressed to equivalent levels as shown in the bottom two panels.

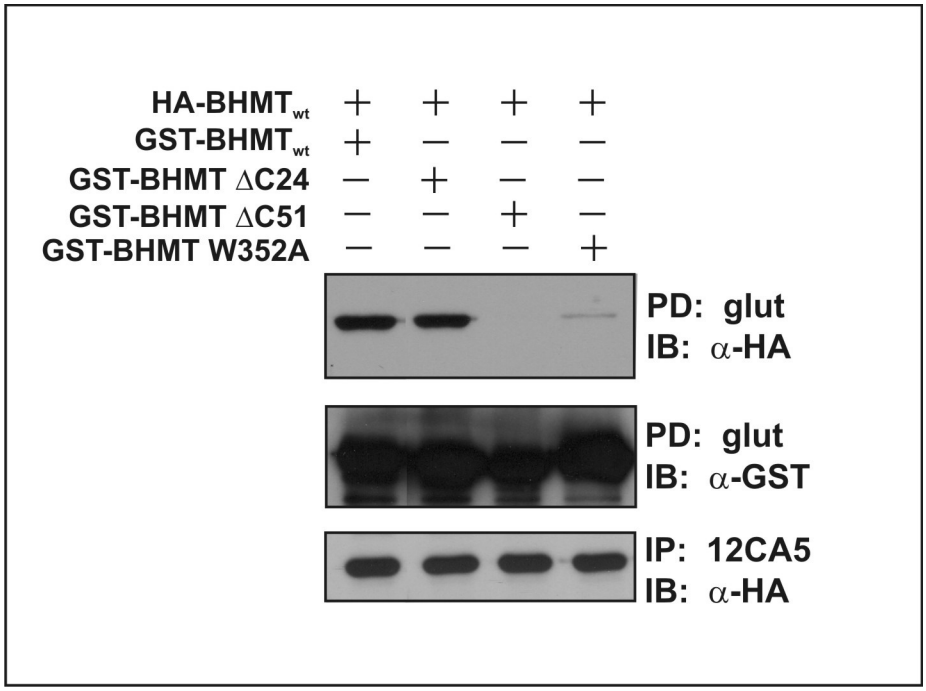
HA-BHMT$_{wt}$ + + + +
GST-BHMT$_{wt}$ + − − −
GST-BHMT ΔC24 − + − −
GST-BHMT ΔC51 − − + −
GST-BHMT W352A − − − +
PD: glut
IB: α-HA
PD: glut
IB: α-GST
IP: 12CA5
IB: α-HA

cathepsin to bind, recognize and cut the L2 region to generate fragment 1, or 2) Quaternary structure of BHMT is important to be recognized by the autophagic machinery and for import into autophagosomes.

3.2.2. BHMT$^{\Delta C51}$ is in autophagosomes

To distinguish between these two possibilities, an assay was designed that would test for the presence of BHMT within autolysosomes/autophagosomes. If both BHMT^{wt} and BHMT$^{\Delta C51}$ trafficked inside of autolysosomes, then the first explanation would be favored. However, if BHMT$^{\Delta C51}$ was not found in autolysosomes, then the data would suggest that quaternary structure was important for cargo selection. The accomplishment of this aim would require two steps. First, a population of intact autophagosomes would be fractionated from cultured cells expressing either GST-BHMT^{wt} or GST-BHMT$^{\Delta C51}$. Second, autophagosome/autolysosome associating proteins such as BHMT would be digested with a protease, with or without a membrane-disrupting detergent. This protection assay would determine if ΔC51 was enclosed within a membrane compartment (Fig. 40A). Resistance to proteolytic digestion in the absence of a detergent would indicate the target protein is enclosed and protected in a membrane structure.

The isolation and enrichment of intact autolysosomes was challenging due to their transient nature, low abundance, and high rate of turnover within the cell. To increase the abundance of autophagosomes and autolysosomes, cells were starved of essential amino acids for 12 hours with protease inhibitors leupeptin and E64d to slow lysosomal proteolysis and turnover of the autolysosomal population. GST-BHMT and HA-LC3B-expressing HEK293 cells treated in this manner were collected, disrupted by dounce

Figure 39. BHMT on a Sucrose gradient. A. Schematic of the sucrose gradient protocol. Transfected HEK293 cells are extracted and processed by differential centrifugation to isolate the light membrane fraction (LMF). The LMF is then loaded on a discontinuous sucrose gradient for ultra-centrifugation. Fractions are collected by upward displacement, numbered 1 at the top to 11 at the bottom of the gradient. Fractions are then analyzed by either glutathione pull-down, immunoprecipitation, or TCA precipitation. B. BHMT fragment 1 co-fractionates with the lysosomal marker LAMP1 in fractions 6 and 8. LC3B peaks in fraction 5.

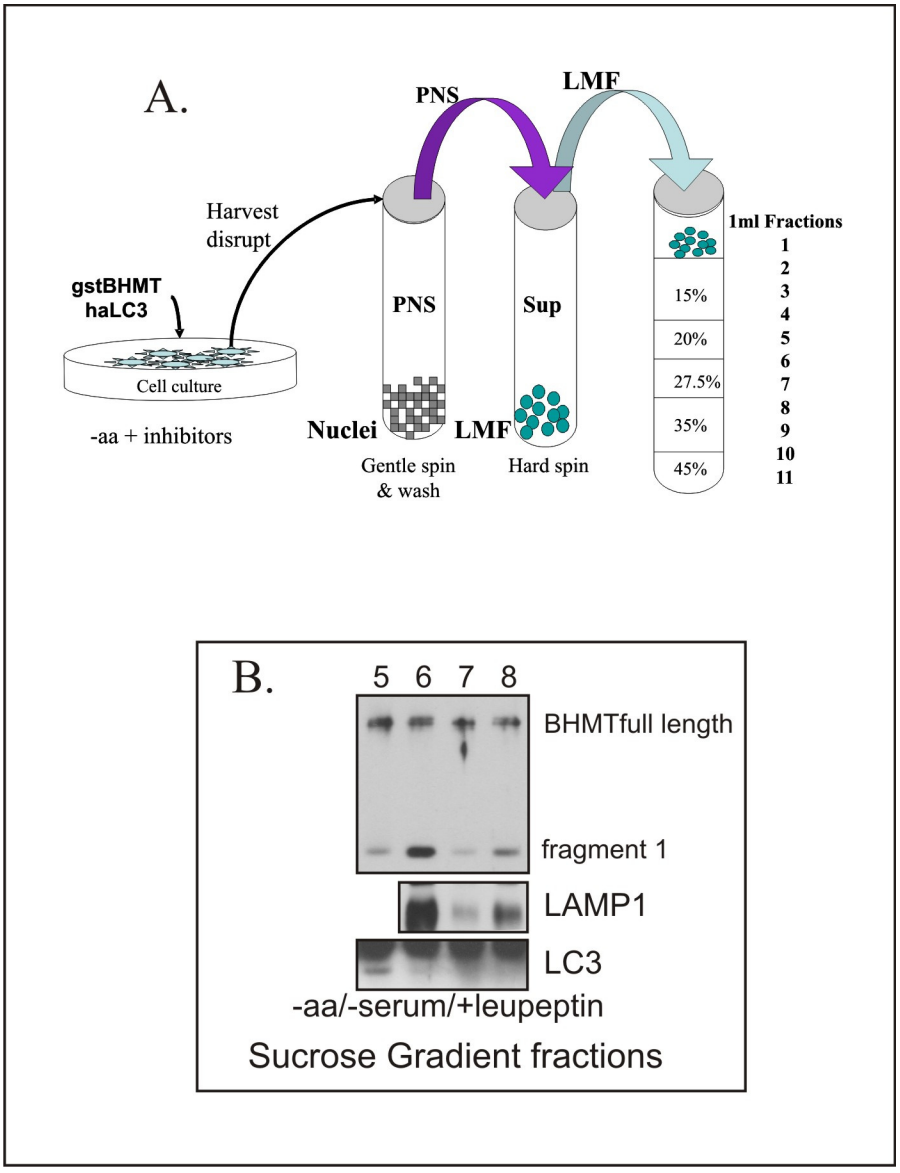
A.
PNS
LMF
Harvest
disrupt
gstBHMT
haLC3
Cell culture
-aa + inhibitors
PNS
Sup
Nuclei
LMF
Gentle spin
& wash
Hard spin
1ml Fractions
1
2
3
4
5
6
7
8
9
10
11
15%
20%
27.5%
35%
45%
B.
5 6 7 8
BHMTfull length
fragment 1
LAMP1
LC3
-aa/-serum/+leupeptin
Sucrose Gradient fractions

Figure 40. Protection assay. A. Schematic of the protection assay protocol. Briefly, sucrose gradient fractions are prepared and incubated for 5 minutes with trypsin to digest outer membrane proteins, and with trypsin and Triton X-100 to digest protein both inside and outside of the enclosed membrane space. B. Validation of conditions for protection assay. Left panel shows total trypsin digest of BHMT in cytosolic fraction. Pooled fractions 5 and 6 are digested with trypsin, with and without the detergent Triton X-100. Full length BHMT, fragment 1 and LC3B-II that remain in the presence of trypsin are within membrane-enclosed vesicles.

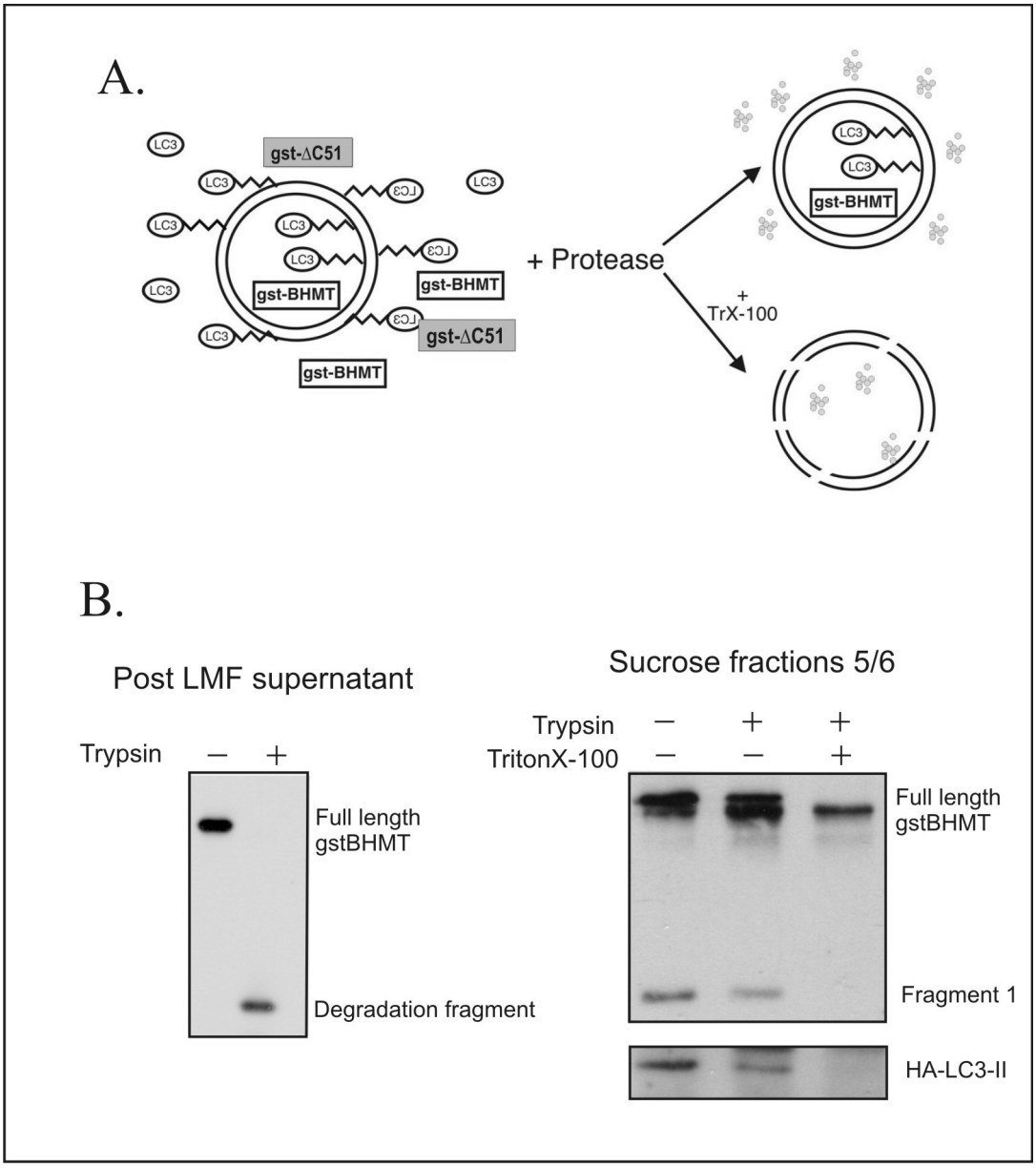
A.
LC3
gst-ΔC51
gst-BHMT
gst-BHMT
gst-ΔC51
gst-BHMT
+ Protease
+
TrX-100
gst-BHMT
B.
Post LMF supernatant
Trypsin – +
Full length
gstBHMT
Degradation fragment
Sucrose fractions 5/6
Trypsin – + +
TritonX-100 – – +
Full length
gstBHMT
Fragment 1
HA-LC3-II

homogenization and gently centrifuged to remove intact nuclei and large membrane remnants. The post-nuclear supernatant (PNS) was collected and centrifuged at high speed to pellet the light membrane fraction (LMF), consisting of autophagosomes, autolysosomes, lysosomes, mitochondria and other small organelles or microsomes. The LMF pellet was washed to remove excess cytoplasmic protein, gently resuspended in the homogenization buffer, and loaded on a prepared discontinuous sucrose gradient. After 2 hours of ultra-centrifugation at 2º C to separate the subcellular organelles by density, 1 ml fractions were collected by upward displacement. The first fraction collected from the top of the gradient was labeled fraction 1 and the densest fraction from the bottom was labeled fraction 11 (Fig. 39A).

Aliquots of fractions from the sucrose gradient were then analyzed for the presence of autolysosomes. Figure 39B is representative of fractions 5 through 8 from cells starved of essential amino acids. LC3B-II, a marker of both autophagosomes and newly fused autolysosomes, accumulated only in cells starved for essential amino acids, with the highest levels in fraction 5. GST-BHMT fragment 1 also accumulated as expected in fractions collected from amino acid starved cells (Fig. 39B). BHMT fragmentation was first observed in fraction 5, and peaked in fractions 6 and 8. A western blot for an endogenous lysosomal membrane protein, lysosome-associated membrane protein 1 (LAMP1), demonstrates that BHMT fragment 1 and LAMP1 co-fractionate and peak in identical fractions, validating that BHMT fragmentation is lysosomal.

Although fragment 1 of $GST_{mod}BHMT^{wt}$ co-fractionated with autolysosomes, full length BHMT could be found in every fraction of the gradient. This could be due to the

abundance of an over-expressed protein that is known to oligomerize and associate with the cytoskeleton. $GST_{mod}BHMT^{wt}$ elutes from a gel filtration column over a broad range of molecular weight fractions, suggesting the propensity of this protein to form higher order complexes (data not shown). Having established that autophagosomes and autolysosomes could be tracked on a sucrose gradient, LC3B-II marked fractions enriched in these vesicles were pooled to test if $GST_{mod}BHMT^{wt}$ was sequestered within vesicles. The post-LMF supernatant, which contained $GST_{mod}BHMT^{wt}$ but was expected to be devoid of vesicular structures, was used as a negative control. In the post-LMF supernatant, trypsin alone was able to fully degrade full-length $GST_{mod}BHMT^{wt}$ (Fig. 40B, left panel). At the end of the 5 minute trypsin digest, all that remained was a fragment approximately the size of GST. Aliquots of pooled fractions 5 and 6 were digested with trypsin alone, or with trypsin plus 0.2% Triton X-100. After the reaction was stopped with soybean trypsin inhibitor (STI), $GST_{mod}BHMT^{wt}$ and HA-LC3B were pulled down with glutathione or HA-antibody attached to Sepharose beads, and run on SDS-PAGE. Approximately half of LC3B-II and full length BHMT, and most of BHMT fragment 1 remained after the trypsin digest (Fig. 40B, right panel). However, LC3B-II, full length BHMT, and BHMT fragment 1 were completely degraded when identical aliquots were digested with trypsin 0.2% TritonX-100 under the same conditions (Fig. 40B, right panel). This assay demonstrates that in fractions 5 and 6, but not in the post-LMF supernatant, some of BHMT and fragment 1 and approximately half of LC3B-II were within intact vesicles, likely autolysosomes and autophagosomes. It is likely that not all vesicles were intact, as a portion of fragment 1 was digested with trypsin alone.

With evidence that the protection assay was functional, sucrose gradients were prepared from the LMF of cells expressing $GST_{mod}BHMT^{wt}$ or GST-$BHMT^{\Delta C51}$. To enrich the LMF with autophagosomes, the HEK293 cells were starved of essential amino acids and serum for 12 hours with the autophagy inhibitor chloroquine (100μM). Prolonged treatment with chloroquine was used to inhibit fusion of autophagosomes and lysosomes, causing an accumulation of autophagosomes loaded with undegraded cargo. After differential centrifugation, the LMF was loaded on discontinuous sucrose gradients and fractions were collected as before. Levels of LC3-II peaked in fractions 5 and 6 and were more broadly distributed throughout the gradient, indicating that the chloroquine-induced block of fusion had created a more heterogeneous population of autophagosomes (Fig. 41A). Aliquots of fractions from each gradient, one from cells expressing $GST_{mod}BHMT^{wt}$ and one from cells expressing GST-$BHMT^{\Delta C51}$, were digested with trypsin as before. Both $GST_{mod}BHMT^{wt}$ and GST-$BHMT^{\Delta C51}$ were protected from the action of trypsin (Fig. 41B) and levels of sequestered protein correlated well with LC3-II. The data show that 1) $BHMT^{\Delta C51}$, like $GST_{mod}BHMT^{wt}$, is sequestered into autophagosomes and 2) the carboxy terminus and/or quaternary structure of BHMT is important for lysosomal cathepsin cleavage to generate fragment 1, but may not play a role in autophagosomal delivery.

3.2.3. $BHMT^{\Delta C51}$ and 3MA

The above data show that $BHMT^{\Delta C51}$ is within autophagosomes and by inference, likely within autolysosomes. A second experiment was designed to validate the actual degradation of ΔC51 in autolysosomes. The above data showed that the carboxy-terminus is important for lysosomal cleavage of "modified" $GST_{mod}BHMT^{wt}$ in

Figure 41. Protection assay with GST-BHMT and GST-BHMT$^{\Delta C51}$. A. HEK293 cells expressing GST-BHMT or GST-BHMT$^{\Delta C51}$ were incubated for 6 hours in media from which essential amino acids and serum had been removed and with 100μM chloroquine to enrich fractions in autophagosomes. Sucrose gradient fractions were prepared as described. A. Equal aliquots of each gradient fraction were precipitated with TCA and prepared for western blotting with antibody against endogenous LC3. With chloroquine, LC3-II is found in multiple lower fractions. LAMP1 is found only in fractions 5 and 6. B. Protection assay was performed in conditions described on each fraction from GST-BHMT and GST-BHMT$^{\Delta C51}$ expressing cells. BHMT and BHMT$^{\Delta C51}$ are both protected from the protease action of trypsin in fractions corresponding well with LC3, suggesting that both BHMT and BHMT$^{\Delta C51}$ are enclosed within autophagosomes.

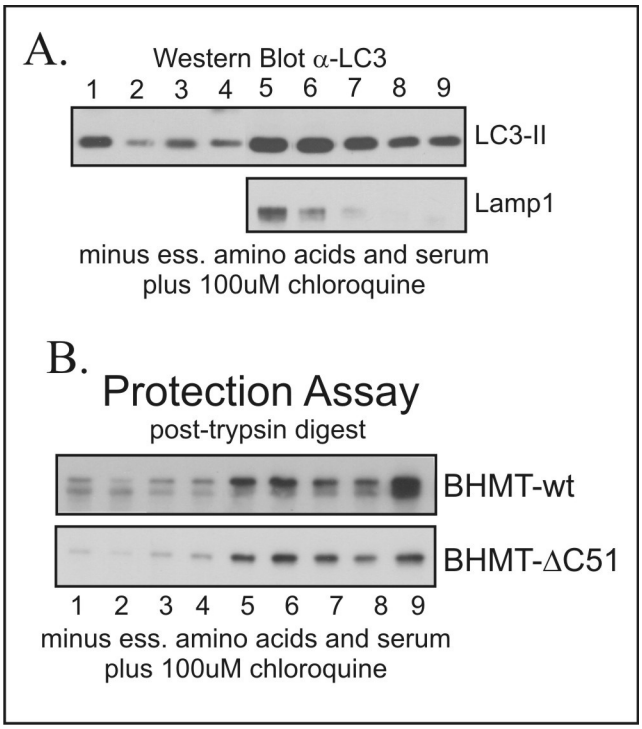
A.
Western Blot α-LC3
1 2 3 4 5 6 7 8 9
LC3-II
Lamp1
minus ess. amino acids and serum
plus 100uM chloroquine
B.
Protection Assay
post-trypsin digest
BHMT-wt
BHMT-ΔC51
1 2 3 4 5 6 7 8 9
minus ess. amino acids and serum
plus 100uM chloroquine

the L2 loop, but the "no thrombin" $GST_{\Delta T}$BHMT has a lysosomal cleavage site outside BHMT that may not be dependent on the carboxy-terminus. The $GST_{\Delta T}$BHMT reporter generated two fragments, fragment 1 and fragment 2′ (Fig. 18). Unlike the original reporter, both fragments of $GST_{\Delta T}$BHMT were invariantly lysosomal. Quaternary structure might not be important for cleavage of GST in this linker region to generate fragment 2′. If this prediction was correct, then fusion of $GST_{\Delta T}$ to $BHMT^{\Delta C51}$ should make a ΔC51 reporter capable of generating fragment 2′ in a manner similar to $GST_{\Delta T}$BHMT.

To test this, ΔC51 was sub-cloned into the $GST_{\Delta T}$ background to match $GST_{\Delta T}$BHMT. The $GST_{\Delta T}$ versions of BHMT and ΔC51 were expressed in HEK293 cells and tested under conditions of amino acid starvation to induce autophagy, and treated with 3MA and wortmannin to inhibit autophagy as before. Both fragments 1 and 2′ in the control $GST_{\Delta T}$BHMT were generated be amino acid starvation and were completely sensitive to 3MA and wortmannin (Fig. 42, left panel). The accumulation of fragment 2′ also increased in the ΔC51 mutant with amino acid starvation, consistent with an autophagic response. However, while completely sensitive to wortmannin, ΔC51 fragment 2′ was partially resistant to the effects of 3MA (Fig. 42, right panel). This was surprising because it suggested that there was a difference between the processing of ΔC51 and full length BHMT.

The sucrose gradient provides a level of resolution between light and dense autolysosomes that might be useful in determining how ΔC51 differs from BHMT. HEK293 cells expressing $GST_{\Delta T}$BHMT or $GST_{\Delta T}BHMT^{\Delta C51}$ were starved of essential amino acids and serum to induce macroautophagy. The LMF fractions from cells

Figure 42. $GST_{\Delta T}BHMT^{\Delta C51}$ generates fragment 2′ under starvation conditions.

The ΔC51 mutant was sub-cloned into the $BHMT_{\Delta T}$ background to see if it would generate fragment 2′. HEK293 cells expressing either $GST_{\Delta T}BHMT$ or $GST_{\Delta T}BHMT^{\Delta C51}$ were starved of essential amino acids and serum to induce autophagy and treated with starvation media with 10mM 3MA or 100nM wortmannin to inhibit autophagy. Cell extracts were prepared for western blot as previously described. In control BHMT cells, fragments 1 and 2′ accumulate under starvation conditions and are inhibited by 3MA and wortmannin (left panel). In starvation conditions, $GST_{\Delta T}BHMT^{\Delta C51}$ generated increased levels of fragment 2′. $GST_{\Delta T}BHMT^{\Delta C51}$ fragment 2′ levels were inhibited by wortmannin, but were 50% resistant to 3MA (right panel).

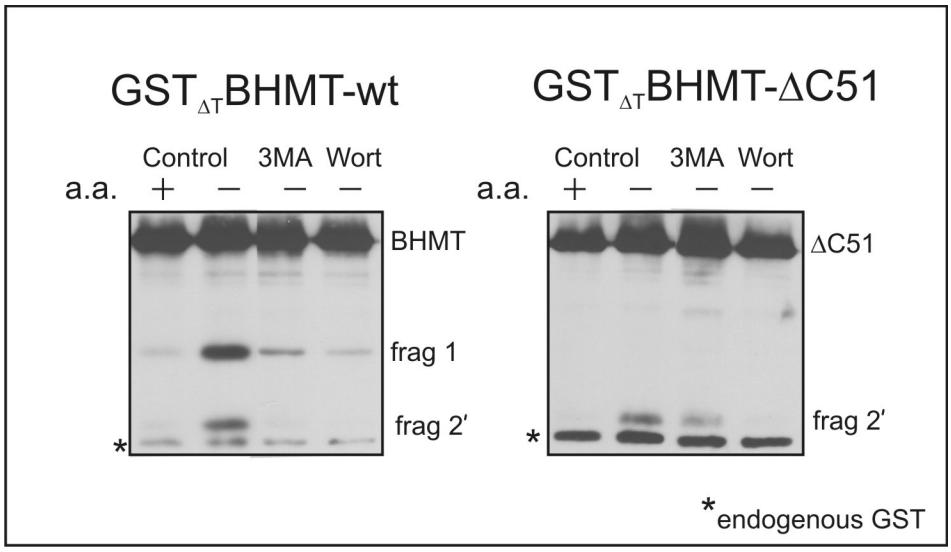
GST$_{\Delta T}$BHMT-wt
Control
3MA
Wort
a.a.
+
–
–
–
BHMT
frag 1
frag 2'
*
GST$_{\Delta T}$BHMT-ΔC51
Control
3MA
Wort
a.a.
+
–
–
–
ΔC51
frag 2'
*
*endogenous GST

Figure 43. $GST_{\Delta T}BHMT^{\Delta C51}$ fragment 2′ co-fractionates with LAMP1 in sucrose gradient fractions. HEK293 cells expressing cells expressing $GST_{\Delta T}BHMT$ or $GST_{\Delta T}BHMT^{\Delta C51}$ were starved of essential amino acids and serum to induce autophagy or $GST_{\Delta T}BHMT^{\Delta C51}$ were starved of essential amino acids and serum to induce autophagy. After 6 hours, the LMF of cell extracts were prepared and separated by density on a sucrose gradient as described. Glutathione extracts and WCE were prepared for western blotting as described. BHMT fragments 1 and 2′, ΔC51 fragment 2′, and LAMP1 cofractionate and peak in fractions 6 and 8. Lower right panel shows distribution of LAMP1-marked vesicles in gradients prepared from 3MA-treated HEK293 cells. Note that in fractions from 3MA-treated cells, distribution of LAMP1 shifts to the lighter fraction.

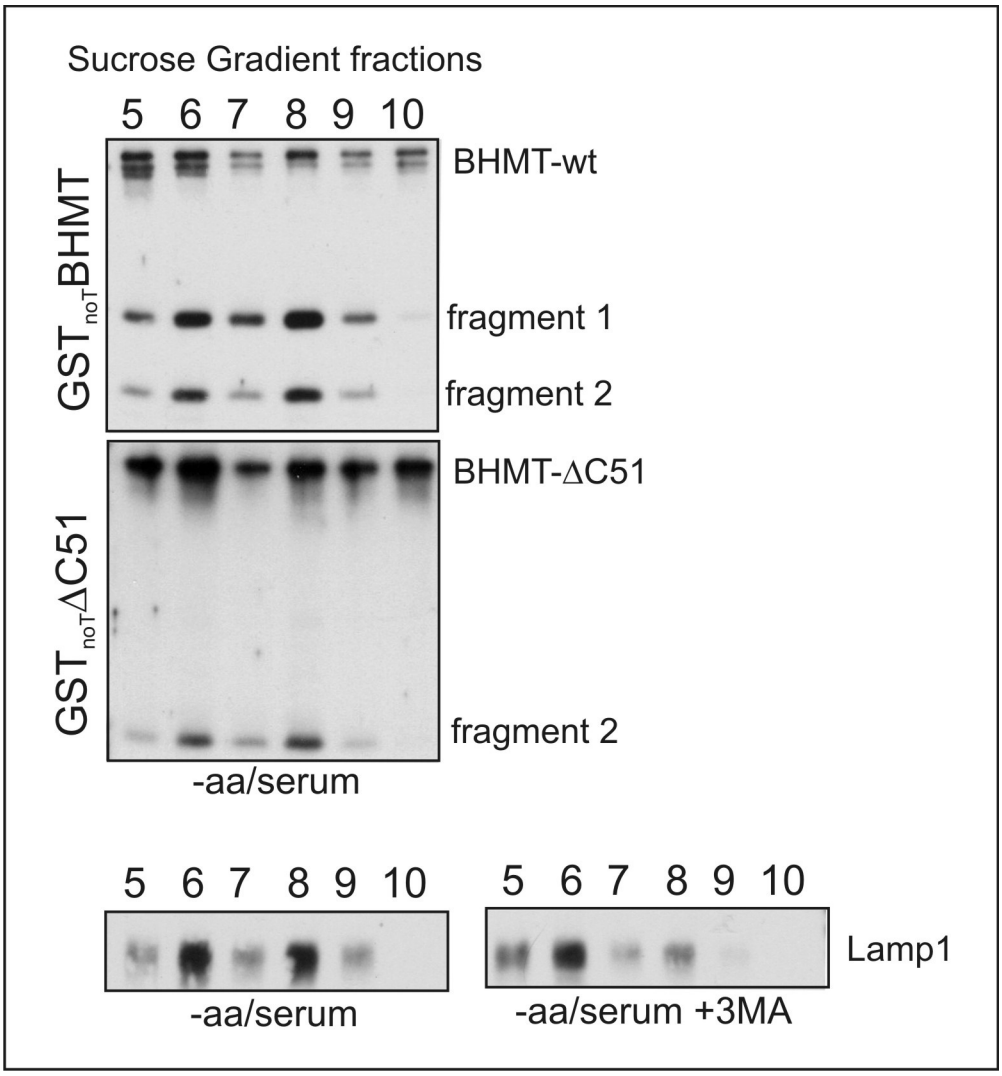
Sucrose Gradient fractions
5 6 7 8 9 10
GST noT BHMT
BHMT-wt
fragment 1
fragment 2
GST noT ΔC51
BHMT-ΔC51
fragment 2
-aa/serum
5 6 7 8 9 10
5 6 7 8 9 10
Lamp1
-aa/serum
-aa/serum +3MA

expressing each BHMT mutant were isolated by differential centrifugation and loaded on sucrose gradients as before. Glutathione pulldowns from gradient fractions were analyzed for GST-tagged proteins and peptides by western blotting. Under amino acid starvation conditions, $GST_{\Delta T}$ BHMT generated fragment 1 and 2′ as expected. $GST_{\Delta T}$ $BHMT^{\Delta C51}$ generated fragment 2′ that co-fractionated perfectly with BHMT fragments 1 and 2′ and with LAMP1 (Fig. 43). This was consistent with the presence of autolysosomes in fractions 6 and 8.

To determine the effect that 3MA might have on the two autolysosome fractions, sucrose gradient fractions were prepared from the LMF of HEK293 cells which were starved of essential amino acids and serum as before, but in the presence of 10mM 3MA. TCA precipitation and western blot analysis of the 3MA-treated fraction, prepared as before, showed decreased LAMP1 staining in the denser fraction 8 (Fig. 43, lower right panel). This is consistent with previous reports that 3MA changes the distribution of lysosome-type vesicles on density gradients[82]. It suggests that 3MA may prevent the formation of denser autolysosomes or other amphisomes.

The resolution provided by the sucrose gradients was used to examine the fractionation pattern of $GST_{\Delta T}$BHMT or $GST_{\Delta T}BHMT^{\Delta C51}$ in the presence or absence of 3MA. HEK293 cells expressing either $GST_{\Delta T}$BHMT or $GST_{\Delta T}BHMT^{\Delta C51}$ were starved of essential amino acids and serum as before, with or without 10mM 3MA. After extraction, the LMFs from each treatment and BHMT reporter were isolated by differential centrifugation and loaded on discontinuous sucrose gradients to resolve autolysosomes by density as before. $GST_{\Delta T}$BHMT fragments 1 and 2′ were observed in fractions 5-10, peaking in fraction 9. Both fragments were completely sensitive to the

effects of 3MA (Fig. 44). As before, $GST_{\Delta T}BHMT^{\Delta C51}$ generated fragment 2′ which co-fractionated with the two fragments of $GST_{\Delta T}BHMT$. However, although fragment 2′ was as sensitive to 3MA in fractions 7 to 10 as control, it was completely resistant in fractions 5 and 6 (Fig. 44). Western blot analysis with antibody against endogenous LC3 showed that LC3-II co-fractionated with BHMT fragments, and like $GST_{\Delta T}BHMT^{\Delta C51}$ was resistant to 3MA only in the middle fractions (Fig. 44). In this experiment, 3MA effectively prevented fragmentation of $GST_{\Delta T}BHMT$ in all fractions, but prevented fragmentation of $GST_{\Delta T}BHMT^{\Delta C51}$ only in the denser fractions. What types of vesicles are in these fractions of different densities?

The LAMP1 data show that 3MA affects the distribution of LAMP1 in the dense fraction of the sucrose gradient. LAMP1 is a membrane-spanning protein found predominantly on lysosomes, but can also be found on some autolysosomes, amphisomes, and late endosomes. To further characterize the nature of the vesicles in the light and dense fractions of the sucrose gradient, a lysosomal disrupting agent, glycyl-L-phenylalanine 2-naphthylamide (GPN) was used. GPN is hydrolyzed by the lysosomal cathepsin C, producing an intralysosomal accumulation of product that osmotically ruptures the lysosomal membrane. GPN is most effective in small mature lysosomes, and is less effective in larger digestive bodies such as autolysosomes and amphisomes where it must compete with other substrates. It does not disrupt intact autophagosomes[83]. Two sets of HEK293 cells, starved of essential amino acids and serum, were collected and gently disrupted by dounce homogenization. One set was incubated for 6 minutes at 37º with the lysosome disrupter GPN, after which both sets were processed as described to separate the LMFs by density on matched sucrose gradients. Fractions 6 -9 were

Figure 44. $GST_{\Delta T}BHMT^{\Delta C51}$ fragment 2′ is resistant to 10mM 3MA in the lighter sucrose gradient fractions. HEK293 cells expressing $GST_{\Delta T}BHMT$ or $GST_{\Delta T}BHMT^{\Delta C51}$ were starved of essential amino acids and serum to induce autophagy or were treated under starvation media with 10mM 3MA. The LMF of each sample was prepared and fractionated by density on a sucrose gradient. Western blots of glutathione pull-downs and TCA precipitation samples were prepared as before. Top panel shows fractions from cells expressing $GST_{\Delta T}BHMT$. Fragments 1 and 2′ show good sensitivity to 3MA. Middle panel shows fractions from cells expressing $GST_{\Delta T}BHMT^{\Delta C51}$. Fragment 2′ is sensitive to 3MA in the denser fractions, 7-10, but is completely resistant to 3MA in fractions 5 and 6. Bottom panel: Like ΔC51, endogenous LC3 is also resistant to 3MA in fractions 5 and6, and sensitive to 3MA in fractions 7-9 (no LC3 is seen in fraction 10).

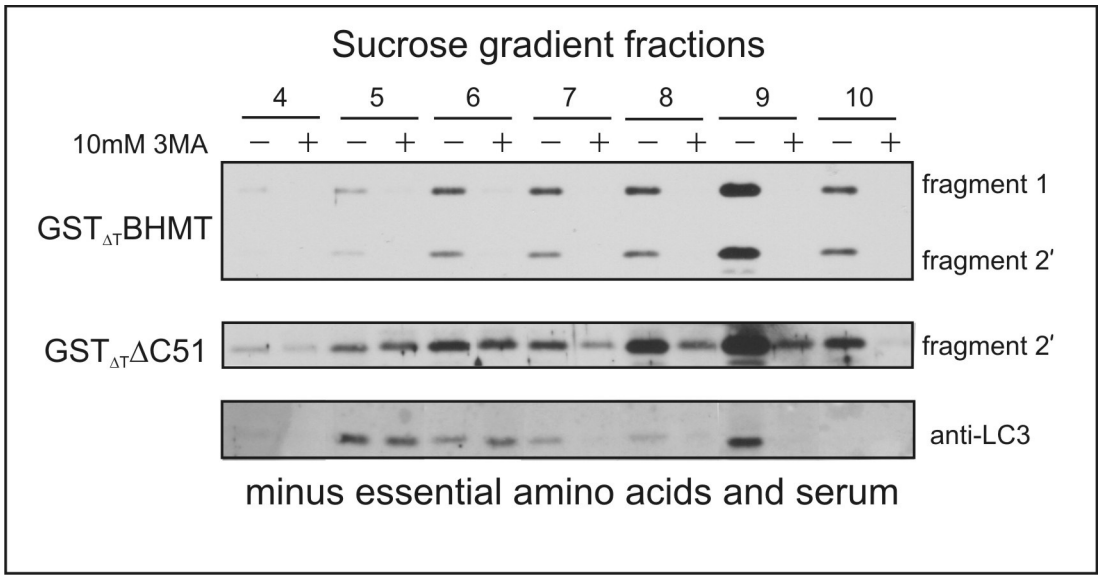
Sucrose gradient fractions
4
5
6
7
8
9
10
10mM 3MA
− + − + − + − + − + − + − +
GST$_{\Delta T}$BHMT
fragment 1
fragment 2′
GST$_{\Delta T}$ΔC51
fragment 2′
anti-LC3
minus essential amino acids and serum

Figure 45. Characterization of sucrose gradient fractions with GPN. HEK293 cells were extracted in PBS and gently dounced to rupture the plasma membrane. One set was exposed to the lysosome disrupter GPN. Cells were then processed as before to obtain the LMF, which was processed on prepared sucrose gradients. Gradient fractions were precipitated with TCA and prepared for western blotting with an antibody against LAMP1. In the GPN-treated samples, LAMP1 was decreased in fraction 6 compared to control. In fraction 8, LAMP1 levels were equivalent between the GPN-treated and control samples. GPN is a more effective inhibitor of cathepsin C in mature lysosomes, which predicts that fraction 6 contains mature lysosomes and that fraction 8 is predominantly amphisomes and autolysosomes.

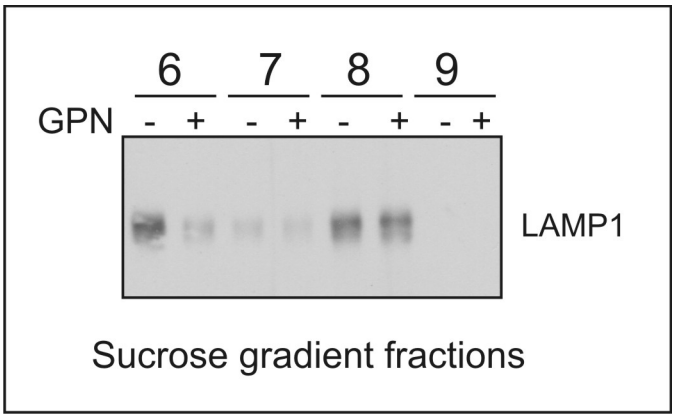
6
7
8
9
GPN
- + - + - + - +
LAMP1
Sucrose gradient fractions

	5/6	8/9
LAMP1	✔	✔
LAMP1 w/ 3MA	✔	⊘
LAMP1 w/ GPN	✔	⊘
LAMP1 w/ chloro	✔	⊘
LC3-II	✔	✔
LC3-II w/ 3MA	✔	⊘
LC3-II w/ chloro	✔	✔
BHMT F1 F2'	✔	✔
BHMT F1 F2' w/ 3MA	⊘	⊘
deltaC51 F2'	✔	✔
deltaC51 F2' w/ 3MA	✔	⊘
lysosomes	✔	⊘
autolysosomes	✔	✔
autophagosomes	✔	✔ ?

Table 5. Characterization of sucrose gradient fractions. Summary of western blot data characterizing the vesicles most likely found in the light (5/6) and dense(8/9) sucrose gradient fractions. ✔ means present. ⊘ means absent.

probed for LAMP1. LAMP1 in the denser fraction was not affected by GPN, while levels of LAMP1 in fraction 6 were reduced, suggesting that in HEK293 cells, mature lysosomes are in the lighter fractions (Fig. 45). The combined data of the previous experiments suggest answers to the following questions:

What type of vesicles are in the light and dense sucrose gradient fractions (See Table 5)? 1) Mature lysosomes are in fractions 5/6 and are not in fractions 8/9. This is supported by the GPN data and LAMP1 antibody staining by western blotting. It is also supported by previous data with chloroquine, which prevents lysosomal fusion. With chloroquine, LAMP1 is only seen in the lighter fractions. 2) Autophagosomes are likely in fractions 5/6. This is supported by the LC3 data and by previous gradient data of amino acid starved cells with the HA-LC3B reporter. 3) Autolysosomes are in fractions 5/6. These fractions are marked by both LAMP1 and LC3-II. BHMT fragment 1 and 2′ demonstrates the presence of functional autolysosomes. 4) Autolysosomes are in fractions 8/9. This is supported by the western blot data of LAMP1 and LC3-II. BHMT fragment 1 and 2′ in the dense fractions supports the presence of functional autolysosomes. 5) Autophagosomes may be in fraction 8/9. The denser fractions are more likely to be digestive organelles, however the data cannot rule out denser autophagosomes. The chloroquine data suggest that dense autophagosomes can form if lysosomal fusion is inhibited.

What is 3MA doing? 1) 3MA quantitatively decreases LAMP1, LC3-II and BHMT fragmentation of either mutant in dense fractions. Therefore, 3MA likely inhibits the formation of dense autolysosomes and perhaps dense autophagosomes. 2) 3MA inhibits the generation of $GST_{\Delta T}$BHMT fragment 1 and 2′ in fractions 5/6. 3) 3MA does

not inhibit fragmentation of $GST_{\Delta T}BHMT^{\Delta C51}$ in fractions 5/6. 4) LC3-II levels are not affected by 3MA in fractions 5/6. This raises the following question:

Does the 3MA-resistant generation of $GST_{\Delta T}BHMT^{\Delta C51}$ fragment 2′ occur in autolysosomes or lysosomes? 1) The protection assay data validate that $GST_{\Delta T}BHMT^{\Delta C51}$ is normally sequestered in autophagosomes, however it does not rule out a compensatory mechanism of lysosomal import of the ΔC51 mutant by 3MA or microautophagy. 2) The co-fractionation of LAMP1 and LC3-II in the presence of 3MA supports a hypothesis of autolysosomal degradation, but it too does not rule out a lysosomal-only mechanism.

The persistence of LC3-II in fractions 5/6 is surprising, because 3MA is thought to block autophagosome formation by inhibiting the Class III PI 3-kinase, Vps34. However, the sucrose data suggest that LC3-II vesicles are formed in the presence of 3MA To determine what affect 3MA might have on the production and turnover of LC3, HEK293 cells stably expressing HA-LC3B-myc were used to test the effects of 3MA on LC3B-II flux in either complete or starvation media. 3MA treatment caused a slight increase in levels of LC3B-II compared to control cells, which suggested that 3MA was not inhibiting LC3B-II formation, but was likely inhibiting LC3B-II flux, similar to the effects of leupeptin and pepstatin A.

If 3MA treatment was in fact revealing LC3B-II flux, than inhibition of the lysosome in 3MA-treated cells should cause an accumulation of LC3B-II. To test this, the HEK293 cells stably expressing HA-LC3B-myc were treated with or without 3MA as before, but with the additional treatment of 25μM chloroquine. The accumulation of

Figure 46. Lysosomal flux of LC3B-II in cells treated with 3MA. HEK293 cells stably expressing HA-LC3B-myc were treated to complete or starvation media for 4 hours, with and without 10mM 3MA, extracted and prepared for western blotting as before. LC3B-II levels in 3MA treated cells were slightly increased compared to control cells (lanes 3 and 4, compared to lanes 1 and 2). A second set of HA-LC3B-myc stable cells were treated under the same condition, except with added 25μM chloroquine for a stronger inhibition of lysosomal turnover. Surprisingly, LC3B-II levels in the 3MA and chloroquine-treated cells were increased almost to the level of the control cells (lanes 7 and 8, compared to 5 and 6). This suggests that LC3B-II continues to be made and degraded in the presence of 3MA.

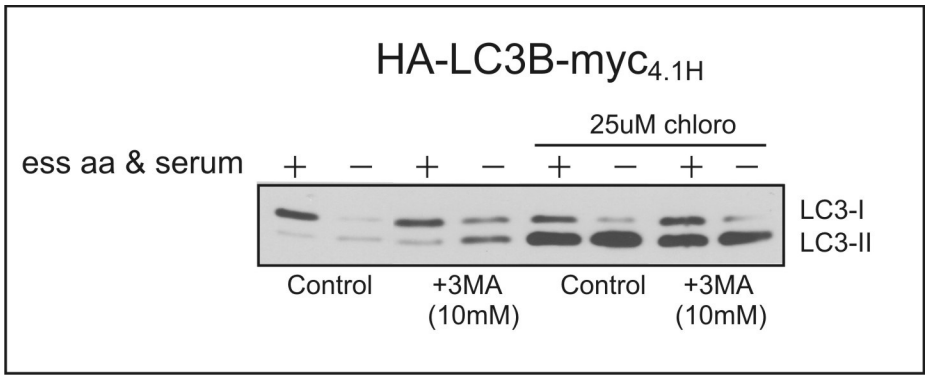
HA-LC3B-myc4.1H
25uM chloro
ess aa & serum
+ − + − + − + −
LC3-I
LC3-II
Control
+3MA (10mM)
Control
+3MA (10mM)

LC3B-II levels in cells treated with 3MA plus chloroquine was significant, reaching levels approximately half of that found in control cells (Fig. 46, lanes 7 and 8, compared to lanes 5 an 6). This demonstrates that in the presence of 3MA, LC3B-II continues to be made and that it is degraded in the lysosome. The surprising conclusion is that LC3B-II, and presumably LC3B-II decorated vesicles, are made and degraded by the lysosome in the presence of 3MA. Quantitatively, LC3B-II turnover in the presence of 3MA is decreased, but is still significant compared to control.

These data support the hypothesis that the fragmentation of $GST_{\Delta T}BHMT^{\Delta C51}$ occurs in autolysosomes in the presence of 3MA, even though $GST_{\Delta T}BHMT$ degradation has been inhibited. This result is surprising. The autophagy field defines macroautophagy almost exclusively in terms of sensitivity to 3MA. The data suggest that there is a 3MA sensitive and a 3MA insensitive macroautophagy. GST-BHMT is processed by the former and ΔC51 by the latter. This is important because 3MA inhibits a signaling molecule, VPS34. It suggests that production of new PI3P is important for the autophagic machinery to recognize BHMT, but is either not necessary or lower levels are necessary for macroautophagy-related degradation of ΔC51. The ability of the BHMT mutants to form higher order structure suggests how these two types of macroautophagy are different. (See discussion).

3.3. Regulation of autophagy: S6 Kinase and mTOR

mTOR is well known for its role in responding to changes in nutrients, mitogens, and ATP to regulate cell growth. In times of stress such as amino acid starvation, mTOR signaling is down-regulated and its downstream effectors p70S6K and 4E-BP1 are hypophosphorylated. This results in reduced translation and increased autophagy. Other

stressors such as hypoxia are well known inhibitors of the mTOR pathway and not surprisingly, there are suggestions in the literature that hypoxia and ischemia induce autophagy. Hypoxia-ischemia creates a severe energy crisis in cells that are deprived of nutrients and the oxygen necessary for energy production, and generally results in cell death. In a physiological context, normal cells exposed to conditions of ischemia after arterial occlusion normally die by apoptosis, although in some models, the mechanism of cell death is proposed to be through excessive autophagy. Evidence in support of the latter includes TEM showing extensive vacuolization and decreased LC3-I levels in damaged tissue compared to control[66]. The question that arises from this data is whether these cells would have sufficient ATP to activate and sustain autophagy under ischemic conditions. Multiple steps of the autophagic process require ATP and even small changes of ATP levels have been shown to slow autophagic proteolysis[84]. It is likely that decreased ATP negatively affects the ATP-dependent steps of LC3 conjugation, lysosome acidification, and vesicle fusion.

Experimental conditions of hypoxia-ischemia can be tested in cell culture and the BHMT and LC3B assays can both be used to measure the effects at two different stages of the autophagic process. HEK293 cells stably expressing either GST_{mod}BHMTmyc or HA-LC3B-myc were used for these experiments to eliminate potential effects of transfection reagents. The two cells lines were maintained in either complete or starvation media, with or without glucose. One set was maintained at normoxia (37ºC, 5% CO_2 and 21% O_2), and a matched set was incubated at hypoxia (37ºC, 5% CO_2, and 1% O_2). The duration of the experiment was approximately five hours. In normoxia, BHMT fragment 1 accumulated normally in conditions of amino acid and serum

starvation. Glucose starvation slightly decreased the level of fragmentation (Fig. 47, lanes 3&4 compared to lanes 1&2). LC3B-II levels were in agreement with BHMT fragmentation, showing induction with amino acid and serum starvation and slightly less LC3B-II with glucose deprivation (Fig. 47, lanes 1-4, second panel from the top). At 1% O_2 with full glucose, autophagy by both BHMT and LC3B assays was not impaired, compared to control (Fig. 47, lanes 6 & 7 compared to lanes 1 & 2). However, in the experimental condition of ischemia, defined as loss of amino aids, serum, and glucose at 1% O_2, LC3B-II levels were severely decreased and accumulation of amino acid starvation-induced BHMT fragment 1 was significantly less than control (Fig. 47, lanes 7 and 8). In this experiment, BHMT fragmentation and LC3B-II levels both suggest that autophagy is inhibited in these conditions of ischemia.

However, even with impaired LC3B processing, there was a small amino acid starvation-induced increase of BHMT fragmentation in ischemia. Some turnover of autophagic cargo did occur in ischemia. It suggests that in ischemia, as amino acid, glucose, O_2 and ATP levels fall, mTOR is down-regulated, and an attempt is made to activate an autophagic response. However, as the ischemic-induced energy crisis continues, the cell utilizes and exhausts the limited resources of LC3-II and ATP in response to the loss of amino acids and autophagy is inhibited. Understanding how cells respond to ischemic conditions has physiological relevance in tumor biology as well as in pathological infarct.

The BHMT assay for autophagy is a good tool to look at the signaling pathways involving mTOR and p70S6K, and phosphorylated S6. Amino acid starvation inactivates the mTOR pathway, which inactivates p70S6K and results in the dephosphorylation of

Figure 47. The BHMT and LC3B assays in a cell culture model of ischemia. HEK293 cells stably expressing either $GST_{mod}BHMTmyc_{4.1}$ or HA-LC3B-myc were incubated for 5 hours in complete media with and without glucose, or in media deficient in essential amino acids and serum, with and without glucose. One set was maintained in conditions of normoxia (37ºC, 5% CO_2 and 21% O_2) and another set was maintained in hypoxia (37ºC, 5% CO_2, and 1% O_2). The cellular condition of ischemia is mimicked in the cells deprived of amino acids, serum, glucose and oxygen (lane 8). Amino acid starvation induced the accumulation of BHMT fragment 1 in both normoxia and hypoxia. No significant increase in fragment 1 was noted with glucose starvation in either normoxia or hypoxia. The combined effects of experimental ischemia inhibited BHMT fragmentation, although a slight increase in fragment 1 is noted in lane 8 compared to lane 7. LC3B-II production was significantly decreased in the absence of glucose and oxygen. Autophagy, by both the BHMT and LC3B assays, was inhibited in conditions of ischemia.

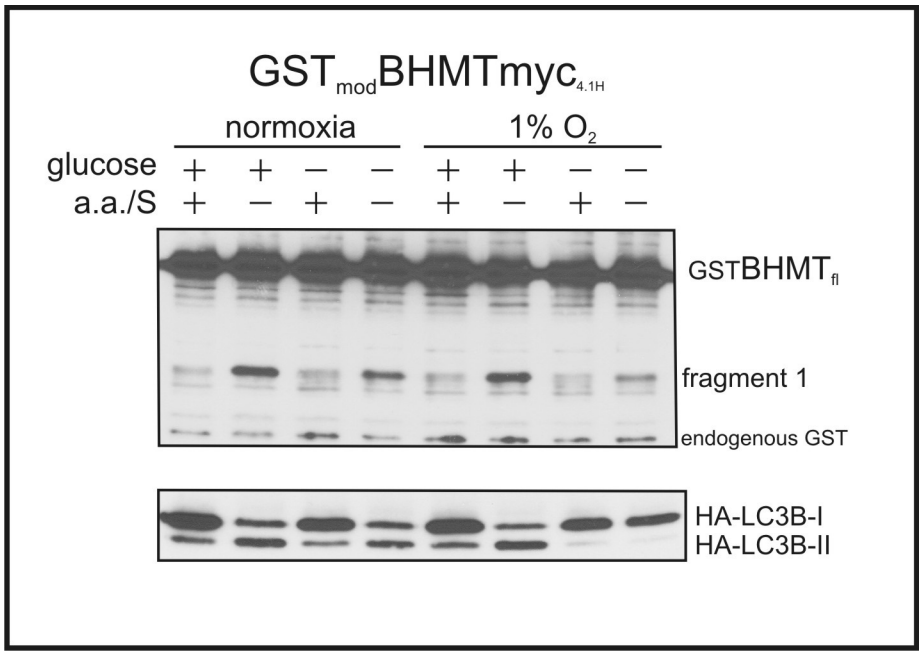
GST mod BHMTmyc 4.1H
normoxia
1% O2
glucose + + − − + + − −
a.a./S + − + − + − + −
GSTBHMT fl
fragment 1
endogenous GST
HA-LC3B-I
HA-LC3B-II

S6[85]. This has led to the suggestion that inactivation of S6K and dephosphorylation of S6 are important events in the induction of autophagy[54]. In order to test if starvation induced S6 dephosphorylation is necessary for the induction of autophagy, a constitutively active allele of S6K was used that is known to be active in the absence of amino acids. HEK293 cells were co-transfected with $GST_{mod}BHMT_{IRES}GFP$ and the constitutively activate allele of p70S6K, $p70S6K^{T389E,D3E}$, or vector control. After allowing sufficient time for expression, the cells were treated in complete media or media deficient in essential amino acids and serum with protease inhibitors, to induce autophagy. After 6 hours, cells were harvested and cells extracts were prepared for glutathione pulldown and western blotting. Expression of GFP is shown as a control of $GST_{mod}BHMT_{IRES}GFP$ transfection efficiency. Western blotting with anti-myc antibody is shown to verify expression of the p70S6K allele. As expected, amino acid starvation significantly increased BHMT fragmentation in the control (Fig. 48, lane 2). Surprisingly, expression of the constitutively active allele of $p70S6K^{T389E,D3E}$ did not inhibit BHMT fragmentation, but rather appeared to slightly increase the accumulation of BHMT fragment 1 in both basal and starvation conditions (Fig. 48, lanes 3 and 4)). The expression $p70S6K^{T389E,D3E}$ is expected to send a positive signal to S6, the downstream substrate of p70S6K. WCE aliquots were prepared for western blotting with an antibody against phospho-S6. In control cells, S6 was dephosphorylated during the 6 hour starvation period, but remained phosphorylated in the presence of the $p70S6K^{T389E,D3E}$ allele as expected (Fig. 49, lanes 2 and 4). Expression levels of total S6 protein are shown in the bottom panel (Fig. 49).

Figure 48. Active p70S6K^{T389E,D3E} does not inhibit autophagy; over-expression of RHEB inhibits autophagy. HEK293 cells expressing $GST_{mod}BHMT_{IRES}GFP$ were transfected with an activated allele of p70S6K^{T389E,D3E} or with mycRHEB. After allowing time for expression, the transfected cells were treated with complete media or were treated under amino acid starvation conditions for 6 hours to induce autophagy. Cell extracts were prepared as previously described for western blotting. In control cells and cells expression the active S6K, levels of BHMT fragment 1 increased in starvation conditions (lanes 1-4). Active S6K was not sufficient to inhibit autophagy, and levels of fragment 1 were actually a little greater than control. In the cells expressing the upstream activator or mTOR, BHMT fragmentation and autophagy were inhibited in starved cells. Controls of expression of the BHMT reporter, RHEB and S6K are shown in panels 2-4. The bottom panel is a western blot of endogenous LC3 from each sample. Neither S6K nor RHEB affect the accumulation of LC3-II levels.

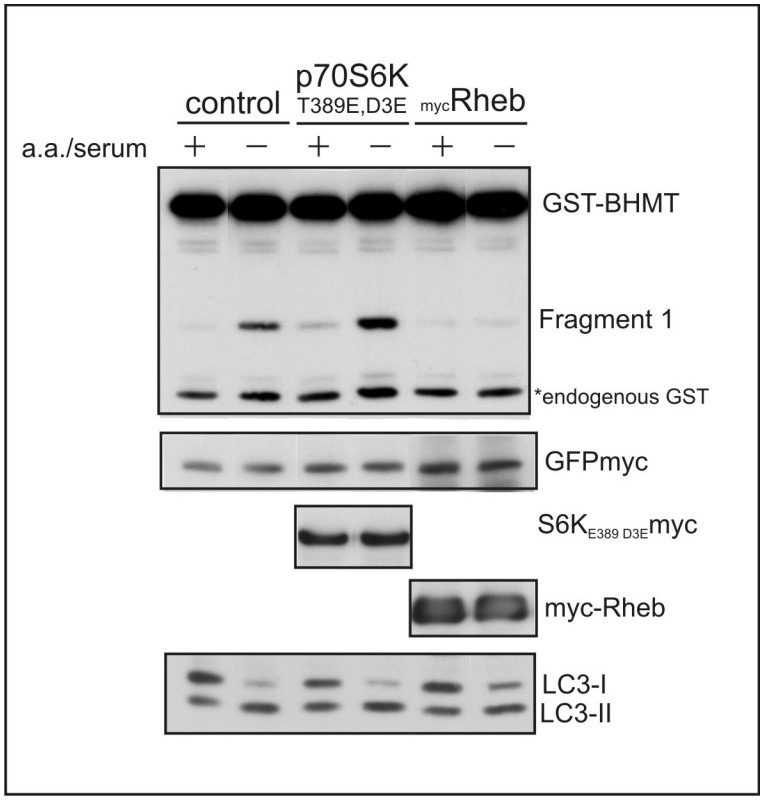
control
p70S6K
T389E,D3E
mycRheb
a.a./serum
+
−
+
−
+
−
GST-BHMT
Fragment 1
*endogenous GST
GFPmyc
S6KE389 D3Emyc
myc-Rheb
LC3-I
LC3-II

Figure 49. S6 phosphorylation in cells with activated p70S6K^{T389E,D3E} and mycRHEB. Western blot of cell extracts from BHMT experiment in Figure 48 with a phospho-specific antibody against S6. Total S6 is shown in bottom panel as a control of expression. As expected, phosphorylation of S6 is decreased in cells starved of essential amino acids, compared to cells in complete media (lane 2 compared to lane 1). Phosphorylation of S6 is protected in cells starved from amino acids that over-express activated p70S6K^{T389E,D3E} or mycRHEB.

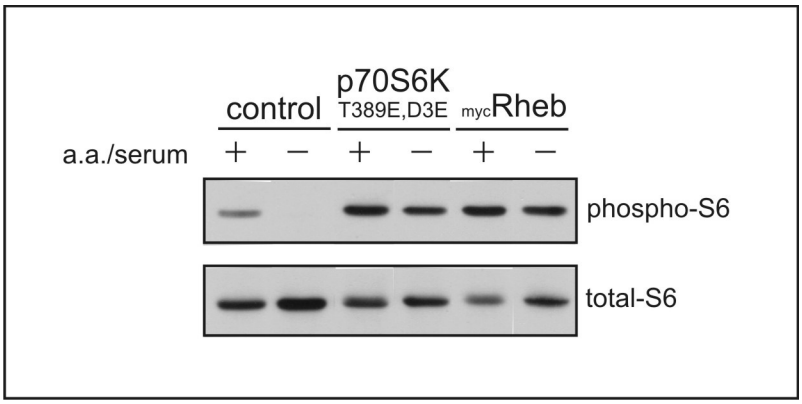
control
p70S6K
T389E,D3E
mycRheb
a.a./serum
+ − + − + −
phospho-S6
total-S6

Figure 50. 4E-BP1 phosphorylation in cells with activated p70S6K^{T389E,D3E} and mycRHEB. Western blot of cell extracts from BHMT experiment as in Figure 48 with a rapamycin control for each condition. Top panel is western blot with a phospho-specific antibody against 4E-BP1. Total 4E-BP1 is shown in bottom panel as a control of expression. In control cells, amino acid starvation causes a band-shift collapse. Rapamycin also causes a slight band shift down of 4E-BP1. Phosphorylation and total levels of 4E-BP1 are equivalent between cells expressing active S6K and control cells in each condition tested. In last four lanes, over-expression of RHEB protects phospho-4E-BP1 in starved cells, but not in rapamycin-treated cells. Note that expression levels of total 4E-BP1 are decreased in cells with over-expressed RHEB. This is most evident in the starved, rapamycin-treated cells (lanes 12).

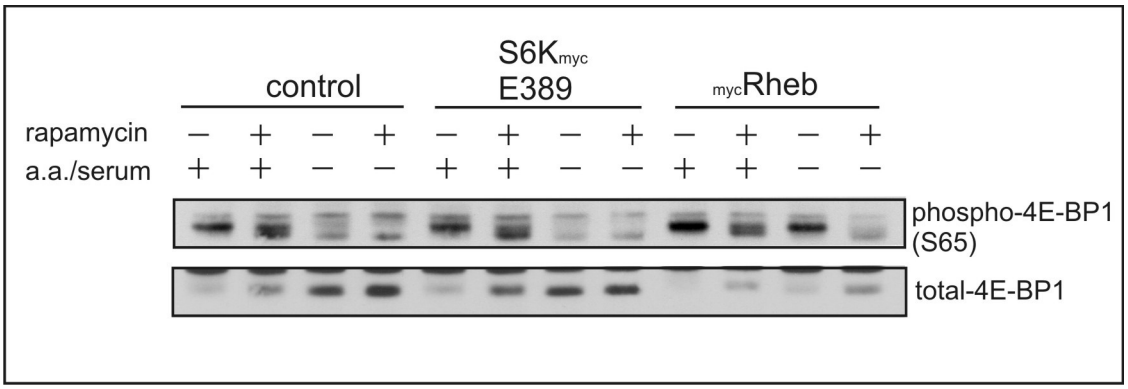
control
S6K$_{myc}$ E389
$_{myc}$Rheb
rapamycin
a.a./serum
phospho-4E-BP1 (S65)
total-4E-BP1

If the amino acid signal for autophagy is through mTOR, then activation of mTOR should inhibit autophagy. Although there are no activated alleles of mTOR, over-expression of its upstream activator RHEB has been shown to activate mTOR in the absence of amino acids. To test the role of mTOR on autophagy, HEK293 cells were co-transfected with $GST_{mod}BHMT_{IRES}GFP$ and mycRHEB or vector control and treated under plus and minus amino acid media conditions as before. Over-expression of mycRHEB completely inhibited the induction of autophagy as judged by the accumulation of BHMT fragment 1 in amino acid starved cells (Fig. 48, lanes 5 and 6). The RHEB data support a hypothesis that the signal to autophagy goes through mTOR and that activation of mTOR is sufficient to inhibit autophagy. Ectopic expression of either $p70S6K^{T389E,D3E}$ or RHEB did not effect levels of LC3-II, shown in the bottom panel of Figure 48.

Like activated S6K, mycRHEB should also send a positive signal to S6. WCE aliquots of samples were prepared for western blotting with an antibody against phopho-S6. In control cells, amino acid and serum starvation inhibited the phosphorylation of S6. In cells expressing the mycRHEB allele, phosphorylation of S6 was retained in minus as well as plus amino acid conditions. Western blot with antibody against total S6 is shown as a control of expression. This suggests that phosphorylation of S6 does not inhibit autophagy and supports the hypothesis that the signal to autophagy does not go through p70S6K or S6.

The RHEB and p70S6K data suggest that the signal to autophagy goes through mTOR but is not through p70S6K. The small increase that was observed in BHMT fragment 1 in cells transfected with activated $p70S6K^{T389E,D3E}$ could suggest that the

over-expressed allele was interfering with a mTOR-dependent pathway parallel to p70S6K. Another well-known effector of mTOR signaling is 4E-BP1, a negative regulator of the translation initiation factor, eIF-4E. To test the effects of RHEB and $p70S6K^{T389E,D3E}$ on 4E-BP1 phosphorylation, an experiment identical to the one in Figure 48 was performed with the addition of a rapamycin control for each condition tested. A western blot was prepared from whole cell extracts with antibody against phosphorylated 4E-BP1. Levels of total 4E-BP1 are shown in the bottom panel as a control (Fig.50). In control and $p70S6K^{T389E,D3E}$ cells, 4E-BP1 was phosphorylated in plus amino acid media, but phosphorylation was inhibited in cells that were starved of amino acids (Fig. 50, lanes 1 and 5, compared to 3 and 7). 4E-BP1 in rapamycin-treated cells shows a slight band-shift down, which can be seen with both phospho and total 4E-BP1 antibodies (lanes 2 and 6). In starved cells expressing the $p70S6K^{T389E,D3E}$ mutant, little change in 4E-BP1 phosphorylation was noted compared to control cells. S6K does not appear to have dominant interfering effect. Expression of ectopic RHEB increased the phosphorylation of 4E-BP1 in either plus or minus amino acid conditions, and rapamycin was effective in blocking the phosphorylation (Fig. 50, lanes 9-12). Surprisingly, the expression of total 4E-BP1 was slightly decreased in the RHEB samples compared to control or $p70S6K^{T389E,D3E}$ (Fig. 50, lane 12). The band-shift pattern of 4E-BP1 makes interpretation of expression difficult in some instances, but rapamycin is effective in collapsing the band-shift, making the decrease in expression more obvious in the rapamycin-treated sample. Sustained mTOR signaling, through the over-expression of RHEB, increased phosphorylation of 4E-BP1 and decreased the expression of the protein.

While the mechanism through which mTOR signals to autophagy is still not known, the 4E-BP1 data suggest that a possible mechanism may involve signaling through 4E-BP1 and the initiation of translation. The potential link between 4E-BP1, translation, and autophagy is consistent with other studies that link autophagy and translation initiation through eIF-2alpha kinase. (See discussion.)

IV. DISCUSSION

4.1 Development of Autophagy Assays

The study of mammalian autophagy has been hindered by the complexity of the process. It requires the coordinate assembly of autophagy-specific proteins to build an autophagosome, an intact cytoskeletal network for trafficking, and a functional lysosome to degrade both the autophagosome and its cargo. Much of the study of autophagy has centered on the autophagosome itself and on the Atg proteins that assemble it. Two of the most commonly used methods to study autophagy involve electron microscopy and LC3. Both are based on the identification and quantification of autophagosomes. Although autophagosome formation is of fundamental importance, its degradation must be considered to understand and study the complete process of autophagy. An ideal assay would measure both sequestration and delivery to the lysosome. One goal of this study was to identify a substrate for macroautophagy that could be used to study the entire process, from engulfment through to lysosomal degradation.

4.1.1. Atg12 and Atg5 Conjugation

Much of what is known about the molecular mechanism of autophagosome formation originated from genetic studies in *S. cerevisiae* mutants that were defective in autophagy. Among the autophagy-specific genes identified by this approach were Atg12, Atg5, Atg7, and Atg10. Together, the proteins coded by these genes function in one of two novel ubiquitin-like conjugations systems required for the maturation of the

autophagosome membrane[26]. Atg12 is a ubiquitin-like modifier that is activated in an ATP dependent step by the E1-like enzyme Atg7, transferred to the E2-like enzyme

Atg10, and finally conjugated to Atg5 through the formation of an isopeptide bond, linking the carboxy-terminal glycine of Atg12 to the ε-amino group of lysine 149 of Atg5. The linked Atg12-Atg5 proteins then form a larger complex with Atg16[26]. This large complex can be found on the convex side of a forming autophagosome and may function as a coating complex to help in the curvature of the forming membrane. The Atg12-Atg5 conjugation system is fully conserved in higher organisms, underscoring the importance not only of this mechanism, but of autophagy itself. In $Atg5^{-/-}$ mouse embryonic fibroblasts (MEFs), autophagosomes do not form, and surprisingly, LC3-I is not conjugated to LC3-II, suggesting functional interaction between the two conjugation systems[27]. If $Atg5^{K130R}$, an Atg5 mutant that cannot link to Atg12, is expressed in $Atg5^{-/-}$ MEFs, $Atg5^{K130R}$ and Atg16 associate with small vesicles in the absence of Atg12, however the small vesicles do not grow[27]. Recent studies have shown that calpain-mediated cleavage of Atg5 produces an Atg5 fragment that induces apoptosis[86], however there is no known function for unconjugated Atg12.

At the beginning of this study, it seemed likely that the formation of new autophagosomes might require the assembly of more Atg12-Atg5 based complexes to coat the newly generated membrane. Changes in levels of either the complex or the individual conjugate partners would then be a novel way to assess the cells demand for new autophagosomes The data demonstrate that levels of the Atg12-Atg5 conjugate are exceedingly stable and do not appear to be regulated by amino acid starvation, inhibition of autophagy, or by levels of new protein synthesis. The conjugation occurs without

autophagy stimulus and appears to be irreversible. It is now known that there is a large cytoplasmic pool of the Atg12-Atg5-Atg16 complex and only a small percentage is associated with autophagosomal membranes[87]. Apparently, the Atg12-Atg5 complex exists in excess to meet cellular demand. The Atg12-Ag5-Atg16 complex does not stay associated with autophagosomes after formation is complete, and it is likely that the cell recycles and reuses the complex, keeping a stable pool available at all times. This makes the Atg5-Atg12 conjugate unsuitable as a measure of autophagy.

Unlike the conjugate, levels of Atg12 dropped significantly with amino acid starvation. This suggested two possible explanations. Either more Atg12 was recruited to the covalent complex during starvation, or it was degraded by another mechanism. Since conjugate levels were unchanged, the latter explanation was more likely. Cycloheximide provided an elegant way to discriminate between the two possibilities. As an autophagy inhibitor, it should protect levels of Atg12 if Atg12 levels are turned over by autophagy. As a translation inhibitor, it should cause levels of Atg12 to drop if Atg12 is degraded through another mechanism. The data support the latter. Cycloheximide also did not protect Atg12 levels during nutrient rich conditions, suggesting that Atg12 stability is not significantly regulated by the nutrient conditions of the cell. A major non-lysosomal mechanism for protein degradation in the cytoplasm is the protesome and data with the proteasome inhibitor MG132 confirm that unconjugated Atg12 was likely degraded by this mechanism.

Unlike ubiquitin, which has many targets, Atg12 is only known to have one, Atg5. Levels of unconjugated Atg12 and Atg5 are thought to be very low. It could be that the only cellular function of Atg12 is to post-translationally modify Atg5. Although

there is one report that suggests that unconjugated murine Atg12 facilitates LC3 processing, the data is based on overexpression and the authors clearly state that there is no evidence of unconjugated, endogeonous Atg12[88]. It is possible that unconjugated Atg12 may be either unnecessary or deleterious to the cell, making quick elimination in the best interest of the cell. Atg8 (LC3), the second ubiquitin-like modifier in autophagy, shares the same E1 enzyme, Atg7, with Atg12 in the conjugation process. In murine cells, Atg12 is the preferred substrate for Atg7, over LC3 and the other murine Atg8 orthologs[89]. This suggests that the Atg12-Atg5 conjugation takes preference over LC3 modification, and supports the idea that free unconjugated Atg12 is undesirable. It is also possible that the preference of Atg7 for Atg12 is to keep an excess supply of Atg12-Ag5 complex.

In conclusion, neither the Atg12-Atg5 conjugation system nor changing Atg12 levels proved suitable for the measurement of autophagy. The stability of the Atg12-Atg5 complex is an interesting observation that may be useful to validate knock-down of conjugation-specific ATG genes. HA-Atg12 and GST-Atg5 not only conjugate to each other, but they form conjugates with their endogenous partners as well (data not shown). The stability of the conjugate in normal cells allows for reliable interpretation of decreases induced by siRNA to Atg7 or Atg10 in future studies. The limited stability of unconjugated Atg12 is an interesting observation which may have physiological relevance.

4.1.2. LC3 conjugation and autophagy

LC3, the mammalian ortholog of Atg8, is a ubiquitin-like modifier in the second UBL conjugation system in autophagy. Pro-LC3 is translated in a form that requires

proteolytic cleavage by Atg4B to expose the carboxy-terminal glycine required for conjugation. It shares the E1-like enzyme Atg7 with the Atg12, but has its own E2-like enzyme, Atg3. Unlike any of the other known UBLs, LC3 does not modify another protein, but is conjugated to a lipid, most likely phosphatidylethanolamine, which anchors LC3-II to the autophagosome membrane[90]. LC3 is one of at least seven Atg8 orthologs in mammals, including GATE-16, GABARAP-I, GABARAP-II, and hAtg8L, LC3A, LC3B, and LC3C[23, 90]. All have been reported to associate with autophagosomes, though other functions are likely. LC3-II is the first, reported protein to specifically associate with autophagosomes, making it a valuable tool to identify these structures.

LC3 processing has been embraced by much of the research community as an assay to measure autophagosomes by both biochemical and fluorescent assays[20, 91]. The later relies on the localization of a chimeric LC3 fused to a fluorescent protein, normally green fluorescent protein (GFP). Cytoplasmic, punctate structures containing GFP-LC3 are thought to represent autophagosomes and autolysosomes. GFP- and RFP-LC3 reporters have been developed in the context of this study and punctate structures can be observed and compared between individual cells (data not shown). However, populations of each are found in both well-fed and starved cells making reproducible and sensitive counting of punctate structures problematic.

The biochemical LC3 assay has been heavily used in the study autophagy, sometimes in conjunction with the fluorescent assay. The lipid attached to LC3-II changes its electrophoretic mobility to create a faster migrating band that can be easily separated from LC3-I by SDS-PAGE. Changes in either levels of LC3-II or in ratios of

LC3-II/LC3-I are often used to assess autophagy[20]. In rare cases when LC3-II cannot be seen, decreased levels of LC3-I have been interpreted as increased autophagy[66]. Recently in the literature, issues concerning interpretations of the LC3 assay were raised by one the original investigators who introduced it[92]. Autophagosomes are not a product of autophagy and therefore, levels of autophagosomes do not always directly or linearly correlate with autophagy. They are intermediate structures in flux, and levels of LC3-II only measure how much is present at a given moment. High rates of autophagy can result in decreased LC3-II and low turnover at the lysosome can increase LC3-II. Both the fluorescent and biochemical LC3 assays have a high potential for false positive and false negative interpretations. However, if carefully used and interpreted, the LC3 assay maintains its value of specificity. For this reason, the biochemical LC3 assay was developed and carefully assessed in this study to provide a tool to independently confirm published findings and to compare autophagosome and autolysosome accumulation with an endpoint assay

During the subcloning of LC3, a mutant with the deletion of a conserved arginine (R68 or R69) in LC3 was discovered that retarded cleavage of pro-LC3 so that all three forms of LC3 were seen on SDS-PAGE. An additional insertion of nine amino acids between the conserved glycine and the translational stop also occurred during subcloning but was found not to affect cleavage. The region of LC3 affected by the deleted arginine is in a stretch of residues that is highly conserved in all the isoforms and orthologs of Atg8 from human to yeast. R68 in particular is 100% conserved in all species examined, with the exception of the plant *Arabidopsis* (Table 3). These residues are very near to a region containing two residues (F77 and F79 in yeast Atg8, F80 and L82 in human LC3)

that in yeast are important for the binding of Atg8 to the protease Atg4[65]. In the structure analysis of human Atg4B, the active site of Atg4B is occupied and inhibited by an autoinhibitory loop[93]. The core region of LC3, potentially involving F80 and L82, binds Atg4B, causing a conformational change to release the autoinhibitory loop and open the active site so that the carboxy-terminal tail of LC3 can bind the open cleft of the protease and be cleaved. Large bulky proteins fused to the carboxy-terminus of LC3 do not affect the ability of Atg4B to cleave LC3 efficiently in an *in-vitro* cleavage assay, supporting the conclusion that the additional 9 amino acids at the carboxy-terminal of the mutant LC3 reporter did not contribute to the delayed processing[94]. In one study of yeast Atg8, an alanine mutation was made in K66 (comparable to R69 in LC3) and tested for the ability to rescue autophagy in Δatg8 cells. No defect was found in the K66A mutant within the limitations of their assay[65]. With the data from the mutant LC3 of this study, it is likely that the K66A mutation would be functional, though delayed in processing.

The mutant LC3 reporter was tested for its response to two classic autophagy inhibitors: chloroquine and 3MA. Chloroquine enters the lysosome and acts as a proton sink, increasing the lysosomal pH and inhibiting lysosomal function and fusion with other vesicles. As expected, levels of LC3-II accumulate in the presence of 100μM chloroquine. 3MA inhibits the Class III PI3K, Vps34. The product of Vps34 activity is phosphatidylinositol 3-phosphate (PI3P) which is found on cytoplasmic vesicles and is thought to be required for autophagy. Although the mechanism is not clear, it is thought that PI3P is necessary for the assembly of Atg proteins at the newly forming autophagosome. One Atg protein that interacts with and possibly regulates Vsp34 is

Beclin1. Some studies have shown that decreased Beclin1 effects LC3-processing, so 3MA effects on LC3 are likely due to inhibition of Vps34[72]. Inhibition by 3MA causes an increase in the proform of LC3 in the mutant reporter, but does not affect accumulation of LC3-II. It is likely that the 3MA-mediated increase in the proform of LC3 is the result of a defect in the recruitment and colocalization of the substrate proLC3 with the Atg4B enzyme. Proteins that bind PI3P do so through FYVE or PX domains, neither of which is found in LC3 or Atg4B. Although interaction of proLC3 and Atg4B may be limited, the data show that LC3-II is still processed in the presence of 3MA. If PI3P is specifically responsible for Atg4B localization to the autophagosome, then in the presence of 3MA, less Atg4B would be available for both the cleavage of proLC3 and the de-lipidating activity or LC3-II necessary for vesicle fusion, thereby affecting autophagy in at least two distinct steps of the process. In the latter scenario, LC3-II levels would be frozen with no new production and no degradation. The mutant LC3 reporter may be useful for future studies on the early processing steps of LC3 processing.

The stable expression of HA-LC3-myc in HEK293 cells was a useful way to study the behavior of LC3 under various conditions. Four conclusions can be drawn from data generated by this reporter. First because some LC3-I may be degraded proteasomally under starvation conditions, LC3-I levels do not necessarily represent changes in autophagy. This is important because decreased levels of LC3-I have been used to invoke increased autophagy in the use of LC3-II to LC3-I ratios and occasionally as a stand-alone marker. It is possible that not all LC3-I observed by western blotting is newly synthesized and modified. Some LC3-II at the autophagosome membrane must be cleaved and removed by Atg4B before vesicle fusion can occur. The electrophoretic

mobility of the released LC3-I would likely be the same as newly modified LC3-I. It has been suggested that released yeast Atg8-I is reused, however the data does not describe the exact site of the second cleavage[95]. Although some deubiquitinating (DUB) enzymes cleave the functionally-related ubiquitin from small adducts, the structure of human Atg4 is most similar to the UBP family of DUB enzymes which cleave the ubiquitin molecule from proteins[93]. Cleavage of LC3 at a peptide bond to remove PE would also remove the carboxy-terminal glycine, making it incompetent for a new round conjugation. If correct, it is conceivable that a pool of incompetent LC3 would be proteasomally degraded during starvation. It also explains why LC3-I levels are not proteasomally degraded in nutrient rich conditions, as this pool of LC3-I is likely newly processed from proLC3.

The second conclusion that was apparent from the LC3 data is that levels of LC3-II do not directly correlate with autophagy and can easily be misinterpreted. Autophagosomes are intermediate, transient vesicles in a constant state of flux and LC3-II levels are 'snapshots' that reflect the balance between synthesis and degradation at a specific moment in the process. Degradation is an important part of the regulatory process and LC3-II levels can increase, decrease, or not change under starvation conditions. The data show that inhibition of lysosome degradation can be used as a tool to demonstrate LC3-II flux at short and long time points, dependent on the strength of the inhibition. The data in this study are consistent with recently published data that lysosomal protease inhibitors are necessary to properly interpret LC3-II levels[92].

Strong lysosomal inhibition shows that a significant amount of LC3-II turns over in nutrient rich conditions. This observation is supported by data published by Kochl et

al. that examined the effect of microtubule disrupting agents on macroautophagy in both full and minimal media[70]. It suggests a significant degree of autophagosome membrane flux during nutrient rich conditions and raises a question about whether amino acid starvation increases LC3-II processing. The chloroquine time course data from this study show that levels of LC3-II accumulate faster under starvation conditions, consistent with an interpretation that LC3-II is processed at a faster rate under starvation conditions. Conceptually however, the unexpected level of LC3-II flux in complete media is not inconsistent with a form of a mammalian Cvt-like pathway or of a cytoplasmic version of pinocytosis, with constant internal LC3-II-marked membrane flux through the lysosome. Interestingly, LC3-II levels appear to be self-limiting. The limiting factor does not appear to be LC3-I, because in nutrient rich media, levels of LC3-I are maintained and still available. It has been suggested that the E1-like conjugating enzyme Atg7 may be limiting[88]. However, overexpression of Atg3, Atg7, or Atg4B does not appear to promote LC3-II processing or autophagy (data not shown). The exact nature of this feedback is not yet known.

The ultimate conclusion of the data generated from the study of LC3 is that LC3-I and LC3-II data must be interpreted cautiously. There is a growing acknowledgement in the field that LC3-II levels alone are not sufficient to measure autophagy. To address this, some studies interpret LC3-II levels only in conjunction with measurement of the degradation of long-lived proteins. Unfortunately, these methods are neither sensitive nor specific for macroautophagy. An ideal assay would measure a product of autophagy at completion, after specific cargo has been sequestered, delivered to the lysosome and degraded.

4.1.3. The BHMT assay

There is a need in the field of mammalian autophagy for an assay that would specifically and sensitively measure the lysosomal degradation of an autophagy cargo protein. This need led to the development of the BHMT assay. Highlights of the discussion will focus on three topics. Why choose BHMT? Is the BHMT measuring macroautophagy? What is the sensitivity and linearity of the BHMT assay?

The decision to turn a metabolic enzyme, betaine homocysteine methyltransferase (BHMT) into a reporter for autophagy began with a published report that rat BHMT associates with purified autolysosomes[96]. One specific proteolytic fragment of rat BHMT was found only on the inside of autolysosomes of rats that were administered the protease inhibitor leupeptin, suggesting that there was a leupeptin-resistant cathepsin specific for a particular site in BHMT[96]. Despite the fact that the authors of a follow-up paper suggested their attempts to create an exogenous BHMT reporter for autophagy had been unsuccessful[68], BHMT was chosen as one of several promising candidates for a plasmid-based reporter assay for autophagy in cell culture.

It was assumed that if proteolytic fragments of BHMT were generated lysosomally, they would not be abundant. However, creation of an epitope-tagged BHMT fusion protein would allow for purification and enrichment of rarified fragments. After several unsuccessful attempts to fuse BHMT to GST, HA or myc epitope tags in an assortment of different combinations, a successful combination was found that fused GST to the amino terminus of BHMT and myc to the carboxy terminus. In conditions known to induce macroautophagy, a leupeptin-resistant GST-fused fragment, termed fragment 1,

of the expected size accumulates quantitatively. Attempts to isolate a carboxy fragment with antibody to myc were not successful (data not shown).

Multiple forms of the BHMT reporter were generated in the course of this study. Each reporter consistently generated fragment(s) in conditions known to induce autophagy, such as starvation from essential amino acids, and to a lesser degree, rapamycin treatment. The starvation-induced generation BHMT fragment(s) was inhibited by every macroautophagy inhibitor tested: 3MA, wortmannin, chloroquine, bafiolomycin A1, puromycin, cycloheximide, and vinblastine. Further validation of the lysosomal nature of the fragments generated from BHMT is found in the co-fractionation of BHMT fragments with the lysosomal marker, LAMP1, in fractions collected from the LMF compartment of cells separated by density on sucrose gradients.

Although the pharmacological data with the BHMT assay suggest that lysosomal import occurs through macroautophagy, other mechanisms of autophagy must be eliminated as either primary or alternative routes to the lysosome for GST-BHMT. One mechanism of autophagy considered is chaperone-mediated autophagy (CMA) which is induced by long term amino acid and serum starvation[10]. There are no known pharmacological inhibitors of CMA, making elimination of a CMA-dependent mechanism difficult. The hsc73 protein recognizes substrates of CMA through exposure of a sequence of amino acids typified by the ribonuclease A sequence, KFERQ[97]. The KFERQ sequence is often degenerate to the point of being unrecognizable, but examination of the human BHMT sequence failed to find any KFERQ-like sequences. The inability to identify a KFERQ sequence in human BHMT is consistent with a published report that KFERQ-like sequences could also not be found in rat BHMT[68].

Unexpectedly, in a published review of chaperone-mediated autophagy, GST was included in a list of known CMA substrates with KFERQ-like sequences[10]. Mutation of the obligate Q or N in KFERQ to an alanine is sufficient to mask recognition by the chaperone complex. The GST^{N43A}BHMT mutation did not change BHMT fragmentation in response to starvation of serum and essential amino acids, or to any of the macroautophagy inhibitors, suggesting that CMA was not a mechanism responsible for BHMT lysosomal import. A recent study found that vinblastine, 3MA, and wortmannin did not inhibit CMA[71] and all were effective in blocking the accumulation of BHMT fragment 1. The pharmacological data of vinblastine, 3MA, and wortmannin support the idea that CMA is not a mechanism of lysosomal import for BHMT.

A third argument against import by CMA can be made from the data on higher order structure. Multimerization of BHMT is necessary for cleavage of the L2 loop to produce fragment 1. The need for oligomerization suggests that BHMT must be imported into the lysosome with quaternary structure intact. During CMA, proteins in the chaperone complex bind LAMP2a at the lysosome membrane and then unfold so that the protein can be threaded through the lysosomal membrane and enter the luminal space. It seems extraordinarily unlikely that BHMT could regain its quaternary structure in the lysosome after entering by the CMA mechanism and be cleaved to generate fragment 1.

In addition, in the course of this study, siRNA targeting LAMP2 successfully reduced expression of LAMP2 protein by approximately 90%. Of the two shRNAs tested, one did not effect BHMT processing and one slightly enhanced BHMT fragmentation (data not shown). The latter result is consistent with a report with selective

knock-down of LAMP2a causes a compensatory increase in macroautophagy[12]. Together, these data support the hypothesis that BHMT is not a substrate for CMA.

Microautophagy is a third mechanism that could import GST-BHMT directly into the lysosome. There is very little published information available about lysosomal invagination and import, although it is generally considered to be a constitutive process, with one exception. In yeast there is a report that TOR positively regulates microautophagy as a mechanism to reduce vacuole size after rapamycin treatment and macroautophagy-induced swelling of the vacuole[9]. The protein complex at the vacuole membrane that mediates this process is conserved in mammals, although the existence of a similar mechanism in mammals is not known. However, in this scenario, rapamycin would be expected to inhibit, not induce degradation. To eliminate microautophagy as a mechanism of BHMT lysosomal import, it was necessary to knock out a macroautophagy-specific gene.

Beclin1, the human Atg6 ortholog, is a good candidate for specific targeting by shRNA because its role in macroautophagy is widely accepted in the autophagy field, its silencing is often cited as validation of macroautophagy, and available antibodies are sensitive enough to demonstrate changes in levels of endogenous protein. Low levels of Beclin1 have been linked to decreased autophagy in MCF7 cells, while over-expression of Beclin1 in MCF7 cells Beclin1 has been shown to induce autophagy and reduce tumorigenicity[38]. It should be noted that in this study, ectopic expression of HA-Beclin1-myc in the cells tested is not sufficient to increase autophagy, as determined by either the LC3 or BHMT assays (data not shown). There could be cell-specific differences between the MCF7 cells in the cited work and the cells used in this study.

Another possibility is that overexpressed Beclin1 in HEK293 cells forms sub-stoichiometric complexes that are not autophagy competent. One study found that overexpessed Beclin1 required the coexpression of a mutant associating protein, PIST, to induce autophagy[98]. Alternatively, the epitope tags fused to Beclin1 may interfere with any autophagy-promoting function. Ectopic expression of Beclin1 without epitope tags should help resolve the latter issue. The data show that shRNA targeting three distinct regions of the Beclin1 mRNA decreased expression of Beclin1 protein. Significantly, depletion of Beclin1 is sufficient to decrease accumulated levels of BHMT fragment 1 in starved cells, establishing unambiguously that the BHMT assay is reading macroautophagy.

The second autophagy-specific target chosen to validate the BHMT assay is the serine-threonine kinase orthologous to yeast Atg1, hULK1. In humans, hULK1 expression has been linked to the trafficking of Atg9 between the trans-Golgi network (TGN) and late endosomes[52]. The link between hULK1 and mAtg9 is consistent with impaired trafficking of Atg9 in yeast Δatg1 mutants between the pre-autophagosomal structure (PAS) and non-PAS structures[47]. Two separate shRNAs targeting hULK1 effectively decreased levels of accumulated BHMT fragment 1 in amino acid starved cells, validating that the BHMT assay is measuring macroautophagy by depletion of a second autophagy gene.

Regarding autophagy, the ability of shRNA targeting ULK1 to inhibit BHMT fragmentation indicates that hULK1 and its isoform hULK2 do not seem to have overlapping functions. hULK1 and hULK2 share the same basic domain structure with an amino terminal kinase domain, a central proline-serine rich domain, and a carboxy-

terminal domain. The catalytic and carboxy-terminal domains are well conserved between the two isoforms, with little conservation noted in the central proline-serine (PS) rich domain[50]. It has been suggested that the human Atg8 orthologs GATE-16, GABARAP, and to limited degree LC3, bind the middle PS domain of hULK1[99]. Future experiments that exchange domains between these two kinases will help determine what regions of the kinase are essential for autophagy.

The above data indicate that hULK1 is important for autophagy and should be studied regarding its role in regulating autophagy. This study attempted to answer three questions regarding hULK1 and autophagy: 1) Is hULK1 specific activity effected when autophagy is induced by amino acid starvation or rapamycin or when cells are treated with autophagy inhibitors? 2) Do levels of hULK1 change in response to the induction of autophagy and is this a mechanism of regulation? 3) Is hULK1 activity required for autophagy?

In yeast, there are two theories regarding Atg1 activity and macroautophagy. Kamada et al. reported that activity was necessary for autophagy while Abeliovich et al. found that Atg1 protein was necessary for macroautophagy and the related Cvt pathway, but its activity was only required for the Cvt pathway[45, 46]. Both studies suggest that Atg1 functions in a complex of proteins and that phosphorylation of Atg13 and Atg1 regulate Atg1 activity. The data in this study show that the catalytically inactive hULK1^{KD} inhibits the generation of fragment 1, suggesting that hULK1 activity may be necessary for mammalian autophagy. However, levels of over-expressed hULK1^{KD} are likely greater than endogenous hULK1, making the formation of sub-stoichiometric complexes possible which could interfere with parallel pathways.

This led to the study of hULK1 specific activity in conditions known to induce or inhibit autophagy. Kamada et al showed that two well known inhibitors of TOR, starvation or rapamycin, increase yeast Atg1 specific activity[45]. In contrast to the yeast data, the results here show that the specific activity of HA-ULK1-myc does not change in response to starvation or rapamycin, and is not affected by inhibitors of autophagy such as 3MA, wortmannin or chloroquine. What might explain this? An obvious explanation would be that yeast Atg1 and human hULK1 are not regulated in the same manner. Some kinases are regulated by levels of expression and there is one report that levels of ULK1 mRNA increase with viral infection in neurons[100]. Since hULK1 mRNA increased in the case of viral infection, and because viral invasion is one way to induce autophagy, it seemed possible that hULK1 levels might increase with amino acid starvation. The data with qPCR show that levels of hULK1 mRNA remain essentially unchanged after 6 hours of amino acid starvation. It does not appear that amino acid starvation regulates hULK1 at the transcriptional level.

How else might hULK1 be regulated? Yeast Atg1 is regulated by the post-translation modification of associating proteins. Atg13 must be de-phosphorylated for Atg1 to be active which suggests that an active phosphatase is required to regulate Atg1 activity. It may be that hULK1 requires the association and/or modification of other proteins for regulated activity that is not reflected in an *in-vitro* assay. It is also possible that the amino or carboxy termini of hULK1 may be important for regulation of its activity. The epitope tags fused to hULK1 may interfere with the regulation of its activity. Little is known about the importance of domains, post-translational modifications, or regulatory proteins for either of the hULKs. Potential issues of

interference caused by the fusion of epitope tags to the hULK1 protein are currently being addressed by making a non-tagged construct for ectopic expression.

It may be that hULK1 is constitutively active and regulated by localization, expression or other mechanism. Autophagy is a membrane trafficking process, and it is possible that hULK1 re-localizes to or from membrane structures in autophagy-stimulating conditions. This is consistent with its role in mAtg9 trafficking. Preliminary studies with the epitope tagged hULK1 have failed to demonstrate differences in distribution between cytosolic, nuclear, or membrane fractions of cell extracts (data not shown). This issue will be revisited with a non-epitope-tagged version of the kinase.

In-vitro kinase assays demonstrate that hULK1 can autophosphorylate, and metabolic labeling with $^{32}PO_4$ shows that hULK1 is phosphorylated *in-vivo*. This suggests that phosphorylation is a mechanism of regulation of hULK1. The activation loop (T-loop) in subdomain VIII of hULK1 contains a cysteine-glycine pair of amino acids that is highly conserved in members of the AGC and CaM kinase families. Kinases that belong to these family groups are phosphorylated on a conserved threonine in the T-loop by an upstream kinase. Mutation of this conserved threonine to an alanine in hULK1 renders hULK1 catalytically inactive (data not shown) suggesting importance of T-loop phosphorylation in the activation of hULK1. In the structurally related hULK2, a priming phosphorylation event is apparently necessary for autophosphorylation and activity, as prolonged treatment with calf intestinal treatment renders hULK2 inactive (data not shown). This phosphorylation event is likely T-loop phosphorylation. The inability of hULK2 to reactivate after prolonged CIP treatment makes it unlikely that hULK2 phosphorylates its own T-loop, although it cannot be ruled out if another priming

phosphorylation is required. hULK2 also shows a high preference for serine over threonine, providing additional evidence that T-loop auto-phosphorylation is unlikely. Interestingly, in the yeast genetic screens, no potential up-stream kinase was identified for Atg1. The failure to identify an up-stream kinase in the autophagy screens supports the yeast model which suggests Atg1 activity is not required for autophagy. Phosphorylation by other kinases may also be important for activity of hULK1 as it has been suggested that PKA may phosphorylate yeast Atg1[101]. Future studies are planned to purify and identify the hULK1 upstream T-loop kinase.

There are no known endogenous substrates of either Atg1 or hULK1. Pull-down experiments and proteomic analysis can be used to identify potential substrates of hULK1. Many of the Atg proteins are phospho-proteins, and hULK1 can phosphorylate some of them *in-vitro* (data not shown). With the tools developed in this study, changes in metabolic labeling of Atg proteins in cells depleted of hULK1 will be used to study effects of hULK1 on Atg post-translational modifications. Regarding activity of hULK1 and autophagy, future experiments are planned that will attempt to rescue the autophagy defect caused by the shRNA-mediated decrease of hULK1 with expression of either the catalytically active or kinase dead alleles of hULK1. If successful, these types of experiments will validate the importance of hULK1 in autophagy and will help determine if catalytic activity is important for autophagy.

In physiology, there are times when circulating amino levels are low, such as after prolonged fasting or in postnatal infancy. Amino acid levels are an important part of the regulation of macroautophagy based on what is reported in the literature[73] and on the response of the BHMT assay. The data show that the BHMT assay is not sensitive to

high levels of essential amino acids. Most of the studies with the BHMT reporter have been done in transformed HEK293 cells that are cultured in DMEM with high amino acid levels. Do transformed cells adapt to high levels of amino acids, or is the cellular sensing mechanism for amino acids unaffected. A linear response of BHMT fragment 1 accumulation to extra-cellular levels of amino acids is only seen when levels of DMEM essential amino acids fall below 10%. This was surprising until levels of the amino acids in DMEM were compared to the normal adult reference ranges. The response of cells in culture is within the physiological range. It appears that cells do not adapt to high levels of amino acids, but maintain sensitivity at more physiological levels. The BHMT assay responds appropriately to physiological levels of essential amino acids, especially when one considers that it is measuring the endpoint of a biological process.

Interestingly, the BHMT assay does not respond equally to the individual essential amino acids. It is possible that the intracellular levels of the essential amino acids may not reflect the extracellular environment within the time frame of the experiment. Bloomaart et al. demonstrated that not all amino acids are in equilibrium with the extracellular environment[73]. However, he also showed that the intracellular levels of a select group of amino acids reflect extracellular concentrations in a linear fashion. His findings included leucine, isoleucine, lysine, phenylalanine and tyrosine, some or all of which were suggested to be amino acids that regulate autophagy[73]. In support of this, the BHMT assay shows sensitivity to leucine, phenylalanine, lysine, and tyrosine. The BHMT assay is also sensitive to arginine, which was not tested in the Bloomaart study.

It is possible that the mechanisms that sense amino acids levels may have selective sensitivity for individual amino acids. How does the cell sense and respond to these particular amino acids? There are two kinases that sense amino acids and both have been implicated in autophagy: mTOR and the eIF2alpha kinase, GCN2[54, 102]. Amino acids, particularly leucine, strongly activate p70S6 kinase through mTOR[103]. How does mTOR sense amino acids? Recent studies suggest that amino acids increase Vps34 activity which in turn activates mTOR[36, 37]. This is counter to reports that amino acid starvation activates Vps34[33], however it is likely that Vps34 functions in distinct complexes that may affect mTOR in opposing ways. How does Vps34 sense amino acids? This mechanism is not yet known and may involve internal and external signals. One report suggests that amino acids may act as a first messenger and signal through plasma membrane receptors[104].

GCN2 responds to levels of intracellular amino acids. GCN2 is an eIF2α kinase that is activated by the deacylation of tRNA. Once activated, it phosphorylates the eukaryote initiation factor 2 alpha (eIF2α) at S51 causing a general translation arrest, but facilitating the translation of GCN4, a transcription factor that has been shown to regulate several autophagy genes[105]. In yeast, amino acid starvation induces autophagy through GCN2; however rapamycin can induce autophagy in the Δgcn2 mutant[102]. One explanation for this could be that GCN2 and TOR activate autophagy through parallel pathways. The BHMT assay indicates that full autophagy activation requires the additive effects of multiple amino acids, supporting the idea that mTOR and GCN2 might respond independently to the same nutrient stress. If true, there could be distinct levels of autophagy activation. Intracellular levels of leucine and the other branched chain amino

acids decrease by as much as 90% within 30 minutes of amino acid withdrawal without affecting the acylation of their respective tRNAs[74]. Thirty minute starvation is sufficient to inactivate mTOR which may activate autophagy initially, followed by a second tier of activation by GCN2. Interestingly, both GCN2 and mTOR regulate translation at the level of initiation, suggesting that translation initiation is an important part of the regulation of autophagy.

Lysosomes are dynamic organelles that differ between cell types in their complement of hydrolytic enzymes. It was tested to see if the BHMT would generate an identifiable fragment in starved cells of other types and species. Cell tested include T98G cells, MCF7 cells, H1299 cells, NIH3T3 cells and C2C12 cells. T98G cells are human glioblastoma cells that are negative for expression of PTEN. Loss of PTEN results in sustained signaling through the PI3 Kinase/Akt pathway, a growth signaling pathway that activates mTOR and is generally thought to suppress macroautophagy[57]. Despite the loss of PTEN, T98G cells were capable of a robust, macroautophagic response to amino acid deprivation. MCF7 cells are human, breast carcinoma cells that are reported to have depleted levels of the autophagy-specific protein, Beclin 1. It has been shown that MCF7 cells have decreased levels of macroautophagy, which could be increased by overexpression of exogenous Beclin 1[38]. The MCF7 cells tested with the BHMT assay were capable responding to amino acid starvation, although the percent increase of accumulated fragment in starved cells compared to control was less than in T98Gs.

H1299 cells are human lung cancer cells that are devoid of the tumor suppressor p53. The induction of p53 has been linked to increased autophagy through several

mechanisms, including negative effects on mTOR and through the lysosomal protein, damage-regulated autophagy modulator DRAM[106, 107]. The dramatic accumulation of BHMT fragment in starved H1299 cells demonstrates that macroautophagy can respond to amino acid starvation in a p53-independent manner. It may be the p53 is required for an autophagic response to genotoxic stress, but is not necessary for a response to amino acid starvation. NIH3T3 cells are immortalized mouse fibroblast and C2C12 cells are immortalized mouse myoblasts. Both mouse cell lines generated a fragment of the same size as fragment 1 in human cells, implicating a similar lysosomal cathepsin. The C2C12 cells did not transfect to a very high efficiency and consequently the level of fragment 1 was low, but fragmentation with starvation still occurred that was sensitive to both 3MA and chloroquine. In conclusion, the lysosomal protease that cleaves BHMT to generate fragment 1 is generally distributed between various cell types and species, broadening the possible applications of the BHMT assay.

4.2. BHMT and higher order structure

The BHMT data suggest that quaternary structure is maintained within the autophagosome. This conclusion is supported by the data that fragment 1 is only generated from BHMT subunits that can form multimers. While it is possible that the cathepsin that cleaves L2 requires an intact carboxy-terminus to bind and cleave, the resistance of the GST-BHMT^{W352A} mutant to generate fragment 1 argues against this possibility.

Second, monomeric and multimeric BHMT molecules are both substrates for macroautophagy. This conclusion is supported by the protection assay and by the generation of fragment 2′ in the GST$_{\Delta T}$BHMT and GST$_{\Delta T}$BHMT$^{\Delta C51}$ reporters.

Quaternary structure of BHMT is not important for the proteolytic cleavage in the region of GST to produce fragment 2′. Although this was not the expected result, it raises an interesting question. Why is BHMT degraded through macroautophagy and not by another mechanism? The BHMT truncation mutants and W352A point mutant all appear to make stable proteins. More severe truncations, however, result in unstable protein that is likely proteasomally degraded soon after translation. An attractive hypothesis is that macroautophagy is a preferred mechanism to remove enzymes or organelles (mitochondria) that contain metal ions, to sequester the oxidizing Zn^{2+}, Cu^{2+} or Fe^{2+} ions that could be harmful to the cytoplasmic environment. In support of this, a rare autosomal recessive disease, mitochondrial myopathy and sideroblastic anemia (MSA), is caused by an unknown gene mutation that maps to the chromosomal region of hULK1[108]. As the name suggests, the disease is marked by excessive accumulation of iron stores, which could be caused by a defect in macroautophagy. The crystal structure of BHMT predicts that although ΔC51 and W352A BHMT mutants cannot oligomerize, they likely assemble into normal $(\alpha/\beta)_8$ barrel subunits, with the Zn^{2+} intact, making them both macroautophagy substrates.

Third, the data of $GST_{\Delta T}BHMT$ and $GST_{\Delta T}BHMT^{\Delta C51}$ on sucrose gradients provide evidence of a 3MA-sensitive and 3MA-resistant macroautophagy. $GST_{\Delta T}BHMT$ is a substrate of the first and $GST_{\Delta T}BHMT^{\Delta C51}$ is a substrate of both. This result is surprising because the autophagy field defines macroautophagy almost exclusively in terms of sensitivity to 3MA.

Does macroautophagy proceed in cells treated with 3MA? 3MA's inhibition of Vps34 is likely partial inhibition. Strong inhibition of PI3K activity with wortmannin is

sufficient to inhibit fragmentation of both forms of BHMT and macroautophagy, which suggests that in cell treated with 3MA, some PI3P is still made. Is it enough to support autophagy? The data of the HA-LC3B reporter show that in the presence of 3MA, LC3-II is produced and lysosomally degraded. Is this LC3-II part of a cargo vesicle?

The data of $GST_{\Delta T}BHMT^{\Delta C51}$ fragment 2′ on the sucrose gradient argue that the LC3-II produced in the presence of 3MA is actively sequestering and delivering $GST_{\Delta T}BHMT^{\Delta C51}$ to the lysosome. What is the difference between the light (5/ 6) fractions and the dense fraction (8) on the sucrose gradient? The dense fractions are sensitive to 3MA and the lighter are resistant. From the sum of the date, the following characterization of fractions 6 and 8 could be made (Table 5). The more buoyant fraction 6 contains autophagosomes, newly formed autolysosomes, and pure lysosomes. Fraction 8 contains denser autolysosomes/amphisomes.

In 3MA treated cells, LAMP1 in fraction 8 is decreased. The decrease of LAMP1 in fraction 8 in 3MA-treated cells suggests that PI3P is required for the fusion events necessary to generate dense autolysosomes/amphisomes. The density shift of LAMP1 from fraction 8 to fraction 6 is consistent with sucrose gradient data from wortmannin treated cells (data not shown). Does the LAMP1 in fraction 5/6 represent lysosomes or more boyant autolysosomes? The co-fractionation of $GST_{\Delta T}BHMT^{\Delta C51}$ fragment 2′ and LC3-II with LAMP1 in 5/6 suggests that autolysosomes form in fractions 5/6 when levels of PI3P are limiting.

Why is $GST_{\Delta T}BHMT^{\Delta C51}$, but not BHMT degraded in 3MA-treated cells? What is the relationship between PI3P and the different abilities of these two mutants to oligomerize? It could be through a mechanism that involves proteins that are regulated

by binding to PI3P. Downstream effectors of hVps34 signaling bind to PI3P through a FYVE domain (first described in proteins Fab1, YOTB/ZK632.12, Vac1, and EEA1) or in some instances through a Phox homology (PX) domain. Despite the importance of PI3P in autophagy, there are very few Atg proteins that actually bind PI3P. The few Atg proteins that have FYVE or PX domains are involved in cargo recognition of the Cvt pathway. Could this type of cargo recognition be involved in mammalian autophagy and in the selection of BHMT? A model of this type of recognition proposes the existence of a FYVE-domain adapter protein that would recognize oligomeric but not monomeric BHMT to bring it to the autophagosome (Fig. 51). Or perhaps BHMT normally forms complexes FYVE-like proteins, as BHMT reportedly associates with both autolysosomes and mitochondria, even though it does not itself have a FYVE domain, PX domain, or other membrane tethering modifications. Thus, when PI3P is available and autophagy is induced, its association with autophagosomes is through a PI3P-dependent mechanism.

If a FYVE adapter-like protein recognizes only BHMT, how does $GST_{\Delta T}BHMT^{\Delta C51}$ become sequestered in autophagosomes? $GST_{\Delta T}BHMT^{\Delta C51}$ is a BHMT monomer in a non-functional conformation. Is there a mechanism that cells use to target misfolded, non-essential, or aggregated proteins for macroautophagy? Reports show that p62/SQSTM1 can function as an adapter-like protein that physically links aggregates of mutant huntingtin protein with LC3 and autophagosomes for degradation[109]. The association between p62 and the mutant huntingtin protein requires p62's ubiquitin-association (UBA) domain. Is this a cellular mechanism that cells use to recognize and remove misfolded proteins by macroautophagy? It is proposed

Figure 51. Proposed model for 3MA-sensitive and 3MA-insensitive macroautophagy. In the proposed model, production of PI3P enriches autophagosomes with its normal cargo through FYVE or PX-containing adapter molecules. When PI3P levels are limiting, this cargo is no longer favored. Abnormal protein structure is recognized by adapter proteins that directly interact with Atg8-orthologs at the autophagosome membrane. These complexes are modeled after p62s proposed role in clearing mutant huntingtin protein.

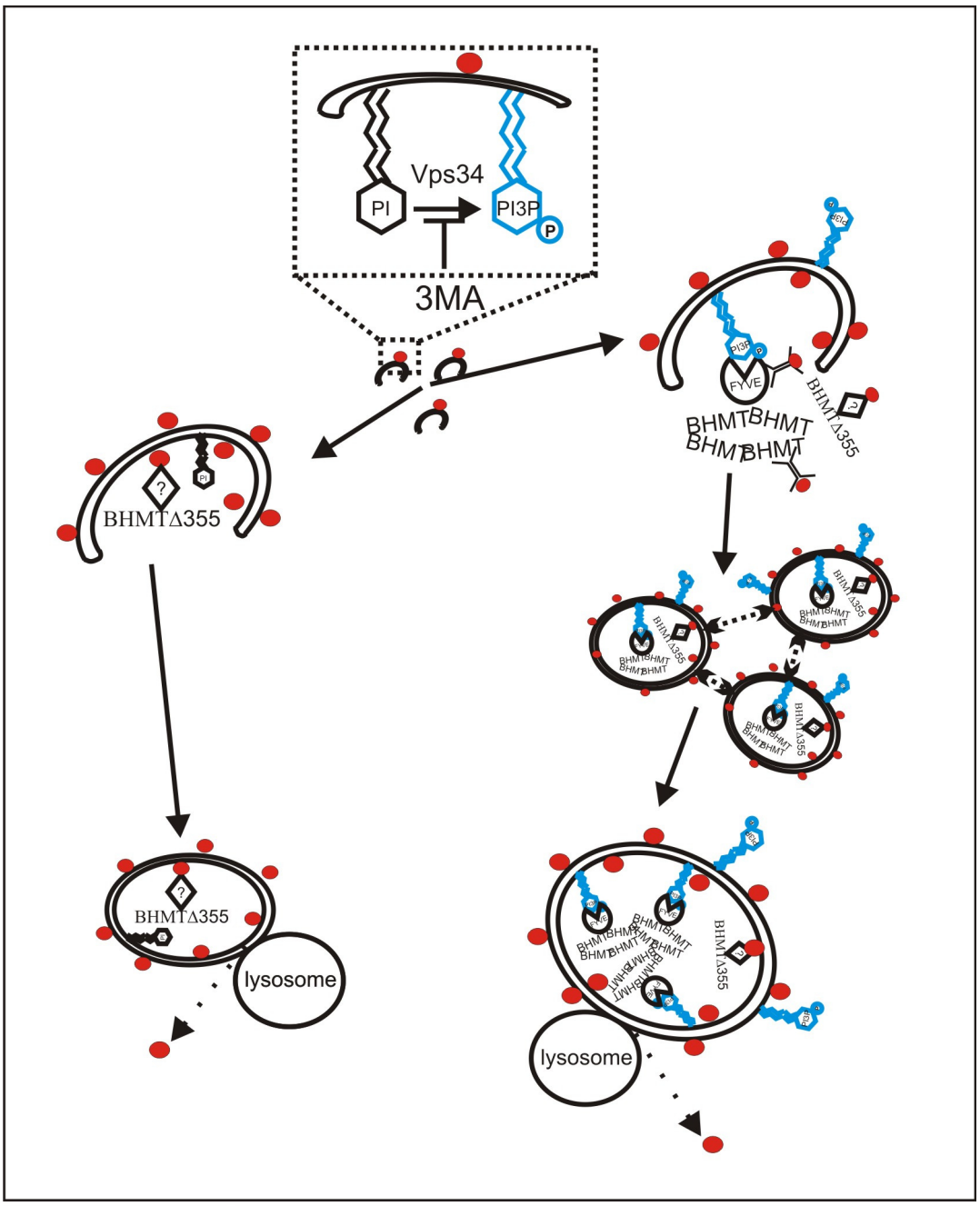
Vps34
PI
PI3P
P
3MA
BHMTΔ355
FYVE
lysosome
LC3
Adaptor for misfolded protein
Adaptor for normal long-lived protein

that this type of mechanism explains the degradation of the $GST_{\Delta T}BHMT^{\Delta C51}$ monomer, and that when PI3P is limiting, degradation of these aggregates continues.

The p62-like adapter mechanism involves direct targeting of aggregates to LC3. Could other Atg8 orthologs have similar roles? And does this explain one of the unanswered questions in autophagy of why there are so many mammalian Atg8 orthologs? When LC3-II was first described as being specific for autophagosomes, the data did not suggest that LC3-II was on all autophagosomes. This suggests that the other Atg8 isoforms may have functions similar to LC3, and indeed, all have been found onautophagosomes. The data that links p62 and LC3 is significant. The plethora of the other Atg8 orthologs suggests that there may be multiple adapters and autophagosome receptors for the clearance of cellular 'garbage' like $GST_{\Delta T}BHMT^{\Delta C51}$.

It is proposed that there are two types of macroautophagy, a signaling autophagy and a structural autophagy (Fig. 51). Both require some PI3P. The signaling autophagy requires sufficient levels of PI3P for recognition of normal cargo such as BHMT. The structural autophagy requires less PI3P and the coordinate activity of the Atg proteins that participate in autophagosome formation. Under starvation conditions with readily available PI3P, both BHMT and $GST_{\Delta T}BHMT^{\Delta C51}$ are degraded. When PI3P is limiting, cargo recognition is limited, but the structural, basal autophagy continues to degrade abnormal cargo, such as $GST_{\Delta T}BHMT^{\Delta C51}$.

In mammalian cells, Vps34 plays a role in trafficking decisions that control the destination of internal vesicles. The proposed model suggests that substrates of the signal-dependent autophagy are more regulated than random. It makes energetic sense to be selective in the process of degradation of proteins that require new synthesis when the

crisis has past. There are other stressors that induce autophagy such as viral or pathogen invasion, where non-specific wholesale degradation of cellular protein might not be desired. However, there are no conditions where accumulated, misfolded, or aggregated protein is desirable. It is this second, structural autophagy that is valuable for the health of the cell and organism.

4.3. Regulation of autophagy and p70S6 Kinase

The protein kinase mTOR plays a central role in the ability of cells to sense growth signals, amino acid levels, and energy in order to make decisions that effect the translation of new proteins, cell growth and proliferation. The signals through mTOR to its downstream effectors p70S6K and 4E-BP1 regulate events involved in the initiation of translation and regulate events in macroautophagy (Fig. 5). If nutrients are readily available from the extracellular milleau, mTOR signals for the cell to grow. When extracellular nutrients are scarce, down-regulation of mTOR signaling increases autophagy to degrade internal proteins for the energy and raw materials necessary for survival.

What is the relationship between p70S6 kinase and autophagy? There is strong correlative evidence of an inverse relationship between phosphorylation of the ribosomal subunit S6 and autophagy in a mammalian setting. The negative correlation between phosphorylated S6 and autophagy has led to a proposed model that places phosphorylated S6 at the endoplasmic reticulum. In the proposed model, the inhibition of mTOR causes de-phosphorylation of S6 and its release from the rough ER. The smooth ER created by the loss of ribosomes is proposed to be one source of the autophagosome membrane[54]. This mechanism directly links mTOR, p70S6 kinase and S6 with autophagy.

In *Drosophila*, it has been proposed that p70S6 kinase must be active for efficient autophagy[58]. How is p70S6 kinase active if TOR is inactive? It has been suggested that residual activity of p70S6 kinase remains when TOR is first inactivated. This activity is both sufficient and required for autophagy. Without TOR activity, it is also self-limiting, preventing uninhibited autophagy from progressing to the point of cell death.

In the current study, using the BHMT assay as a measure of macroautophagy, there is no correlation between the phosphorylation of S6 and autophagy. Both the constitutively active allele of S6K and RHEB increase the signal to S6 in the absence of amino acids. However RHEB inhibits autophagy and active S6K does not inhibit autophagy, suggesting that the inhibitory signal to autophagy is through mTOR, but does not go through the p70S6K arm of the pathway.

The constitutively active S6K does cause a slight increase in levels of BHMT fragment 1. If the model from Scott et al. in *Drosophila* is correct, then S6K activity may be pushing a maximum signal to autophagy. An alternate explanation is that the over-expressed allele may have a dominant interfering effect by sequestering mTOR. Others have shown that this can have a negative effect on mTOR's other substrate, 4E-BP1. However, the phosphorylation data with 4E-BP1 suggest that in this instance that activated S6K did not inhibit mTOR signaling to 4E-BP1.

Interestingly, the RHEB-mediated sustained positive signal through the mTOR pathway caused hyperphosphorylation of 4E-BP1 and decreased total 4E-BP1 protein. Decreased levels of a negative regulator of eIF-4E cause unregulated translation, which may lead to tumorigenesis. The RHEB-induced decrease of 4E-BP1 could be a

mechanism that explains how a strong positive signal through the mTOR pathway might lead to cancer. Does the mTOR signal to autophagy go through 4E-BP1? The hypothesis is attractive because it links the signal to autophagy with a signal for the initiation of translation. It is also consistent with the role of the eIF2α kinases, which also inhibit translation initiation and promote autophagy[102]. Future studies will explore the potential relationship between eIF4E and autophagy. In conclusion, the above data confirm that the signal to autophagy is through mTOR, but that it does not go through p70S6 kinase.

The re-addition of amino acids to cells increases Vps34 activity and activates mTOR signaling, thereby inhibiting autophagy. However autophagy also requires Vps34 activity. Autophagy's need for Vps34 activity is supported by the data that fragmentation of both BHMT mutants is completely inhibited by wortmannin. How is it that both mTOR and autophagy require Vps34 activity and both are inhibited by wortmannin, but active mTOR inhibits autophagy? It could be explained in terms of levels of PI3P. Vps34 activity increases levels of PI3P, a well known way to modulate signaling pathways through the recruitment of proteins with FYVE and PX domains. It is likely that the Vps34 activation of mTOR may involve these types of PI3P-dependent molecules with a low affinity for PI3P. Thus high levels of PI3P would activate mTOR. Amino acid starvation would drop PI3P to levels that are high enough to support autophagy, but too low to activate mTOR. A decrease in mTOR signaling would then increase autophagy.

The 3MA treatment of cells expressing the two types of BHMT cargo suggests that modulating levels of PI3P during starvation that might effect the selection of cargo.

Figure 52. Proposed model for Vps34, PI3P, and mTOR regulation of autophagy. In nutrient rich conditions, PI3P levels are high, mTOR is active and autophagy is at basal levels. With amino acid starvation, PI3P levels decrease, mTOR signaling is decreased and the inhibition on autophagy is relieved. In ischemia, Vps34 activity decreases and PI3P levels fall. In these conditions, autophagy of normal cargo ceases, but autophagy continues that targets misfolded proteins that are likely to accumulate in ischemic conditions.

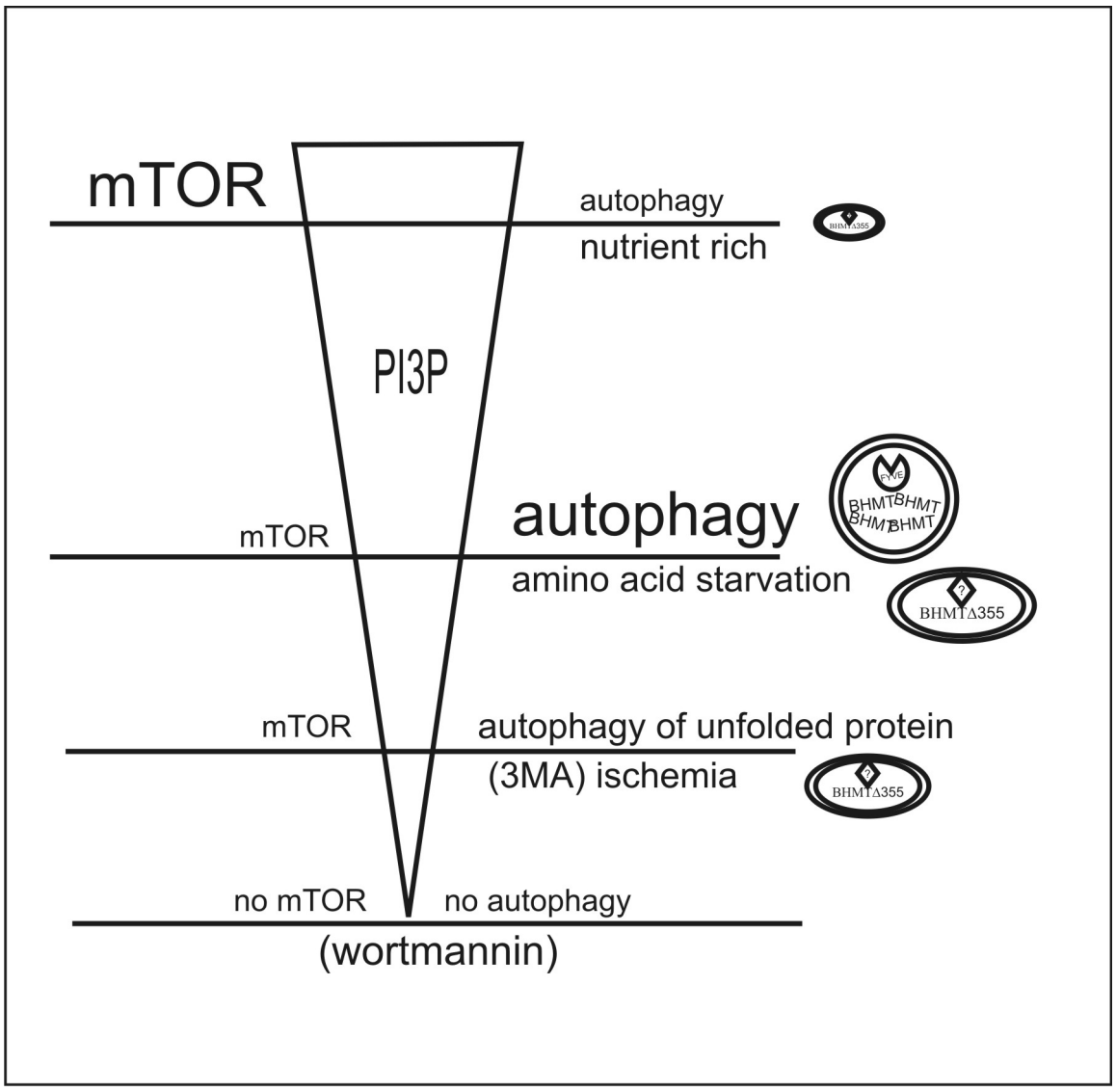
mTOR
autophagy
nutrient rich
PI3P
mTOR
autophagy
amino acid starvation
BHMTΔ355
mTOR
autophagy of unfolded protein
(3MA) ischemia
BHMTΔ355
no mTOR
no autophagy
(wortmannin)

A model has been proposed in which adapter proteins facilitate the selection and degradation of cytoplasmic proteins. Regulated cargo requires the recognition of PI3P by FYVE or PX proteins. However, structurally abnormal protein continues to be degraded when PI3P levels are low. However, if Vps34 activity is completely inhibited, as happens with wortmannin treatment, autophagy cannot proceed.

This suggests that there are levels of PI3P in the cell that effect the progression of autophagy (Fig. 52). At high levels, mTOR is active and autophagy is inhibited. At low levels, mTOR is inactive and autophagy is active. If PI3P levels continue to decrease, autophagy also becomes inhibited. Under what physiological condition might this occur? The data show that ischemia is one situation where both mTOR and autophagy are inhibited.mTOR signaling is down-regulated in response to decreased levels of amino acids and ATP. The ischemia experiment was designed to determine how these cellular stressors affect autophagy. It has been suggested in the literature that cells subjected to conditions of ischemia induce autophagy as a means of survival[110]. This mechanism is proposed to explain how apoptosis-defective (i.e. $Bax^{-/-}/Bak^{-/-}$) solid tumors survive in a nutrient-poor environment, until an adequate blood supply can be established to supply nutrients[110]. Is autophagy induced in ischemia? In an *in-vitro* model of ischemia, Degenhardt et al, concluded ischemia induced autophagy, based on GFP-LC3 localization[110]. The data here, using a similar model of ischemia, show that autophagy as measured by BHMT was inhibited in ischemic conditions, and was slightly inhibited by loss amino acids and glucose. It is likely that the limited response was due to decreased levels of ATP. Autophagy is very energy dependent. Multiple steps of the

autophagic process require ATP and even small changes of ATP levels have been shown to slow autophagic proteolysis[84].

In ischemic conditions, defined as loss of nutrients, serum, glucose and low oxygen, both LC3-II processing and BHMT fragmentation were strongly inhibited. Down-regulation of mTOR does not necessarily mean that the cell has increased autophagy. It is likely that inactive mTOR relieves an inhibitor signal that allows autophagy to proceed as long as sufficient ATP is available for the events required for autophagy. However, even in full ischemia, a small increase of BHMT fragment is observed under amino acid starvation conditions, suggesting that some autophagy was induced. But the severe decrease in LC3-II suggests that as ATP levels drop, the ATP-dependent step of LC3 processing is likely negatively affected.

Together, the data suggest that Vps34 activity and levels of PI3P determine if mTOR is active or inactive (Fig. 52). If mTOR signaling is down-regulated and autophagy is active, modulation of PI3P levels can determine the type of cargo that will be degraded. A severe decrease in PI3P will inhibit autophagy. Ischemia is a situation where mTOR is off and there is only a small autophagy response. Could this be an example of PI3P levels dropping below a threshold necessary to support autophagy? It is likely that the glucose starvation and ischemia conditions also decrease PI3P. This is consistent with the published report that glucose starvation or AICAR, an activator of AMPK decreases Vps34 activity[37]. In addition, conditions of glucose deprivation and hypoxia are two potential stressors that cells face in a physiological situation. Decreased ATP and oxygen can ultimately lead to the production of misfolded proteins. Under these conditions, clearance of unfolded proteins would be a priority, and the proposed

mechanism might explain how cells are able to mount a response to selectively remove this population of aggregate-prone protein. This model predicts that $BHMT^{\Delta C51}$ under the same stress conditions would continue to generate fragment 2´. Future experiments are planned to test ΔC51 in this cell culture model of ischemia.

Diseases of aging such as Alzheimer's, Parkinson's, Huntington's, and Inclusion Body Myositis are all major neurological and muscular diseases associated with the accumulation of aggregated proteins. Therapeutic strategies that increase autophagy can help alleviate the cellular stress of abnormal protein accumulation. Rapamycin, a negative inhibitor of mTOR, has already shown promise as a drug of choice by increasing the degradation of mutant huntingtin protein. The studies here predict that in times of nutrient stress, the cell has adapted macroautophagy such that misfolded proteins are preferentially degraded for the benefit of the cell.

V. REFERENCES

1. Reggiori, F. and D.J. Klionsky, *Autophagy in the eukaryotic cell.* Eukaryot Cell, 2002. **1**(1): p. 11-21.

2. Lum, J.J., R.J. DeBerardinis, and C.B. Thompson, *Autophagy in metazoans: cell survival in the land of plenty.* Nat Rev Mol Cell Biol, 2005. **6**(6): p. 439-48.

3. Rusten, T.E. and H. Stenmark, *Developmental biology: moonlighting at the pole.* Nature, 2007. **445**(7127): p. 497-9.

4. Melendez, A., et al., *Autophagy genes are essential for dauer development and life-span extension in C. elegans.* Science, 2003. **301**(5638): p. 1387-91.

5. Kotoulas, O.B., S.A. Kalamidas, and D.J. Kondomerkos, *Glycogen autophagy in glucose homeostasis.* Pathol Res Pract, 2006. **202**(9): p. 631-8.

6. Cuervo, A.M., *Autophagy: in sickness and in health.* Trends Cell Biol, 2004. **14**(2): p. 70-7.

7. Shintani, T. and D.J. Klionsky, *Autophagy in health and disease: a double-edged sword.* Science, 2004. **306**(5698): p. 990-5.

8. Klionsky, D.J., *The molecular machinery of autophagy: unanswered questions.* J Cell Sci, 2005. **118**(Pt 1): p. 7-18.

9. Dubouloz, F., et al., *The TOR and EGO protein complexes orchestrate microautophagy in yeast.* Mol Cell, 2005. **19**(1): p. 15-26.

10. Majeski, A.E. and J.F. Dice, *Mechanisms of chaperone-mediated autophagy.* Int J Biochem Cell Biol, 2004. **36**(12): p. 2435-44.

11. Eskelinen, E.L., et al., *Disturbed cholesterol traffic but normal proteolytic function in LAMP-1/LAMP-2 double-deficient fibroblasts.* Mol Biol Cell, 2004. **15**(7): p. 3132-45.

12. Massey, A.C., et al., *Consequences of the selective blockage of chaperone-mediated autophagy.* Proc Natl Acad Sci U S A, 2006. **103**(15): p. 5805-10.

13. Yorimitsu, T. and D.J. Klionsky, *Autophagy: molecular machinery for self-eating.* Cell Death Differ, 2005. **12 Suppl 2**: p. 1542-52.

14. Tsukada, M. and Y. Ohsumi, *Isolation and characterization of autophagy-defective mutants of Saccharomyces cerevisiae.* FEBS Lett, 1993. **333**(1-2): p. 169-74.

15. Thumm, M., et al., *Isolation of autophagocytosis mutants of Saccharomyces cerevisiae.* FEBS Lett, 1994. **349**(2): p. 275-80.

16. Klionsky, D.J., et al., *A unified nomenclature for yeast autophagy-related genes.* Dev Cell, 2003. **5**(4): p. 539-45.

17. Ohsumi, Y. and N. Mizushima, *Two ubiquitin-like conjugation systems essential for autophagy.* Semin Cell Dev Biol, 2004. **15**(2): p. 231-6.

18. Mizushima, N., et al., *A new protein conjugation system in human. The counterpart of the yeast Apg12p conjugation system essential for autophagy.* J Biol Chem, 1998. **273**(51): p. 33889-92.

19. Abeliovich, H., et al., *Dissection of autophagosome biogenesis into distinct nucleation and expansion steps.* J Cell Biol, 2000. **151**(5): p. 1025-34.

20. Kabeya, Y., et al., *LC3, a mammalian homologue of yeast Apg8p, is localized in autophagosome membranes after processing.* Embo J, 2000. **19**(21): p. 5720-8.

21. He, H., et al., *Post-translational modifications of three members of the human MAP1LC3 family and detection of a novel type of modification for MAP1LC3B.* J Biol Chem, 2003. **278**(31): p. 29278-87.

22. Tanida, I., et al., *GATE-16 and GABARAP are authentic modifiers mediated by Apg7 and Apg3.* Biochem Biophys Res Commun, 2003. **300**(3): p. 637-44.

23. Tanida, I., et al., *Atg8L/Apg8L is the fourth mammalian modifier of mammalian Atg8 conjugation mediated by human Atg4B, Atg7 and Atg3.* Febs J, 2006. **273**(11): p. 2553-62.

24. Mizushima, N., et al., *A protein conjugation system essential for autophagy.* Nature, 1998. **395**(6700): p. 395-8.

25. Mizushima, N., T. Noda, and Y. Ohsumi, *Apg16p is required for the function of the Apg12p-Apg5p conjugate in the yeast autophagy pathway.* Embo J, 1999. **18**(14): p. 3888-96.

26. Mizushima, N., T. Yoshimori, and Y. Ohsumi, *Role of the Apg12 conjugation system in mammalian autophagy.* Int J Biochem Cell Biol, 2003. **35**(5): p. 553-61.

27. Mizushima, N., et al., *Dissection of autophagosome formation using Apg5-deficient mouse embryonic stem cells.* J Cell Biol, 2001. **152**(4): p. 657-68.

28. Komatsu, M., et al., *Impairment of starvation-induced and constitutive autophagy in Atg7-deficient mice.* J Cell Biol, 2005. **169**(3): p. 425-34.

29. Komatsu, M., et al., *Loss of autophagy in the central nervous system causes neurodegeneration in mice.* Nature, 2006. **441**(7095): p. 880-4.

30. Hara, T., et al., *Suppression of basal autophagy in neural cells causes neurodegenerative disease in mice.* Nature, 2006. **441**(7095): p. 885-9.

31. Kametaka, S., et al., *Apg14p and Apg6/Vps30p form a protein complex essential for autophagy in the yeast, Saccharomyces cerevisiae.* J Biol Chem, 1998. **273**(35): p. 22284-91.

32. Kihara, A., et al., *Two distinct Vps34 phosphatidylinositol 3-kinase complexes function in autophagy and carboxypeptidase Y sorting in Saccharomyces cerevisiae.* J Cell Biol, 2001. **152**(3): p. 519-30.

33. Petiot, A., et al., *Distinct classes of phosphatidylinositol 3'-kinases are involved in signaling pathways that control macroautophagy in HT-29 cells.* J Biol Chem, 2000. **275**(2): p. 992-8.

34. Eskelinen, E.L., et al., *Inhibition of autophagy in mitotic animal cells.* Traffic, 2002. **3**(12): p. 878-93.

35. Walker, D.M., et al., *Characterization of MTMR3. an inositol lipid 3-phosphatase with novel substrate specificity.* Curr Biol, 2001. **11**(20): p. 1600-5.

36. Nobukuni, T., et al., *Amino acids mediate mTOR/raptor signaling through activation of class 3 phosphatidylinositol 3OH-kinase.* Proc Natl Acad Sci U S A, 2005. **102**(40): p. 14238-43.

37. Byfield, M.P., J.T. Murray, and J.M. Backer, *hVps34 is a nutrient-regulated lipid kinase required for activation of p70 S6 kinase.* J Biol Chem, 2005. **280**(38): p. 33076-82.

38. Liang, X.H., et al., *Induction of autophagy and inhibition of tumorigenesis by beclin 1.* Nature, 1999. **402**(6762): p. 672-6.

39. Kihara, A., et al., *Beclin-phosphatidylinositol 3-kinase complex functions at the trans-Golgi network.* EMBO Rep, 2001. **2**(4): p. 330-5.

40. Liang, X.H., et al., *Protection against fatal Sindbis virus encephalitis by beclin, a novel Bcl-2-interacting protein.* J Virol, 1998. **72**(11): p. 8586-96.

41. Qu, X., et al., *Promotion of tumorigenesis by heterozygous disruption of the beclin 1 autophagy gene.* J Clin Invest, 2003. **112**(12): p. 1809-20.

42. Yue, Z., et al., *Beclin 1, an autophagy gene essential for early embryonic development, is a haploinsufficient tumor suppressor.* Proc Natl Acad Sci U S A, 2003. **100**(25): p. 15077-82.

43. Pattingre, S., et al., *Bcl-2 antiapoptotic proteins inhibit Beclin 1-dependent autophagy.* Cell, 2005. **122**(6): p. 927-39.

44. Matsuura, A., et al., *Apg1p, a novel protein kinase required for the autophagic process in Saccharomyces cerevisiae.* Gene, 1997. **192**(2): p. 245-50.

45. Kamada, Y., et al., *Tor-mediated induction of autophagy via an Apg1 protein kinase complex.* J Cell Biol, 2000. **150**(6): p. 1507-13.

46. Abeliovich, H., et al., *Chemical genetic analysis of Apg1 reveals a non-kinase role in the induction of autophagy.* Mol Biol Cell, 2003. **14**(2): p. 477-90.

47. Reggiori, F., et al., *The Atg1-Atg13 complex regulates Atg9 and Atg23 retrieval transport from the pre-autophagosomal structure.* Dev Cell, 2004. **6**(1): p. 79-90.

48. Tekinay, T., et al., *Function of the Dictyostelium discoideum Atg1 kinase during autophagy and development.* Eukaryot Cell, 2006. **5**(10): p. 1797-806.

49. Scott, R.C., G. Juhasz, and T.P. Neufeld, *Direct induction of autophagy by Atg1 inhibits cell growth and induces apoptotic cell death.* Curr Biol, 2007. **17**(1): p. 1-11.

50. Kuroyanagi, H., et al., *Human ULK1, a novel serine/threonine kinase related to UNC-51 kinase of Caenorhabditis elegans: cDNA cloning, expression, and chromosomal assignment.* Genomics, 1998. **51**(1): p. 76-85.

51. Yan, J., et al., *Mouse ULK2, a novel member of the UNC-51-like protein kinases: unique features of functional domains.* Oncogene, 1999. **18**(43): p. 5850-9.

52. Young, A.R., et al., *Starvation and ULK1-dependent cycling of mammalian Atg9 between the TGN and endosomes.* J Cell Sci, 2006. **119**(Pt 18): p. 3888-900.

53. Sarbassov, D.D., S.M. Ali, and D.M. Sabatini, *Growing roles for the mTOR pathway.* Curr Opin Cell Biol, 2005. **17**(6): p. 596-603.

54. Blommaart, E.F., et al., *Phosphorylation of ribosomal protein S6 is inhibitory for autophagy in isolated rat hepatocytes.* J Biol Chem, 1995. **270**(5): p. 2320-6.

55. Lee, S.B., et al., *ATG1, an autophagy regulator, inhibits cell growth by negatively regulating S6 kinase.* EMBO Rep, 2007.

56. Hay, N. and N. Sonenberg, *Upstream and downstream of mTOR.* Genes Dev, 2004. **18**(16): p. 1926-45.

57. Arico, S., et al., *The tumor suppressor PTEN positively regulates macroautophagy by inhibiting the phosphatidylinositol 3-kinase/protein kinase B pathway.* J Biol Chem, 2001. **276**(38): p. 35243-6.

58. Scott, R.C., O. Schuldiner, and T.P. Neufeld, *Role and regulation of starvation-induced autophagy in the Drosophila fat body.* Dev Cell, 2004. **7**(2): p. 167-78.

59. Dann, S.G. and G. Thomas, *The amino acid sensitive TOR pathway from yeast to mammals.* FEBS Lett, 2006. **580**(12): p. 2821-9.

60. Pantuck, A.J., et al., *Mammalian target of rapamycin inhibitors in renal cell carcinoma: current status and future applications.* Semin Oncol, 2006. **33**(5): p. 607-13.

61. Kondo, Y., et al., *The role of autophagy in cancer development and response to therapy.* Nat Rev Cancer, 2005. **5**(9): p. 726-34.

62. Berger, Z., et al., *Rapamycin alleviates toxicity of different aggregate-prone proteins.* Hum Mol Genet, 2006. **15**(3): p. 433-42.

63. Cuervo, A.M., et al., *Autophagy and aging: the importance of maintaining "clean" cells.* Autophagy, 2005. **1**(3): p. 131-40.

64. Schmid, D., et al., *Autophagy in innate and adaptive immunity against intracellular pathogens.* J Mol Med, 2006. **84**(3): p. 194-202.

65. Amar, N., et al., *Two newly identified sites in the ubiquitin-like protein Atg8 are essential for autophagy.* EMBO Rep, 2006. **7**(6): p. 635-42.

66. Adhami, F., et al., *Cerebral ischemia-hypoxia induces intravascular coagulation and autophagy.* Am J Pathol, 2006. **169**(2): p. 566-83.

67. Mizushima, N., *Methods for monitoring autophagy.* Int J Biochem Cell Biol, 2004. **36**(12): p. 2491-502.

68. Furuya, N., et al., *Leupeptin-induced appearance of partial fragment of betaine homocysteine methyltransferase during autophagic maturation in rat hepatocytes.* J Biochem (Tokyo), 2001. **129**(2): p. 313-20.

69. Gonzalez, B., et al., *Crystal structure of rat liver betaine homocysteine s-methyltransferase reveals new oligomerization features and conformational changes upon substrate binding.* J Mol Biol, 2004. **338**(4): p. 771-82.

70. Kochl, R., et al., *Microtubules facilitate autophagosome formation and fusion of autophagosomes with endosomes.* Traffic, 2006. **7**(2): p. 129-45.

71. Finn, P.F., et al., *Effects of small molecules on chaperone-mediated autophagy.* Autophagy, 2005. **1**(3): p. 141-5.

72. Zeng, X., J.H. Overmeyer, and W.A. Maltese, *Functional specificity of the mammalian Beclin-Vps34 PI 3-kinase complex in macroautophagy versus endocytosis and lysosomal enzyme trafficking.* J Cell Sci, 2006. **119**(Pt 2): p. 259-70.

73. Blommaart, P.J., et al., *Effects of intracellular amino acid concentrations, cyclic AMP, and dexamethasone on lysosomal proteolysis in primary cultures of perinatal rat hepatocytes.* J Biol Chem, 1993. **268**(3): p. 1610-7.

74. Dennis, P.B., et al., *Mammalian TOR: a homeostatic ATP sensor.* Science, 2001. **294**(5544): p. 1102-5.

75. Muno, D., et al., *Effect of metabolic alterations on the density and the contents of cathepsins B, H and L of lysosomes in rat macrophages.* Eur J Biochem, 1990. **191**(1): p. 91-8.

76. Holen, I., P.B. Gordon, and P.O. Seglen, *Protein kinase-dependent effects of okadaic acid on hepatocytic autophagy and cytoskeletal integrity.* Biochem J, 1992. **284 (Pt 3)**: p. 633-6.

77. Holen, I., P.B. Gordon, and P.O. Seglen, *Inhibition of hepatocytic autophagy by okadaic acid and other protein phosphatase inhibitors.* Eur J Biochem, 1993. **215**(1): p. 113-22.

78. Inbal, B., et al., *DAP kinase and DRP-1 mediate membrane blebbing and the formation of autophagic vesicles during programmed cell death.* J Cell Biol, 2002. **157**(3): p. 455-68.

79. Wu, H., et al., *Elongation factor-2 kinase regulates autophagy in human glioblastoma cells.* Cancer Res, 2006. **66**(6): p. 3015-23.

80. Szegedi, S.S. and T.A. Garrow, *Oligomerization is required for betaine-homocysteine S-methyltransferase function.* Arch Biochem Biophys, 2004. **426**(1): p. 32-42.

81. Millian, N.S. and T.A. Garrow, *Human betaine-homocysteine methyltransferase is a zinc metalloenzyme.* Arch Biochem Biophys, 1998. **356**(1): p. 93-8.

82. Mousavi, S.A., et al., *Phosphoinositide 3-kinase regulates maturation of lysosomes in rat hepatocytes.* Biochem J, 2003. **372**(Pt 3): p. 861-9.

83. Berg, T.O., et al., *Use of glycyl-L-phenylalanine 2-naphthylamide, a lysosome-disrupting cathepsin C substrate, to distinguish between lysosomes and prelysosomal endocytic vacuoles.* Biochem J, 1994. **300 (Pt 1)**: p. 229-36.

84. Schellens, J.P. and A.J. Meijer, *Energy depletion and autophagy. Cytochemical and biochemical studies in isolated rat hepatocytes.* Histochem J, 1991. **23**(10): p. 460-6.

85. Thomas, G., *The S6 kinase signaling pathway in the control of development and growth.* Biol Res, 2002. **35**(2): p. 305-13.

86. Yousefi, S., et al., *Calpain-mediated cleavage of Atg5 switches autophagy to apoptosis.* Nat Cell Biol, 2006. **8**(10): p. 1124-32.

87. Kuma, A., et al., *Formation of the approximately 350-kDa Apg12-Apg5.Apg16 multimeric complex, mediated by Apg16 oligomerization, is essential for autophagy in yeast.* J Biol Chem, 2002. **277**(21): p. 18619-25.

88. Tanida, I., et al., *Mammalian Apg12p, but not the Apg12p.Apg5p conjugate, facilitates LC3 processing.* Biochem Biophys Res Commun, 2002. **296**(5): p. 1164-70.

89. Tanida, I., et al., *Murine Apg12p has a substrate preference for murine Apg7p over three Apg8p homologs.* Biochem Biophys Res Commun, 2002. **292**(1): p. 256-62.

90. Tanida, I., T. Ueno, and E. Kominami, *LC3 conjugation system in mammalian autophagy.* Int J Biochem Cell Biol, 2004. **36**(12): p. 2503-18.

91. Martinet, W., et al., *In situ detection of starvation-induced autophagy.* J Histochem Cytochem, 2006. **54**(1): p. 85-96.

92. Tanida, I., et al., *Lysosomal turnover, but not a cellular level, of endogenous LC3 is a marker for autophagy.* Autophagy, 2005. **1**(2): p. 84-91.

93. Sugawara, K., et al., *Structural basis for the specificity and catalysis of human Atg4B responsible for mammalian autophagy.* J Biol Chem, 2005. **280**(48): p. 40058-65.
94. Yoshimura, K., et al., *Effects of RNA interference of Atg4B on the limited proteolysis of LC3 in PC12 cells and expression of Atg4B in various rat tissues.* Autophagy, 2006. **2**(3): p. 200-8.

95. Kirisako, T., et al., *The reversible modification regulates the membrane-binding state of Apg8/Aut7 essential for autophagy and the cytoplasm to vacuole targeting pathway.* J Cell Biol, 2000. **151**(2): p. 263-76.

96. Ueno, T., et al., *Autolysosomal membrane-associated betaine homocysteine methyltransferase. Limited degradation fragment of a sequestered cytosolic enzyme monitoring autophagy.* J Biol Chem, 1999. **274**(21): p. 15222-9.

97. Wing, S.S., et al., *Proteins containing peptide sequences related to Lys-Phe-Glu-Arg-Gln are selectively depleted in liver and heart, but not skeletal muscle, of fasted rats.* Biochem J, 1991. **275 (Pt 1)**: p. 165-9.

98. Yue, Z., et al., *A novel protein complex linking the delta 2 glutamate receptor and autophagy: implications for neurodegeneration in lurcher mice.* Neuron, 2002. **35**(5): p. 921-33.

99. Okazaki, N., et al., *Interaction of the Unc-51-like kinase and microtubule-associated protein light chain 3 related proteins in the brain: possible role of vesicular transport in axonal elongation.* Brain Res Mol Brain Res, 2000. **85**(1-2): p. 1-12.

100. Kramer, M.F., et al., *Latent herpes simplex virus infection of sensory neurons alters neuronal gene expression.* J Virol, 2003. **77**(17): p. 9533-41.

101. Budovskaya, Y.V., et al., *An evolutionary proteomics approach identifies substrates of the cAMP-dependent protein kinase.* Proc Natl Acad Sci U S A, 2005. **102**(39): p. 13933-8.

102. Talloczy, Z., et al., *Regulation of starvation- and virus-induced autophagy by the eIF2alpha kinase signaling pathway.* Proc Natl Acad Sci U S A, 2002. **99**(1): p. 190-5.

103. Cota, D., et al., *Hypothalamic mTOR signaling regulates food intake.* Science, 2006. **312**(5775): p. 927-30.

104. Tang, X., et al., *Muscarinic receptor-mediated activation of p70 S6 kinase 1 (S6K1) in 1321N1 astrocytoma cells: permissive role of phosphoinositide 3-kinase.* Biochem J, 2003. **374**(Pt 1): p. 137-43.

105. Wek, R.C., H.Y. Jiang, and T.G. Anthony, *Coping with stress: eIF2 kinases and translational control.* Biochem Soc Trans, 2006. **34**(Pt 1): p. 7-11.

106. Crighton, D., et al., *DRAM, a p53-induced modulator of autophagy, is critical for apoptosis.* Cell, 2006. **126**(1): p. 121-34.

107. Feng, Z., et al., *The coordinate regulation of the p53 and mTOR pathways in cells.* Proc Natl Acad Sci U S A, 2005. **102**(23): p. 8204-9.

108. Casas, K., et al., *Gene responsible for mitochondrial myopathy and sideroblastic anemia (MSA) maps to chromosome 12q24.33.* Am J Med Genet A, 2004. **127**(1): p. 44-9.

109. Bjorkoy, G., et al., *p62/SQSTM1 forms protein aggregates degraded by autophagy and has a protective effect on huntingtin-induced cell death.* J Cell Biol, 2005. **171**(4): p. 603-14.

110. Degenhardt, K., et al., *Autophagy promotes tumor cell survival and restricts necrosis, inflammation, and tumorigenesis.* Cancer Cell, 2006. **10**(1): p. 51-64.